FLUID DISPERSION ASSOCIATED WITH LAMINAR FLOW OF NON-NEWTONIAN FLUIDS

by

WEI SHIN HWANG

B. S., National Taiwan University, 1955

A MASTER'S THESIS

submitted in partial fulfillment of the

requirements for the degree

MASTER OF SCIENCE

Department of Chemical Engineering

KANSAS STATE UNIVERSITY
Manhattan, Kansas

1964

Approved by:

Liang-Tseng Fan

Major Professor

TABLE OF CONTENTS

Page

I. INTRODUCTION

Understanding the behavior of non-Newtonian fluids such as molten plastics, pulps, slurries, emulsions, and colloidal solutions which do not obey Newton's law of viscosity in motion is becoming increasingly important industrially. Much attention so far has been given to the mechanism by which momentum and heat are transferred to a moving non-Newtonian fluid under the simple flow configurations.

One area of fluid flow which has received extensive treatment in recent years is that of fluid dispersion. The importance of fluid dispersion in continuous flow systems has been well recognized and a number of theories and models of fluid dispersion have been proposed. In flow systems, fluid dispersion plays a significant role in the system's performances. Even in heterogeneous systems such as solid particles, liquid droplets, and gas bubbles distributed in fluids, dispersion characteristics affect their performances. However, both analytical and experimental investigations of the fluid dispersion have been mainly confined to Newtonian fluids. The literature of fluid dispersion in non-Newtonian flow is almost non-existent, but fluid dispersion is as important in the processing of non-Newtonian fluids as it is in the processing of Newtonian fluids. A partial listing of the areas in which dispersion of non-Newtonian fluids is of importance is given below:

(1) Dispersion of food additives

(2) Manufacture of pastes

(3) Paint mixing

(4) Processing of heavy oils, coal tar, and coal pastes

(5) Plastic processing and molding

(6) Pulp digestors

(7) Production of various colloidal solutions

(8) Continuous processing of glass

(9) Biological blood flow

(10) Polymerization

The major studies of mixing of non-Newtonian fluids have been carried out in batch mixing tanks by Metzner and co-workers (1,2). McKelvey (3) in his recent book has briefly considered mixing in polymer processing. Typical examples of mixing processes given by him are the dispersion of carbon black in polyethylene with a Banbury mixer, the compounding of a rubber formulation on a roller mill, and the blending of two polymers in an extruder. McKelvey's work is also mainly concerned with efficiency of mixing and a determination of the "goodness" of mixing also in batch systems.

An important tool, commonly used in the study of fluid mixing or dispersion in continuous flow systems, is the analysis of residence or holding time distribution of a tracer in the fluid flowing through the systems. The (exit) residence time distribution is defined as the fraction of material introduced into a system at a dimensionless time $\theta = 0$, which appears at the outlet of the system between θ and $\theta + d\theta$ (4). The residence time distribution function or exit age distribution may be regarded as the response of a flow system to a Dirac delta

function input of a tracer material (5). The residence time distribution function may be directly related to the degree of fluid dispersion and thus can be used to develop either physical or mathematical models to represent dispersion characteristics of flow systems.

This thesis will be concerned mainly with the development of some mathematical models to represent the characteristics of non-Newtonian fluid dispersion in flow systems.

In cylindrical coordinates a mathematical expression of a flow model for which both convection and radial and longitudinal diffusion are considered to be equally important is

$$\frac{\partial C}{\partial t} = D_L \frac{\partial^2 C}{\partial x^2} + D_R \left(\frac{\partial^2 C}{\partial r^2} + \frac{1}{r}\frac{\partial C}{\partial r}\right) - V_x(r)\frac{\partial C}{\partial x}$$

where the following assumptions are made: D_L and D_R are independent of position and concentration gradient, no chemical reaction occurs in the system, and flow is isothermal and steady.

When both the radial and longitudinal diffusions are negligible, the steady-state velocity profile becomes the only factor governing the overall or apparent fluid dispersion. This specific case is often called a convective (velocity profile) model. Such a model is extensively treated in this thesis. Age distribution curves for flow of fluids which have the properties of either the Bingham plastic or Ostwald-de Waele fluid are calculated based on such a model. Comparisons of the convective model with other models such as the Taylor dispersion, perfectly-mixed-tanks-in-series, and others are also presented.

When the variation of the axial velocity with radial

position and the lateral material transport by molecular diffusion are assumed to be the dominant dispersion mechanism, the equation previously shown is called a dispersion model. Such a model for the Ostwald-de Waele fluid flowing through an open-open circular conduit is treated in Chapter V. Age distribution functions (curves) are presented in order to show the effects of dispersion coefficients and flow-behavior index on the performance of the flow.

II. BACKGROUND INFORMATION

NATURE OF FLUID DISPERSION

1. Mathematical Representation

The degree to which the fluid flowing through a flow system is mixed or dispersed may be characterized by either the distribution of residence times of the fluid elements flowing through the system or the concentration profile of the fluid in the system. Theoretically, both of these relationships may be obtained analytically.

A full mathematical description for the conservation of mass and the equation of motion for any component of the system may be written as follows (6).

$$\frac{\partial C_i}{\partial t} = -\left(\nabla \cdot \left\{C_i \vec{v} + \vec{J}_i\right\}\right) + r_i \; ; \; i = 1, 2, \ldots n \tag{1}$$

$$\frac{\partial}{\partial t} \rho \vec{v} = -\left[\nabla \cdot \left\{\vec{v}\vec{v} + \vec{\vec{\pi}}\right\}\right] + \sum_{i=1}^{n} \rho_i \vec{g}_i \tag{2}$$

These equations are seldom used in the complete form given above because the exact solution of these equations is beyond the capability of present day mathematics. The normal procedure is to disregard terms that are physically negligible or identically zero, thereby obtaining simpler equations for a given situation. For example, consider an isothermal and incompressible fluid of constant mass density and viscosity. Equations (1) and (2) become

$$\frac{\partial C_i}{\partial t} = -\vec{v} \cdot \nabla C_i - \nabla \cdot \vec{J}_i + r_i \tag{3}$$

$$\frac{D\vec{v}}{Dt} = -\nabla P - \left[\nabla \cdot \vec{\vec{\tau}}\right] + \rho \vec{g} \qquad (4)$$

For a given physical situation of simple geometry (e.g., flow through a circular tube, Equations (3) and (4) are relatively easily solved for laminar flow. This is because in laminar flow the molar flux $\vec{J}_i$ and stress tensor $\vec{\vec{\tau}}$ are expressed in terms of Fick's law of diffusion and Newton's law of viscosity (for Newtonian fluids only). When considering turbulent flow $\vec{J}_i$ and $\vec{\vec{\tau}}$ are given by (6)

$$\vec{J}_i = \vec{J}_i^{(l)} + \vec{J}_i^{(t)} \qquad (5)$$

$$\vec{\vec{\tau}} = \vec{\vec{\tau}}^{(l)} + \vec{\vec{\tau}}^{(t)} \qquad (6)$$

The superscripts (l) and (t) refer to laminar and turbulent contributions respectively. The $\vec{J}_i^{(l)}$ and $\vec{\vec{\tau}}_i^{(l)}$ can be given by the same expressions as for purely laminar flow. The difficulty here is that only semi-empirical expressions are available for $\vec{J}_i^{(t)}$ and $\vec{\vec{\tau}}^{(t)}$.

If the geometry of the system becomes complicated, even the laminar flow situation is impossible, or at least, very difficult to solve. It is, therefore, convenient to treat fluid dispersion from semi-empirical and/or mathematical or physical modeling techniques. Furthermore, it is essential to confirm results from such a treatment experimentally.

2. Age Distributions

The discussion which follows is based mainly on that

presented by Levenspiel (5) in his book.

a. Internal age distribution, $\underline{I}(\theta)$. The vessel contains, in general, fluid elements of varying ages, age being the time the fluid elements have spent in the vessel. Let $\underline{I}(\theta)$ be the internal age distribution function, which is defined so that $\underline{I}(\theta)d\theta$ is the fraction of fluid elements with ages between θ and $\theta + d\theta$. A typical plot of $\underline{I}(\theta)$ versus θ is given in Figure 1. It follows that the area under the curve is one, i.e.

$$\int_0^\infty \underline{I}(\theta)d\theta = 1 \tag{7}$$

The fraction of fluid with ages less than θ_1 is shown in Figure 1 as the shaded area and is given by

$$\int_0^{\theta_1} \underline{I}(\theta)d\theta \tag{8}$$

The fraction of fluid with ages greater than θ_1 is

$$\int_{\theta_1}^\infty \underline{I}(\theta)d\theta = 1 - \int_0^{\theta_1} \underline{I}(\theta)d\theta \tag{9}$$

The internal age distribution $\underline{I}(t)$ based on time rather than reduced time is related to $\underline{I}(\theta)$ as

$$\underline{I}(\theta) = \bar{t}\, \underline{I}(t) \text{ with } \int_0^\infty \underline{I}(t)dt = 1 \tag{10}$$

b. Exit age distribution or residence time distribution function (r.t.d.f.), $\underline{E}(\theta)$. In a manner similar to $\underline{I}(\theta)$, let $\underline{E}(\theta)$ denote the distribution of ages of all fluid elements leaving the vessel. $\underline{E}(\theta)$ is defined so that $\underline{E}(\theta)d\theta$ is the

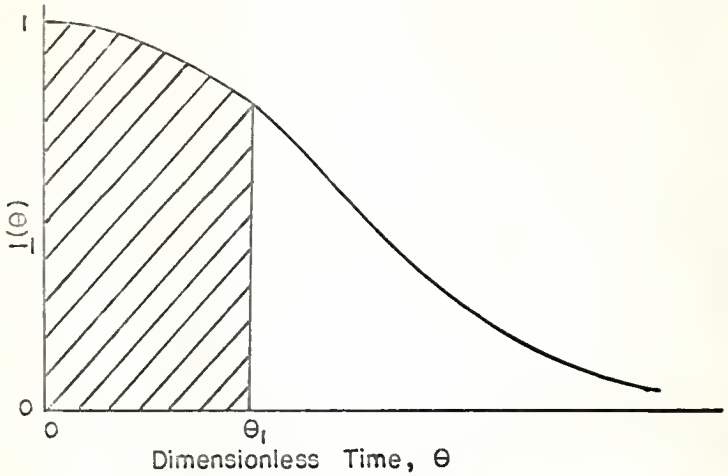

Fig. 1. Typical internal age distribution curve.

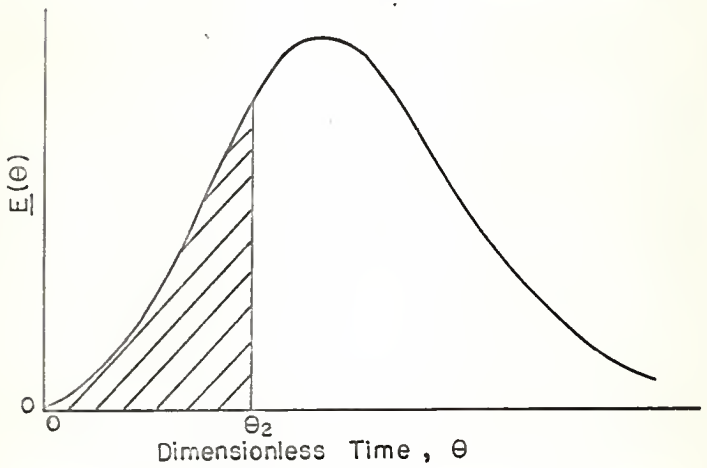

Fig. 2. Typical exit age distribution curve.

fraction of material in the exit stream between the ages of θ and $\theta+d\theta$. It follows that

$$\int_0^\infty \underline{E}(\theta)d\theta = 1 \tag{11}$$

A typical $\underline{E}(\theta)$ curve is given in Figure 2. The fraction of material in the exit stream younger than age θ_2, the shaded area of Figure 2, is

$$\int_0^{\theta_2} \underline{E}(\theta)d\theta \tag{12}$$

and the fraction older than θ_2 is

$$\int_{\theta_2}^\infty \underline{E}(\theta)d\theta = 1 - \int_0^{\theta_2} \underline{E}(\theta)d\theta \tag{13}$$

$\underline{E}(\theta)$ is variously referred to as the exit age distribution function, the exit residence time distribution, or simply the residence time distribution function (r.t.d.f.). If time, t, is used instead of θ,

$$\underline{E}(\theta) = \bar{t}\ \underline{E}(t) \text{ with } \int_0^\infty \underline{E}(t)dt = 1 \tag{14}$$

c. Cumulative (exit) age distribution, $\underline{F}(\theta)$. With no tracer initially present, let a step function (Appendix 1) in time of tracer be introduced into the fluid entering the vessel in such a manner that the volumetric flow rate to the vessel remains constant. Then the concentration-time curve for the tracer in the exit fluid system, measured in terms of tracer concentration in the entering stream, C_o, and reduced time θ is called the

cumulative (exit) age distribution curve or F-curve. As shown in Figure 3 the range of F is $0 \leq F \leq 1$.

d. The C-curve. The curve which describes the concentration-time function of tracer in the exit stream of a vessel in response to a Dirac delta function or unit impulse input (Appendix 2) is called the C-curve. As with the F-curve, the range and domain are dimensionless. Concentrations are measured in terms of the initial concentration, C^o, as if it were evenly distributed throughout the vessel.

$$C^o = \int_0^\infty C d\theta = \frac{1}{\bar{t}} \int_0^\infty C dt \tag{15}$$

Time is measured in a reduced unit with this choice of unit

$$\int_0^\infty C d\theta = 1 \tag{16}$$

Figure 4 shows a typical C-curve. The terms F, C, I, and E were introduced by Danckwerts (4). They are interrelated as follows (3):

$$F(\theta) + I(\theta) = 1 \tag{17}$$

$$C(\theta) = E(\theta) \tag{18}$$

$$F(\theta) = 1 - I(\theta) = \int_0^\theta E(\theta) d\theta = \int_0^\theta C(\theta) d\theta \tag{19}$$

FLOW MODELS

The use of flow models to represent actual dispersion characteristics or the corresponding residence time distributions of flow systems is, as mentioned in the first chapter, a very

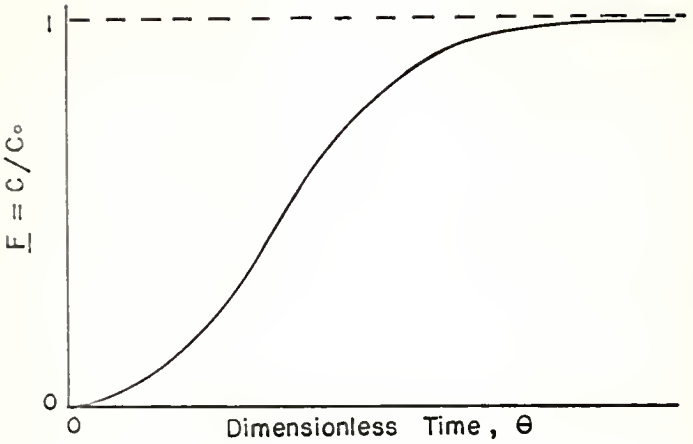

Fig.3. Typical F-curve.

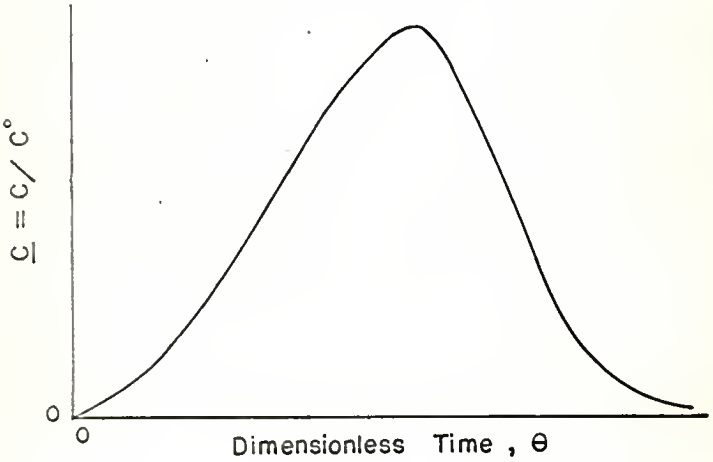

Fig.4. Typical C-curve.

fruitful approach to the prediction of system performance. The parameters of models can be correlated with the physical properties of the fluid, vessel geometry, and flow rates. Once these correlations are found, performance predictions can be made without resort to experimentation for all types of fluid processing.

Two ideal flow patterns, which are often used to approximate real systems, are plug flow and complete mixing. Patterns of flow other than plug or complete mixing flow may be called non-ideal flow patterns (5). Many types of models are available to describe non-ideal flow patterns within vessels, e.g., the dispersion models, convective models*, perfectly-mixed-tanks-in-series models, mixed models, and others (5).

The models may vary in complexity depending on the number of parameters included. As the number of parameters used increases, so does the difficulty in establishing general correlations. In general, therefore, it is best to use as few parameters as is consistent with adequate description of the system of interest (5).

1. The Dispersion Model

The mathematical representation of one of the general forms of the dispersion model is given by

$$\frac{\partial C}{\partial t} + \nabla \cdot (-D \nabla C) + \nabla \cdot (\vec{v} C) + \psi (C) = 0 \qquad (20)$$

*The convective model has often been called the velocity profile model.

where D is the dispersion coefficient, $\vec{v}$ the fluid velocity vector, C the concentration, and t is the time. The values of D are different in different directions, and thus the coefficient may be represented by a second order tensor. The first term of Equation (20) represents the change of concentration with respect to time. The second term is an extension of Fick's law or net outflow due to dispersion. The third term stands for the velocity gradient and the fourth term represents the depletion of material caused by the progress of a rate process.

A very important special form of the equation of continuity is that of an incompressible fluid for which

$$\nabla \cdot \vec{v} = 0$$

Since the third term of Equation (20) may be written as

$$\nabla \cdot (\vec{v}C) = \vec{v} \cdot \nabla C + C(\nabla \cdot \vec{v})$$

$$= \vec{v} \cdot \nabla C$$

Equation (20) thus becomes

$$\frac{\partial C}{\partial t} - \nabla \cdot (- D \nabla C) + \vec{v} \cdot C + \psi(C) = 0 \qquad (21)$$

For symmetrical axial flow in cylindrical tubes as encountered in most of the chemical processes, Equation (21) reduces to

$$\frac{\partial C}{\partial t} - \frac{\partial}{\partial x}\left[D_L(r) \frac{\partial C}{\partial x} \right] - \frac{1}{r} \frac{\partial}{\partial r}\left[D_R(r)\, r \frac{\partial C}{\partial r} \right] + V_x(r) \frac{\partial C}{\partial x} + \psi(C) = 0 \qquad (22)$$

The lack of analytical solutions of this equation makes the

evaluation of the dispersion coefficients extremely difficult. Therefore, further simplification of Equation (21) often becomes necessary.

a. The axial dispersed plug flow model. The most often treated dispersion model is the axial dispersed plug flow model, which is obtained from Equation (21) by making the following assumptions: Only the dispersion in the axial direction is significant, the dispersion coefficient, D, is independent of position and concentration gradients, and the fluid flows with an average axial velocity component $\bar{V}_x$.

With these assumptions, Equation (21) reduces to

$$\frac{\partial C}{\partial t} = D \frac{\partial^2 C}{\partial x^2} - \bar{V}_x \frac{\partial C}{\partial x} - \Psi(C) \qquad (23)$$

The usual way of finding the value of D is through unsteady tracer injection experiments. For a Dirac delta function input of an inert tracer Equation (23) becomes, in terms of reduced quantities and variables,

$$\frac{\partial C^*}{\partial \theta} + \frac{\partial C^*}{\partial \eta} - \frac{1}{Pe} \frac{\partial^2 C}{\partial \eta^2} = \delta(\eta - \eta_o)\, \delta(\theta) \qquad (24)$$

where δ is the Dirac delta function

$$\eta = \frac{x}{L}$$

L = characteristic length of the system

$$Pe = \frac{\bar{V}\, L}{D}$$

With the selection of proper boundary conditions to be used with

Equation (24), the residence time distribution function of the system can be calculated.

b. The dispersed plug flow model. The dispersed plug flow model takes into account the dispersion in both the axial and radial directions. As with the axial dispersed plug flow model, the dispersion coefficients are assumed to be independent of position and concentration gradients, and the fluid is assumed to flow with an average axial velocity component $\bar{v}_x$. With these assumptions, Equation (22) becomes

$$\frac{\partial C}{\partial t} = D_L \frac{\partial^2 C}{\partial x^2} + D_R \left(\frac{\partial^2 C}{\partial r^2} + \frac{1}{r}\frac{\partial C}{\partial r}\right) - \bar{v}_x \frac{\partial C}{\partial x} - \Psi(C) \qquad (25)$$

The method of solution is similar to that of the axial dispersed plug flow model except for modification, which keeps both axial and radial dispersions in the equations.

2. Dispersion (Diffusion) Model with Velocity Profile

Consider a steady-state flow inside a circular tube. There exists a developed velocity profile, and owing to molecular and turbulent diffusion, both axial and radial mixing will occur. The presence of a velocity profile will increase the mixing along the overall flow direction.

Suppose that the following assumptions are valid for flow through a circular conduit; D_L and D_R are independent of position and concentration gradient, no chemical reaction occurs in the system, and steady-state flow inside the tube is assumed.

Then Equation (22) reduces to

$$\frac{\partial C}{\partial t} = D_L \frac{\partial^2 C}{\partial x^2} + D_R \left(\frac{\partial^2 C}{\partial r^2} + \frac{1}{r}\frac{\partial C}{\partial r}\right) - V_x(r) \frac{\partial C}{\partial x} \tag{26}$$

For laminar flow of Newtonian fluids,

$$D_R = D_L = D_m \text{ (molecular diffusivity)}$$

and

$$V_x(r) = V_m\left[1 - \left(\frac{r}{R}\right)^2\right] \tag{27}$$

where V_m represents velocity at central axis and R is the radius of the tube.

Taylor (7, 8, 9) and Tichacek et al. (10) considered solutions of Equation (26) and compared the results with experimental data. When the diffusion terms in the above equation are negligible, the velocity profile alone accounts for the "apparent" mixing. The residence time distribution functions for this case have been solved by Miyauchi (11) and Sheppard (12). This specific case is often termed convective model.

3. Perfectly-Mixed-Tanks-in-Series Model

The perfectly-mixed-tanks-in-series model was first applied to distillation plates by Kirschbaum (13) who called it the pool model. It gives tracer response curves that are somewhat similar in shape to those found from the dispersion model. This is a one-parameter model, the parameter being the number of tanks in series.

Consider j tanks in series, each having the same volume, a material balance around the i-th tank gives

$$vC_{i-1} = vC_i + V_i \frac{dC_i}{dt} \tag{28}$$

The C-curve may be found by solving the set of equations (28) for i = 1, 2, 3,...,j with the condition that the input to the first tank, i = 1, is a Dirac delta function of tracer. Solving Equations (28) by the use of Laplace transforms gives (5)

$$\underline{C} = \frac{j^j \theta^{j-1}}{(j-1)!} e^{-j\theta} \tag{29}$$

The mean and the variance are

$$\mu = 1 \tag{30}$$

$$\sigma^2 = \frac{1}{j} \tag{31}$$

Hence, the experimental C-curve data can be used to determine a variance σ^2 and thus j.

Several authors (14, 15, 16) have discussed the similarity between the axial dispersed plug flow model and perfectly-mixed tanks-in-series-model. Various methods of comparison have been suggested. Kramers and Alberda (14) used the variance for the doubly infinite vessel which is

$$\sigma^2 \approx \frac{2}{Pe} = 2 \frac{D}{\bar{V}_x L} \tag{32}$$

Comparing this with Equation (31) gives

$$\frac{1}{j} = \frac{2}{Pe} \tag{33}$$

Equation (33) extrapolates properly to $j \rightarrow \infty$ as $1/Pe \rightarrow 0$ (or $D \rightarrow 0$), but does not extrapolate to $j = 1$ as $1/Pe \rightarrow \infty$ (or $D \rightarrow \infty$). Levenspiel (15) has shown that the reason for the incorrect extrapolation of Equation (33) as $1/Pe \rightarrow \infty$ (or $D \rightarrow \infty$) is that the doubly infinite vessel is not the proper one to use for the comparison. The closed vessel must be used. Then from van der Laan (17), it gives

$$\frac{1}{j} = \frac{2}{Pe} - \frac{2}{Pe^2}\left(1 - e^{-Pe}\right) \qquad (34)$$

This expression extrapolates properly to $j = 1$ for $1/Pe \rightarrow \infty$ (or $D \rightarrow \infty$) small values of $1/Pe$ it reduces to Equation (33). These comparisons are the basis for the statement that an infinite number of stirred-tanks-in-series is equivalent to plug flow (11, 15) because $j \rightarrow \infty$ as $1/Pe \rightarrow 0$ (or $D \rightarrow 0$).

CHARACTERISTICS OF NON-NEWTONIAN FLOW

The distinguishing feature of non-Newtonian systems appears to be that the colloidal rather than molecular properties are of significance. Philippoff (18) has summarized the properties of colloidal particles which are relevant in determining their rheological behavior.

The completely general case is that of a fluid for which the relationship between shear stress and rate of shear is non-linear, time dependent, and is also dependent upon the extent of the deformation. Consequently, the non-Newtonian systems may be divided into three broad classifications; time-independent non-Newtonian fluids, time-dependent non-Newtonian fluids, and

systems which have many characteristics of a solid, primarily that of elastic recovery from the deformation, which occurs upon flow. To date engineering research in this area has been concerned mostly with the first of these classifications. Some work has been done with paints and foods, which generally fall in the second catagory.

The time independent non-Newtonian fluids can be divided into three classes, whose shear stress and shear rate behaviors for a two dimensional flow with one-dimensional rheological statement are shown in Figure 5.

The so-called Bingham plastic or plastic fluid is the simplest of all non-Newtonian fluids in the sense that the relationship between stress and shear rate differs from that of a Newtonian fluid in that the linear relationship does not pass through the origin. Thus a finite shearing stress, τ_o, is necessary to initiate movement. For example, slurries of approximately equi-dimensional particles in a liquid would be most likely to exhibit Bingham plastic behavior (19). Specific examples are drilling muds, nuclear fuel suspensions, suspensions of chalk, grains and rock, and sewage sludge (20).

The general rheological statement between shear stress tensor, $\overrightarrow{\overrightarrow{\tau}}$, and rate of deformation tensor, $\overrightarrow{\overrightarrow{\Delta}}$ is represented according to Bird et al. (6) as

$$\overrightarrow{\overrightarrow{\tau}} = -\left\{\mu_o - \frac{\tau_o}{\sqrt{\frac{1}{2}\left(\overrightarrow{\overrightarrow{\Delta}} : \overrightarrow{\overrightarrow{\Delta}}\right)}}\right\} \Delta \quad \text{for } \frac{1}{2}\left(\overrightarrow{\overrightarrow{\tau}} : \overrightarrow{\overrightarrow{\tau}}\right) > \tau_o^2 \tag{35}$$

$$\overrightarrow{\overrightarrow{\Delta}} = 0 \qquad \text{for } \frac{1}{2}\left(\overrightarrow{\overrightarrow{\tau}} : \overrightarrow{\overrightarrow{\tau}}\right) < \tau_o^2 \tag{36}$$

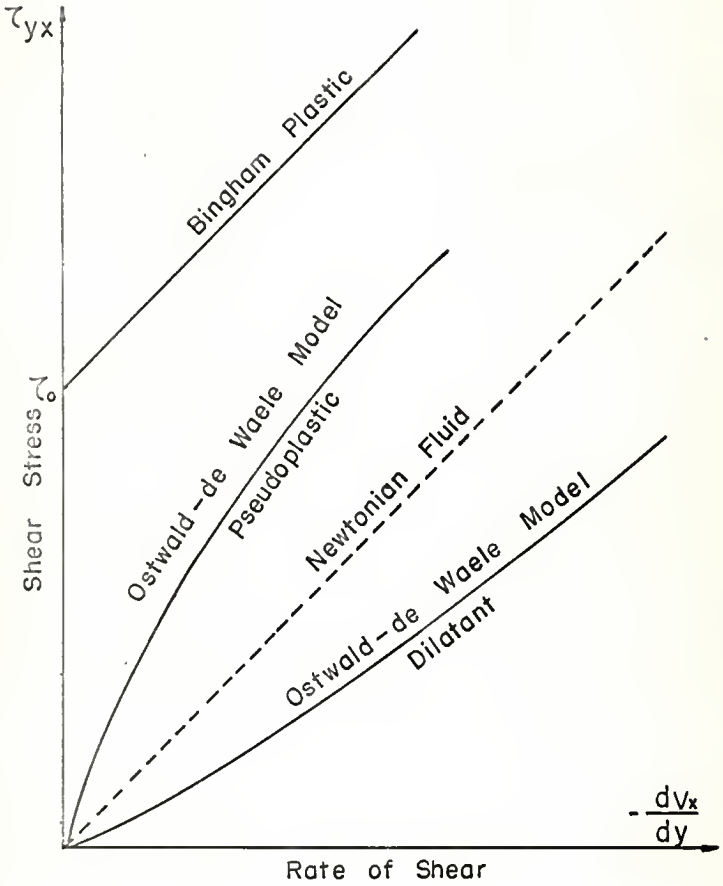

Fig. 5. Steady-state non-Newtonian fluids (6).

In the flow of a pseudoplastic fluid, Ostwald-de Waele fluid, or power-law fluid, the apparent viscosity gradually decreases with increased values of shear rates, that is, the intermolecular or interparticle interactions smoothly decrease with increasing rates of shear.

Examples of fluids which exhibit pseudoplastic behavior include polymeric solutions or melts, such as rubbers, cellulose acetate, and napalm; suspensions such as paints, mayonnaise, paper pulp, and detergent slurries, and even dilute suspensions of inert, unsolvated solids (21).

The pseudoplastic fluid may be characterized by the following relationship between shear stress tensor and rate of deformation tensor (6):

$$\overrightarrow{\overrightarrow{\tau}} = -\left\{m\left|\sqrt{\frac{1}{2}\left(\overrightarrow{\overrightarrow{\Delta}} : \overrightarrow{\overrightarrow{\Delta}}\right)}\right|^{\nu-1}\right\}\overrightarrow{\overrightarrow{\Delta}} \tag{37}$$

The apparent viscosity of dilatant fluids gradually increases with increasing shear rate. The best explanation for dilatant behavior may still be the original explanation given by Reynolds in 1888 (22). This explanation suggests that all suspensions of solids in liquids should exhibit dilatant behavior at high solids contents. Few data are available for evaluating this conclusion.

The time-dependent non-Newtonian fluids may be divided into two groups, depending on whether the shear stress increases or decreases with time of shear at a constant shearing rate (23). The former are termed rheopectic and the latter thixotropic

fluids (23).

The causes of thixotropic and rheopectic behavior are possibly very similar to those for pseudoplasticity and dilatancy. The alignment of asymmetrical molecules or particles in pseudoplasticity cannot always be expected to be instantaneous with respect to time. Therefore, it seems that the pseudoplastic behavior may be that form of thixotropy which has too small a time element to be measured on most instruments in current use. The same argument may be applied to the relationship between rheopexy and dilatancy (21).

III. LITERATURE SURVEY

The convective model of dispersion in Newtonian fluids was proposed by several investigators (4, 11, 12, 24, 25) to predict residence time distribution functions of the flow in circular conduits. Employing the fully developed laminar flow velocity profile, they obtained the following (or equivalent) expressions of the cumulative age distribution for the model when the entrance effect is considered. The cumulative age distribution at the outlet of the system corresponds to the response to a step function input of a tracer or a second fluid

$$\left.\begin{aligned} \underline{F}(\theta) &= 1 - \frac{1}{2\theta} \quad , \quad \text{for} \quad \theta > 1/2 \\ &= 0 \quad , \quad \text{for} \quad \theta < 1/2 \end{aligned}\right\} \qquad (1)$$

Entrance effect consideration will be briefly described as follows: We may resolve the fluid in the tube into a series of laminar sleeves. When the fluid flows through the section, $x = 0$ and $x = X$ (X/R being small), initially filled with a uniformly distributed tracer, the tracer may be resolved into a corresponding series of laminar rings. Since the tracer is uniform in the section mentioned, or in other words, it is uniform in length and concentration, the amount of the tracer per unit cross-sectional area entering each ring will be constant everywhere. When we relate the amount of tracer which this ring delivers at the outflow to the time of delivery, we can obtain the residence time distribution of a tracer in the

fluid flowing through the tube. This is the case in which the entrance effect is considered (12, 25). Exit age distribution for the model in which the entrance effect is considered is the response to a Dirac delta function input of a tracer and is expressed by

$$\left.\begin{aligned} \underline{E}(\theta) &= \frac{1}{2\theta^2} \quad , \quad \text{for} \quad \theta > \tfrac{1}{2} \\ &= 0 \quad , \quad \text{for} \quad \theta < \tfrac{1}{2} \end{aligned}\right\} \qquad (2)$$

Now, suppose that the distribution of a tracer is uniform at the inflow when taken with respect to time coordinates rather than to space coordinates. The central laminae of the flow will receive more tracer than will peripheral ones when a relatively long pipe, as actually encountered in many practical situations, is used. Thus, the moving laminae contain tracer in proportion to the fluid velocity (12, 25). This generates a case in which the entrance effect can be neglected. For this case, they (4, 11, 12, 24, 25) obtained the following expressions for the cumulative and exit age distributions:

$$\left.\begin{aligned} \underline{F}(\theta) &= 1 - \frac{1}{(2\theta)^2} \quad , \quad \text{for} \quad \theta > 1/2 \\ &= 0 \quad , \quad \text{for} \quad \theta < 1/2 \end{aligned}\right\} \qquad (3)$$

and

$$\left.\begin{aligned} \underline{E}(\theta) &= \frac{1}{2\theta^3} \quad , \quad \text{for} \quad \theta > 1/2 \\ &= 0 \quad , \quad \text{for} \quad \theta < 1/2 \end{aligned}\right\} \qquad (4)$$

A solid curve in Figure 6 is the graphical representation of Equation (4). Miyauchi (11), however, indicated that such a curve is generally deformed, probably due to diffusion accompanying the flow as shown by the dotted line.

Gonzalez-Fernandez (25) considered the case with a more generalized velocity profile for the laminar flow of a Newtonian fluid. He also proposed the velocity profile for Newtonian fluid flow at a low Reynolds number with slippage at the tube wall as follows:

$$V_x(r) = V_R + (V_m' - V_R) \left[1 - \left(\frac{r}{R}\right)^2\right] \qquad (5)$$

As described above, most of the convective models considered are only for laminar flow of Newtonian fluids. Actually, non-Newtonian flow predominates in many industrial systems as mentioned in the introductory chapter.

In order to give a more precise description of the dispersion characteristics of fluids, axial and radial diffusions and the velocity profile should be considered simultaneously. The mathematical expression of such a model is shown by Equation (2.26). The general solutions to this equation do not exist. Thus, some terms that are physically negligible or identically zero may be disregarded in order to obtain simpler equations for a given situation as mentioned previously.

Taylor (7) simplified Equation (2.26) by considering that the variation of axial velocity with radial position and radial transport by molecular diffusion to be the main mechanism of

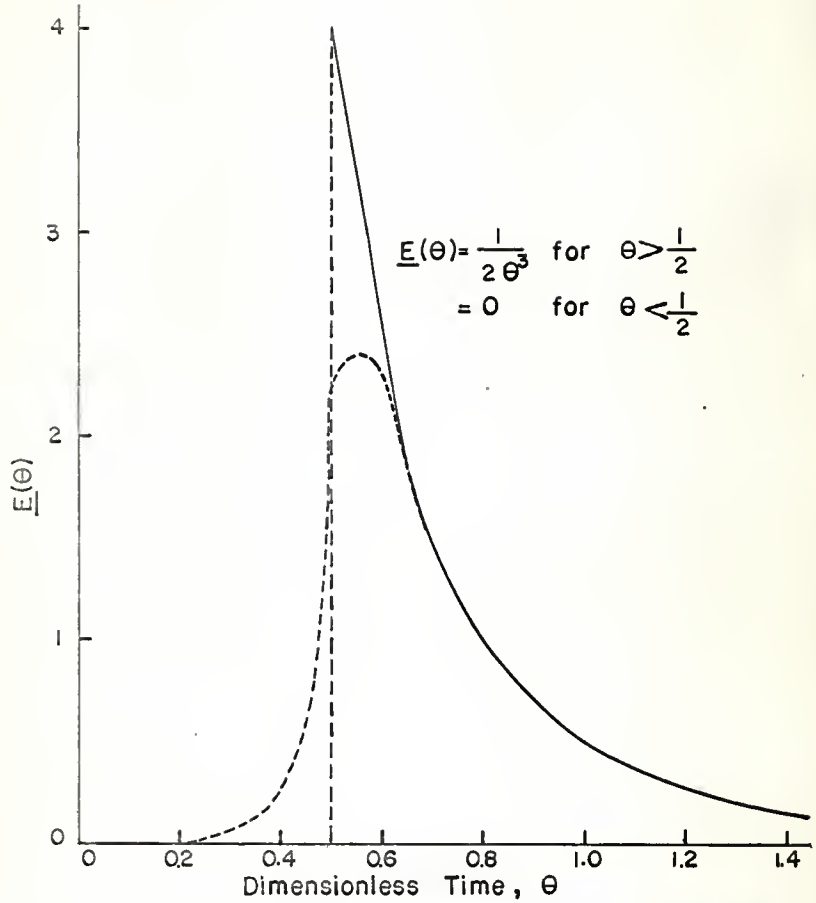

Fig. 6. Residence time distribution function of the convective model for laminar flow of a Newtonian fluid in a cylindrical tube.

dispersion of soluble tracer during laminar flow of a Newtonian fluid in an open tube. The corresponding diffusion equation is

$$D_m\left(\frac{\partial^2 C}{\partial r^2} + \frac{1}{r}\frac{\partial C}{\partial r}\right) - V_m\left[1 - \left(\frac{r}{R}\right)^2\right]\frac{\partial C}{\partial x} = \frac{\partial C}{\partial t} \qquad (6)$$

where D_m is the molecular diffusivity which is equal to D_R, the radial diffusion coefficient, as shown in Equation (2.27).

Since it would be difficult to find a complete solution of Equation (6), Taylor in his first paper (7) presented approximate solutions, which are valid under the following two limiting conditions:

> "The changes in C due to convective transport along the tube take place in a time which is so short that the effect of molecular diffusion may be neglected."
>
> "The time necessary for appreciable effects to appear, owing to convective transport, is long compared with the 'time of decay' during which radial variations of concentration are reduced to a fraction of their initial value through the action of molecular diffusion."

The calculated distributions of C_m along a tube for the first condition have been given by him (7) as follows:

When input of a tracer in the flow is an impulse

$$\left.\begin{aligned} C_m &= \frac{C_o X}{V_m t} \quad , \quad 0 < x < V_m t \\ &= 0 \quad , \quad x < 0 \text{ and } x > V_m t \end{aligned}\right\} \qquad (7)$$

For the step input of a tracer,

$$\left.\begin{aligned} C_m &= C_o \quad , \quad x < 0 \\ C_m &= C_o \left(1 - \frac{x}{V_m t}\right) \quad , \quad 0 < x < V_m t \\ C_m &= 0 \quad , \quad x > V_m t \end{aligned}\right\} \tag{8}$$

For the finite pulse input of a tracer the distribution is described by, if $t < X/V_m$

$$\left.\begin{aligned} C_m &= 0, \quad x < 0 \\ C_m &= C_o x/V_m t \quad , \quad 0 < x < V_m t \\ C_m &= C_o \quad , \quad V_m t < x < X \\ C_m &= C_o \left(1 - \frac{x-X}{V_m t}\right) \quad , \quad X < x < X + V_m t \\ C_m &= 0 \quad , \quad x > X + V_m t \end{aligned}\right\} \tag{9}$$

If $t > X/V_m$, it is given by

$$\left.\begin{aligned} C_m &= 0 \quad , \quad x < 0 \\ C_m &= C_o \left(x/V_m t\right) \quad , \quad 0 < x < X \\ C_m &= C_o \left(X/V_m t\right), \quad X < x < V_m t \\ C_m &= C_o \left(\frac{X + V_m t - x}{V_m t}\right) \quad , \quad V_m t < x < V_m t + X \\ C_m &= 0 \quad , \quad x > X + V_m t \end{aligned}\right\} \tag{10}$$

It should be noted that the first simplification proposed by

Taylor can be considered as the origin of the convective model whose residence time distribution functions are given by Equations (1), (2), (3), and (4).

If the molecular diffusion becomes the dominant dispersion mechanism of a tracer in a fluid flow and if the second condition is valid, the time necessary for convection, L/V_m, to make an appreciable change in C was given by (7)

$$\frac{L}{V_m} \gg \frac{R^2}{(3.8)^2 D_m} \tag{11}$$

Letting $x_1 = x - \frac{1}{2} V_m t$ and $\rho = \frac{r}{R}$, Taylor transformed Equation (6) into the following form

$$\frac{\partial^2 C}{\partial \rho^2} + \frac{1}{\rho} \frac{\partial C}{\partial \rho} = \frac{R^2}{D_m} \frac{\partial C}{t} + \frac{R^2 V_m}{D_m} \left(\frac{1}{2} - \rho^2\right) \frac{\partial C}{\partial x_1} \tag{12}$$

Since the mean velocity across planes, for which x_1 is constant, is zero, the transfer of C across such planes depends only on the radial variation of C. Therefore, if it is assumed that the radial variation of C is small, and thus $\partial C/\partial t$ is also small. Then, Equation (12) may be written as

$$\frac{\partial^2 C}{\partial \rho^2} + \frac{1}{\rho} \frac{C}{\partial \rho} = \frac{R^2 V_m}{D_m} \left(\frac{1}{2} - \rho^2\right) \frac{\partial C}{\partial x_1} \tag{13}$$

Furthermore, since $\partial C/\partial x_1$ is independent of ρ, if $\partial C/\partial \rho$ is very small, the solution obtained is

$$C = C_{x_1} + A \left(\rho^2 - \frac{1}{2} \rho^4\right) \tag{14}$$

where C_{x_1} is the concentration at $\rho = 0$ and A is a constant.

Substituting Equation (14) into Equation (13) one obtains

$$A = \frac{R^2 V_m}{8D_m} \frac{\partial C}{\partial x_1} \tag{15}$$

The rate of transfer of C across the section at x_1 is

$$Q = 2\pi R^2 \int_0^1 V_m \left(\frac{1}{2} - \rho^2\right) C \rho \, d\rho \tag{16}$$

Thus, on substituting for C from Equation (14), and integrating gives

$$Q = - \frac{\pi R^4 V_m^2}{192 D_m} \frac{\partial C_{x_1}}{\partial x_1} \tag{17}$$

Now C_{x_1} is replaced by C_m, the mean concentration, since radial variation of C is assumed to be small. Thus, on comparison with Fick's law of diffusion, the expression obtained for the diffusion coefficient is

$$K = \frac{R^2 V_m^2}{192 D_m} \tag{18}$$

Hence,

$$\frac{\partial Q}{\partial x_1} = - \pi R^2 \frac{\partial C_m}{\partial t}$$

or

$$K \frac{\partial^2 C_m}{\partial x_1^2} = \frac{\partial C_m}{\partial t} \tag{19}$$

because there is no loss or gain of matter.

The solution to Equation (19) for an infinitely long tube with introduction of a unit impulse input or a Dirac delta function input at time equal to zero is

$$C_m \pi R^2 = \frac{1}{(4\pi Kt)^{\frac{1}{2}}} \exp\left\{ -\left[x - 1/2\ (V_m t)\right]^2 / 4Kt \right\} \qquad (20)$$

In a later paper (9) Taylor gave further consideration to the assumption that axially directed molecular diffusion is negligible compared with axial transport by convection. This assumption is inherent in Equation (6) and thus limits the applicability of Equations (18) and (20). He showed that his previous derivation of Equation (18) is valid when D_m is sufficiently small compared with K.

Aris (26) removed this restriction by showing Equation (20) to be valid when it satisfies the criterion of Equation (11) and if the effective diffusion coefficient is defined as the sum of K (as given by Equation (19) and the molecular diffusivity, D_m. Blockwell (27) in his study of liquid dispersion in long capillary tubes obtained effective dispersion coefficients, which showed an agreement with the work by Aris (26).

Taylor in his later paper (8) extended the method of analysis of laminar flow in round empty tubes to turbulent flow through open tubes. Several investigators (5, 28, 29, 30, 31) later used this model to study dispersion in packed units.

When both diffusion and convection are equally important in effecting dispersion, Equations (1) through (20) should be modified. Solutions of Equation (6) by numerical and analytical

have been presented in the literature (32, 33). For the analytical solution, Farrel and Leonard (33) started with Equation (6) and obtained the Laplace transformation of the residence time distribution function resulting from a unit impulse input $\bar{C}(s, \tau_1)$.

$$\bar{C}(s,\tau_1) = \sum_{m=1}^{\infty} A_m \left[\exp(-\alpha_m^2 \eta_1) \frac{\int_0^1 (1-\rho^2)\rho F_m(\lambda,\rho)d\rho}{\int_0^1 (1-\rho^2)\rho\, d\,\rho} \right] \quad (21)$$

where

$\lambda = \frac{sR^2}{4D_m}$ = Dimensionless Laplace parameter

$\eta = \frac{4xD_m}{V_m R^2}$ = Dimensionless axial coordinate, or dispersion parameter

$\rho = \frac{r}{R}$ = Dimensionless radial coordinate

α_m = m-th eigen value

A_m = m-th eigen constant

$F_m(\lambda, \rho)$ = m-th eigen function

They compared the transformed residence time distribution function for the two-dimensional case with the limiting one-dimensional models for a definite range of operating conditions. Second and third central moments of the one and two-dimensional models were also compared. The two-dimensional solution was shown to predict a more skewed distribution than the one-

dimensional models of equal mean and variance.

Nichols and Lamb (34) gave the general solution of first-order chemical reaction in laminar tubular flow with axial and radial diffusion considered. They solved the general equation shown in Equation (22) by using a formal series expansion of the dependent variable with a Bessel function representation of the radial eigen functions.

$$\frac{D_R}{r}\frac{\partial}{\partial r}\left(r\frac{\partial C}{\partial r}\right) + D_L\frac{\partial^2 C}{\partial x^2} = V_x(r)\frac{\partial C}{\partial x} + kC \qquad (22)$$

They also summarized a number of special cases of the general equation, which were treated.

In turbulent flow, the diffusivity tensor D, in Equation (2.20) is no longer the representation of molecular diffusivity as in Equation (6). It should be taken as the sum of the "molecular diffusivity," D_m and "eddy diffusivity," ϵ_D, that is, $D = D_m + \epsilon_D$ (35).

D_m can be given by the same expressions as for purely laminar flow. The difficulty here is that only semiempirical expressions are available for ϵ_D. Values of ϵ_D are always non-isotropic, but it is sufficiently accurate for many applications to use the mean value of ϵ_D. Not only is it difficult to solve for turbulent flow, but also very difficult or even impossible to solve the laminar flow case if the geometry of the physical system becomes complicated. It is, therefore, convenient to treat fluid mixing in turbulent flow from semi-empirical modeling techniques. Furthermore, it is essential to confirm results from

such a treatment experimentally.

Taylor (8) also studied axial mixing in turbulent flow regions. For fully developed turbulent flow region Taylor used the Reynolds analogy to determine dispersion coefficients in terms of Fanning friction factor f as

$$\frac{D_L}{\bar{V}_x \, d_t} = 3.57 \sqrt{f} \qquad (23)$$

where D_L is the axial dispersion coefficient, $\bar{V}_x$ is the average velocity, and d_t the inside diameter of the tube; f is the Fanning friction factor and is related to the Reynolds number. Tichacek, Barkelew, and Baron (10) repeated Taylor's analysis by using actually measured average velocity profiles and accounting for the eddy diffusivity ϵ_D as well as molecular diffusivity D_m. According to their analysis, $D_L/\bar{V}_x \, d_t$ is dependent on the Reynolds number, pipe roughness (or friction factor) and Schmidt number. For high values of f, the Schmidt number affected the values of $D_L/\bar{V}_x \, d_t$. They reported that their theoretical data are applicable with less than 25% error as shown by comparison with Taylor's experimental data. Vanderveen (36) determined the value of D_L for Reynolds numbers between 4×10^3 and 10^4. He found experimentally that values of $D_L/\bar{V}_x \, d_t$ showed significant deviations from Taylor's theory in the range studied. The results fall between Taylor's model and the results of Tichacek et al. (10). Vanderveen (36) reported that the data obtained were believed to be reliable to within 10% throughout the range of Reynolds numbers studied, but did not agree with Tichacek's results.

IV. CONVECTIVE MODELS

The importance of the study of the characteristics of non-Newtonian fluid dispersion in continuous flow systems and the usefulness of models to represent real flow systems have been mentioned in the previous chapters. Starting from this chapter, the analysis of residence time distributions for some flow models will be discussed. First of all, convective models will be treated extensively in this chapter for fluids which can be represented by the Bingham plastic and Ostwald-de Waele models. The convective model is such a model that both radial and longitudinal dispersion terms in Equation (2.26) are negligible and only the effect of the velocity profile of the fluid becomes the major influence on the fluid dispersion. Steady and iso-thermal flow situations and ducts of constant geometrical configurations are to be assumed. Models for which both diffusion and convective terms cannot be neglected will be discussed in the next chapter.

FLOW THROUGH CYLINDRICAL TUBES

1. Bingham Plastic

As previously described, a substance that has the following general rheological statement between shear stress tensor, $\overline{\overline{\tau}}$, and rate of deformation tensor, $\overline{\overline{\Delta}}$, is called the Bingham plastic (6):

$$\vec{\vec{\tau}} = -\left\{\mu_o - \frac{\tau_o}{\sqrt{\frac{1}{2}\left(\vec{\vec{\Delta}} : \vec{\vec{\Delta}}\right)}}\right\}\vec{\vec{\Delta}} \quad \text{for} \quad \frac{1}{2}\left(\vec{\vec{\tau}} : \vec{\vec{\tau}}\right) > \tau_o^2 \tag{1}$$

$$\vec{\vec{\Delta}} = 0 \quad \text{for} \quad \frac{1}{2}\left(\vec{\vec{\tau}} : \vec{\vec{\tau}}\right) < \tau_o^2 \tag{2}$$

where μ_o and τ_o are rheological constants.

In any situation, Equations (1) and (2) are to be combined with the equation of continuity

$$(\nabla \cdot \vec{v}) = 0 \tag{3}$$

and the equation of motion

$$\rho \frac{D\vec{v}}{Dt} = -\nabla P - \left[\nabla \cdot \tau\right] \tag{4}$$

and solved subject to certain boundary conditions (37).

For flow through a cylindrical tube with length L and radius R, for which a one-dimensional rheological statement (37) in cylindrical coordinates is valid (See Figure 7), Equations (1) and (2) reduce to (Appendix 3) (6)

$$\tau_{rx} = \tau_o - \mu_o \frac{dV_x}{dr} \quad \text{for} \quad \tau_{rx} > \tau_o \tag{5}$$

$$\frac{dV_x}{dr} = 0 \quad \text{for} \quad \tau_{rx} < \tau_o \tag{6}$$

and the equation of motion at steady state reduces to

$$\frac{1}{r}\frac{\partial}{\partial r}\left(r\,\tau_{rx}\right) = -\frac{\partial P}{\partial x} \tag{7}$$

Since the right-hand side of Equation (7) is not a function of

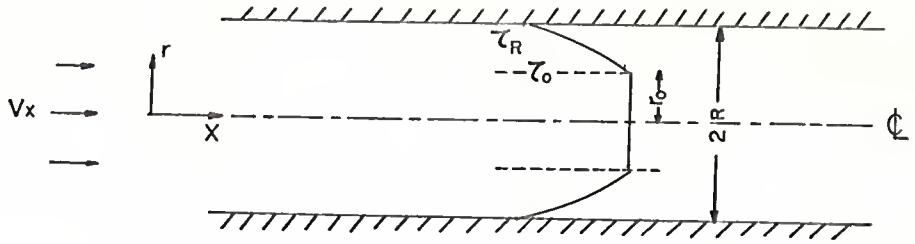

Fig. 7. Velocity profile of the Bingham plastic fluid in a cylindrical tube (3).

r, it can be integrated to give

$$\tau_{rx} = \left(-\frac{\partial P}{\partial x}\right)\frac{r}{2} + \frac{C_1}{r} \tag{8}$$

where C_1 is the constant of integration. Because, at r = 0, the momentum flux is never infinite, the constant C_1 must be zero. Equation (8) thus becomes

$$\tau_{rx} = \left(-\frac{\partial P}{\partial x}\right)\frac{r}{2} \tag{9}$$

Combining Equations (5) and (9) and applying the boundary condition $V_x = 0$ at r = R, one can obtain the following velocity profile of the Bingham plastic fluid flowing through a pipe (Appendix 4) (38).

$$V_m = \frac{(-\Delta P)R^2}{4\mu_o L}(1 - \xi)^2 \quad \text{for } r \leq r_o \tag{10}$$

$$V_x(r) = V_m\left[1 - \frac{\left(\frac{r}{R} - \xi\right)^2}{(1 - \xi)^2}\right] \text{for } r \geq r_o \tag{11}$$

where

$$\xi = \frac{r_o}{R} = \frac{\tau_o}{\tau_R}$$

and

ΔP = the pressure drop over L

The mean velocity of the fluid is obtained by summing all the velocities over a cross-section and then dividing by the cross-sectional area (Appendix 5) (6)

$$\bar{V}_x = \frac{(-\Delta P)R^2}{8\mu_o L}\left(1 - \frac{4}{3}\xi + \frac{1}{3}\xi^4\right) \tag{12}$$

or

$$\bar{V}_x = \frac{V_m}{2}\left[\frac{1 - \frac{4}{3}\xi + \frac{1}{3}\xi^4}{(1-\xi)^2}\right] \tag{13}$$

Let $\alpha = \dfrac{1 - \frac{4}{3}\xi + \frac{1}{3}\xi^4}{(1-\xi)^2}$, Equation (13) becomes

$$\bar{V}_x = \frac{V_m}{2}\,\alpha \tag{14}$$

The residence time distribution functions of the Bingham plastic fluid flowing through a round pipe for an iso-thermal situation will be developed here. If one assumes that the fluid is everywhere in unaccelerated laminar flow, and both entrance effects and molecular diffusion are negligible, the response to a step function input of a tracer can be obtained through the following manipulations. The F-curve, as it was defined in Chapter II of this thesis, can be expressed mathematically as follows (11, 12, 25):

$$\underline{F}(\theta) = \frac{\int_o^r V_x(r) \cdot 2\pi r\, dr}{\int_0^R \bar{V}_x \cdot 2\pi r\, dr} = \frac{2\int_o^r V_x(r) r\, dr}{\bar{V}_x R^2} \tag{15}$$

As shown in Figure 7, the Bingham plastic is a fluid which,

theoretically, has a plug flow portion with radius r_o through the center of the pipe. Therefore Equation (15) can be rewritten as (39)

$$\underline{F}(\theta) = \underline{F_1}(\theta) + \underline{F_2}(\theta) \tag{16}$$

where

$$\underline{F_1}(\theta) = \frac{2}{\bar{V}_x R^2} \int_0^{r_o} V_m r dr \tag{17}$$

and

$$\underline{F_2}(\theta) = \frac{2}{\bar{V}_x R^2} \int_{r_o}^{r} V_m \left[1 - \frac{\left(\frac{r}{R} - \xi\right)^2}{(1 - \xi)^2}\right] r dr \tag{18}$$

Introducing a unit step function $U_s(\theta - \frac{\alpha}{2})$, which has the properties

$$U_s(\theta - \tfrac{\alpha}{2}) = \begin{cases} 0 & \text{for } \theta < \frac{\alpha}{2} \\ 1 & \text{for } \theta > \frac{\alpha}{2} \end{cases} \tag{19}$$

into Equation (17) and combining the result with Equation (14), we have

$$\underline{F_1}(\theta) = \frac{2\xi^2}{\alpha} \cdot U_s\left(\theta - \tfrac{\alpha}{2}\right) \tag{20}$$

where θ is a dimensionless time defined as a ratio of reaction time to holding time or mean residence time. The response to a Dirac delta function input is obtained by taking the derivative of $\underline{F}(\theta)$ with respect to θ as shown in Equation (2.19) and is

given by

$$\underline{E}_1(\theta) = \frac{d\underline{F}_1(\theta)}{d\theta} = \frac{2\xi^2}{\alpha} \cdot \delta\left(\theta - \frac{\alpha}{2}\right) \tag{21}$$

where $\delta(\theta - \frac{\alpha}{2})$ is a Dirac delta (Appendix 2) function and is defined as

$$\delta\left(\theta - \frac{\alpha}{2}\right) = \begin{cases} 0 & \text{for } \theta \neq \frac{\alpha}{2} \\ 1 & \text{for } \theta = \frac{\alpha}{2} \end{cases} \tag{22}$$

By knowing that

$$\frac{V_x(r)}{V_m} = \frac{\alpha V_x(r)}{2\bar{V}_x} = \frac{\alpha}{2\theta} \tag{23}$$

Equation (18) can be simplified to (Appendix 6)

$$\underline{F}_2(\theta) = \int_{\frac{\alpha}{2}}^{\theta} \frac{(1-\xi)\alpha}{2\theta^3} \left(\frac{\xi}{\sqrt{1 - \frac{\alpha}{2\theta}}} + 1 - \xi\right) d\theta \tag{24}$$

$$\cong (1-\xi)\alpha \left[\frac{1-\xi}{\alpha^2} + \frac{\sqrt{2}\xi}{3} \cdot \frac{2\theta-\alpha}{\theta^{3/2}} - \frac{1-\xi}{4\theta^2}\right]$$

The residence time distribution function is, then (39)

$$\underline{E}_2(\theta) = \frac{(1-\xi)\alpha}{2\theta^3} \left(\frac{\xi}{\sqrt{1 - \frac{\alpha}{2\theta}}} + 1 - \xi\right) \tag{25}$$

Therefore, Equation (16) becomes

$$\underline{F}(\theta) = \frac{2\xi^2}{\alpha} \cdot U_s(\theta - \frac{\alpha}{2}) + \int_{\frac{\alpha}{2}}^{\theta} \frac{(1-\xi)\alpha}{2\theta^3} \left(\frac{\xi}{\sqrt{1 - \frac{\alpha}{2\theta}}} + 1 - \xi\right) d\theta \quad \text{for } \theta > \frac{\alpha}{2}$$

$$= 0 \quad \text{for } \theta < \frac{\alpha}{2} \qquad (26)$$

The residence time distribution function for the Bingham plastic fluid flowing through a pipe is then

$$\underline{E}(\theta) = \frac{2\xi^2}{\alpha} \cdot \delta(\theta - \frac{\alpha}{2}) + \frac{(1-\xi)\alpha}{2\theta^3} \left(\frac{\xi}{\sqrt{1 - \frac{\alpha}{2\theta}}} + 1 - \xi\right) \quad \text{for } \theta > \frac{\alpha}{2}$$

$$= 0 \quad \text{for } \theta < \frac{\alpha}{2} \qquad (27)$$

For the special case when $\xi = 0$ and $\alpha = 1$, Equations (26) and (27) reduce to the Newtonian case represented by Equations (3.3) and (3.4).

2. Ostwald-de Waele Model

In the case for which a one-dimensional rheological statement is valid, Equation (2.37) written in a cylindrical coordinate reduces to

$$\tau_{rx} = - m \left| \frac{dV_x}{dr} \right|^{\nu-1} \left(\frac{dV_x}{dr}\right) \qquad (28)$$

where m and ν are rheological parameters.

Solving the governing differential equation subject to

appropriate boundary conditions, one obtains (Appendix 7) (6)

$$\tau_{rx} = m(-\frac{dV_x}{dr})^{\nu} = (-\frac{\partial P}{\partial x})\frac{r}{2} \tag{29}$$

With the boundary condition $V_x = 0$ at $r = R$, Equation (29) is solved to be (3)

$$V_x(r) = (\frac{-\Delta P}{2mL})^{n} \frac{R^{n+1}}{n+1}\left[1 - (\frac{r}{R})^{n+1}\right] \tag{30}$$

where $n = \frac{1}{\nu}$ and ΔP is the pressure drop over L. The maximum velocity occurs at $r = 0$, and thus has the value (3)

$$V_m = (\frac{-\Delta P}{2mL})^{n} \frac{R^{n+1}}{n+1} \tag{31}$$

Combining Equations (30) and (31) yields (3, 21)

$$V_x(r) = V_m\left[1 - (\frac{r}{R})^{n+1}\right] \tag{32}$$

Figure 8 shows the velocity profiles based on Equations (32). For $n = 0$, the fluid is a highly non-Newtonian dilatant, while the fluid becomes so called "plug flow" when $n \to \infty$. For Newtonian fluids $n = 1$. Hence, Equation (32) represents general velocity profiles for various values of n.

The average velocity, $\bar{V}_x$, is calculated by

$$\bar{V}_x = \frac{\int_0^{2\pi}\int_0^{R} V_x(r)\,r\,dr\,d\theta}{\int_0^{2\pi}\int_0^{R} r\,dr\,d\theta} = (\frac{-\Delta P}{2mL})(\frac{R^{n+1}}{n+1})(\frac{n+1}{n+3})$$

or

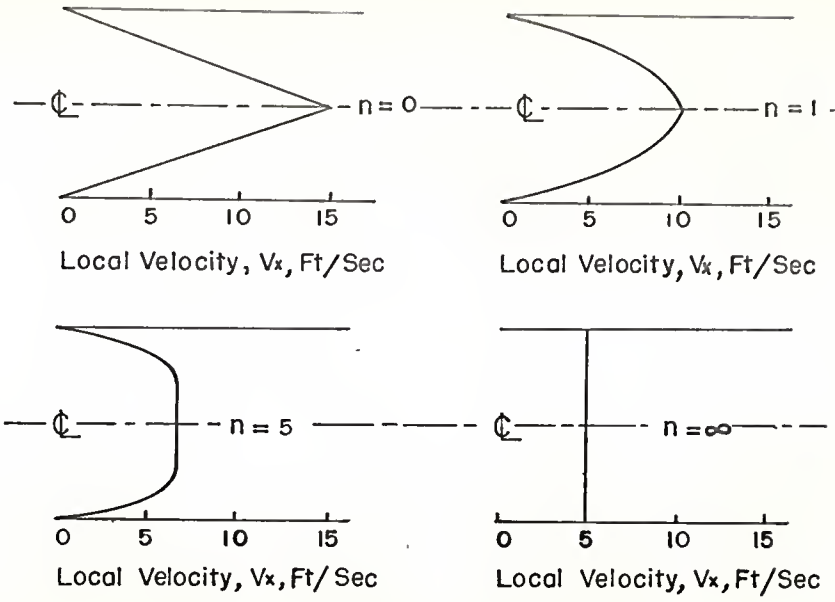

Fig.8. Dependence of velocity profiles upon flow-behavior index (21).

$$\bar{V}_x = \left(\frac{n+1}{n+3}\right)V_m$$

The residence time distribution functions of the Ostwald-de Waele fluid flowing through a pipe will be developed for the two different cases with and without entrance effect consideration. When the entrance effect is considered, the F-function is (25)

$$\underline{F}(\theta) = \frac{2}{R^2} \int_0^r r\, dr \tag{34}$$

Furthermore, Equations (32) and (33) show that

$$\frac{r}{R} = \left[1 - \frac{V_x(r)}{V_m}\right]^{\frac{1}{n+1}}$$

$$= \left[1 - \frac{1}{\left(\frac{n+3}{n+1}\right)\theta}\right]^{\frac{1}{n+1}} \tag{35}$$

Hence the F-curve can be obtained by substituting Equation (35) into Equation (34) as (39)

$$\left.\begin{aligned} \underline{F}(\theta) &= \int_{\frac{n+1}{n+3}}^{\theta} \frac{2}{n+3} \frac{1}{\theta^2\left[1 - \frac{1}{\left(\frac{n+3}{n+1}\right)\theta}\right]^{\frac{n-1}{n+1}}} d\theta \\ &\qquad \text{for} \quad \theta > \frac{n+1}{n+3} \\ &= 0 \qquad \text{for} \quad \theta < \frac{n+1}{n+3} \end{aligned}\right\} \tag{36}$$

The E-curve (39), residence time distribution function, is obtained by simply differentiating Equation (36) with respect to θ

$$\left.\begin{aligned} \underline{E}(\theta) &= \frac{2}{n+3} \frac{1}{\theta^2\left[1 - \frac{1}{(\frac{n+3}{n+1})\theta}\right]^{\frac{n-1}{n+1}}} \quad \text{for } \theta > \frac{n+1}{n+3} \\ &= 0 \qquad\qquad\qquad\qquad \text{for } \theta < \frac{n+1}{n+3} \end{aligned}\right\} \quad (37)$$

When the entrance effect is not considered the F-function is (11, 12, 25)

$$\underline{F}(\theta) = \frac{2}{R^2 \underline{V}_x} \int_0^r V_x(r) r \, dr$$

Therefore, the F-curve is

$$\left.\begin{aligned} \underline{F}(\theta) &= \int_{\frac{n+1}{n+3}}^{\theta} \frac{2}{n+3} \frac{1}{\theta^3\left[1 - \frac{1}{(\frac{n+3}{n+1})\theta}\right]^{\frac{n-1}{n+1}}} d\theta \quad \text{for } \theta > \frac{n+1}{n+3} \\ &= 0 \qquad\qquad\qquad\qquad\qquad\qquad\qquad\qquad \text{for } \theta < \frac{n+1}{n+3} \end{aligned}\right\} \quad (38)$$

The E-curve is then

$$\left.\begin{aligned} \underline{E}(\theta) &= \frac{2}{n+3} \frac{1}{\theta^3\left[1 - \frac{1}{(\frac{n+3}{n+1})\theta}\right]^{\frac{n-1}{n+1}}} \quad \text{for } \theta > \frac{n+1}{n+3} \\ &= 0 \qquad\qquad\qquad\qquad\qquad\qquad\qquad\qquad \text{for } \theta < \frac{n+1}{n+3} \end{aligned}\right\} \quad (39)$$

For the special case when n = 1 Equations (36), (37), (38), and (39) reduce to the Newtonian case, as shown by Equations (3.1), (3.2), (3.3), and (3.4).

FLOW THROUGH A SLIT BETWEEN PARALLEL PLATES

1. Bingham Plastic

An analysis of the Bingham plastic fluid flowing through a two-dimensional thin slit between parallel plates at steady state is presented in this section. The coordinate axes are chosen as shown in Figure 9. For a one-dimensional rheological statement, Equations (2.35) and (2.36) reduce to

$$\tau_{yx} = \tau_o - \mu_o \frac{dV_x}{dy} \qquad \text{for } \tau_{yx} > \tau_o \tag{40}$$

$$\frac{dV_x}{dy} = 0 \qquad \text{for } \tau_{yx} < \tau_o \tag{41}$$

The velocity profile can be obtained by combining the above equations with the equation of motion and solving the resulting equation subject to appropriate boundary conditions, which state that momentum flux is finite at the center of a slit and velocity is zero at the wall. The velocity profile, thus obtained is (Appendix 8)

$$V_m = \frac{(-\Delta P)H^2}{2\mu_o L}(1 - \zeta)^2 \qquad \text{for } y \leq y_o \tag{42}$$

$$V_x(y) = V_m \left[1 - \frac{(\frac{y}{H} - \zeta)^2}{(1 - \zeta)^2}\right] \qquad \text{for } y \geq y_o \tag{43}$$

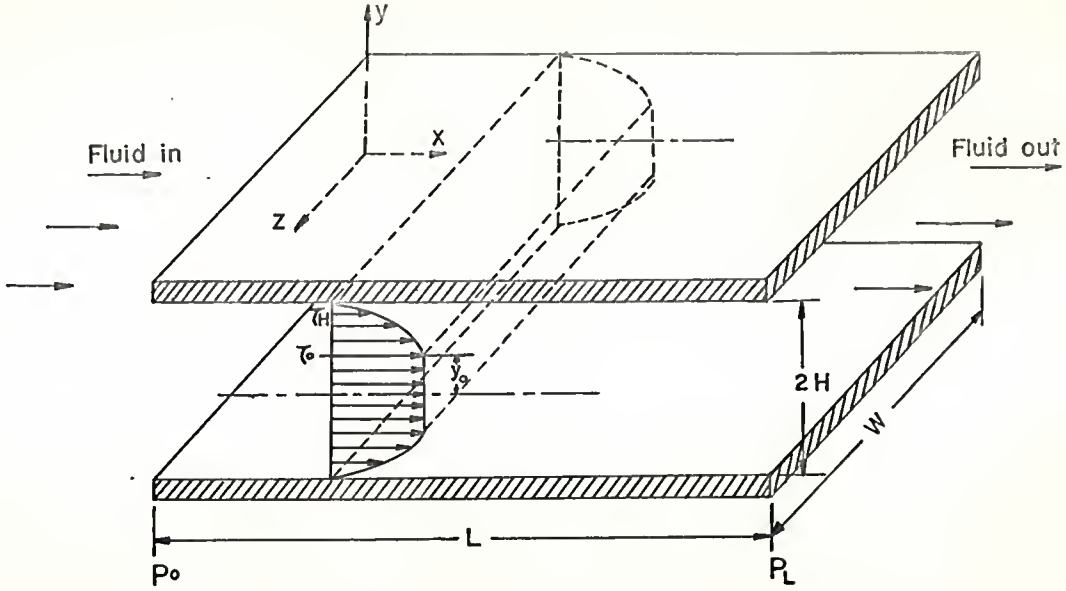

Fig. 9. Velocity profile of the Bingham plastic fluid in a slit.

where

$$\zeta = \frac{y_o}{H} = \frac{\tau_o}{\tau H}$$

ΔP = the pressure drop over L

The mean velocity of the fluid is (Appendix 9):

$$\bar{V}_x = \frac{(-\Delta P)H^2}{3\mu_o L}\left(1 - \frac{3}{2}\zeta + \frac{1}{2}\zeta^2\right) \tag{44}$$

When $\zeta = 0$, Equations (43) and (44) reduce to Newtonian case (6). Dividing Equation (44) by Equation (42) yields

$$\bar{V}_x = \frac{2}{3} V_m \beta \tag{45}$$

where

$$\beta = \frac{1 - \frac{3}{2}\zeta + \frac{1}{2}\zeta^2}{(1 - \zeta)^2} \tag{46}$$

When the entrance effect is negligible, a response to a unit step function input is

$$\underline{F}(\theta) = \frac{1}{2HW\bar{V}_x} \int_o^W \int_o^y 2 V_x(y)\, dy\, dz$$

$$= \frac{1}{H\bar{V}_x} \int_o^y V_x(y)\, dy$$

$$= \underline{F}_1(\theta) + \underline{F}_2(\theta) \tag{47}$$

where

$$\underline{F}_1(\theta) = \frac{1}{H\bar{V}_x} \int_o^{y_o} V_m\, dy \tag{48}$$

and

$$\underline{F}_2(\theta) = \frac{1}{H\,\overline{V}_x} \int_{yo}^{y} V_m \left[1 - \frac{\left(\frac{y}{H} - \zeta\right)^2}{(1-\zeta)^2}\right] d\,y \tag{49}$$

Solutions to Equations (48) and (49) are

$$\underline{F}_1(\theta) = \frac{3\zeta}{2\beta} \cdot U_s \left(\theta - \frac{2}{3}\beta\right) \tag{50}$$

and

$$\underline{F}_2(\theta) = \int_{\frac{2}{3}\beta}^{\theta} \frac{(1-\zeta)\beta}{3\theta^3} \frac{d\,\theta}{\sqrt{1 - \frac{2\beta}{3\theta}}} \tag{51}$$

Detailed derivation of Equation (51) is given in Appendix 10.

The $\underline{F}$-function and $\underline{E}$-function are, therefore,

$$\left.\begin{aligned} \underline{F}(\theta) &= \frac{3\zeta}{2\beta} \cdot U_s\left(\theta - \frac{2}{3}\beta\right) + \int_{\frac{2}{3}}^{\theta} \frac{(1-\zeta)\beta}{3\theta^3} \frac{d\theta}{\sqrt{1 - \frac{2\beta}{3\theta}}} \\ &\qquad \text{for } \theta > \frac{2}{3}\beta \\ &= 0 \qquad \text{for } \theta < \frac{2}{3}\beta \end{aligned}\right\} \tag{52}$$

and

$$\left.\begin{aligned} \underline{E}(\theta) &= \frac{3\zeta}{2\beta}\cdot\delta \left(\theta - \frac{2}{3}\beta\right) + \frac{(1-\zeta)\beta}{3\theta^3} \frac{1}{\sqrt{1 - \frac{2\beta}{3\theta}}} \\ &\qquad \text{for } \theta > \frac{2}{3}\beta \\ &= 0 \qquad \text{for } \theta < \frac{2}{3}\beta \end{aligned}\right\} \tag{53}$$

For the case $\zeta = 0$ and $\beta = 1$, Equations (52) and (53) reduce to those for the Newtonian flow, that is,

$$\left.\begin{aligned} \underline{F}(\theta) &= \int_{\frac{2}{3}}^{\theta} \frac{1}{3\theta^3} \frac{d\theta}{\sqrt{1 - \frac{2}{3\theta}}} && \text{for } \theta > \tfrac{2}{3} \\ &= 0 && \text{for } \theta < \tfrac{2}{3} \end{aligned}\right\} \quad (54)$$

and

$$\left.\begin{aligned} \underline{E}(\theta) &= \frac{1}{3\theta^3\sqrt{1 - \frac{2}{3\theta}}} && \text{for } \theta > \tfrac{2}{3} \\ &= 0 && \text{for } \theta < \tfrac{2}{3} \end{aligned}\right\} \quad (55)$$

2. Ostwald-de Waele Model

Referring to Figure 10, the velocity profile of the Ostwald-de Waele fluid flowing through a two-dimensional thin slit at steady-state can be obtained by solving the equation of motion in conjunction with Equation (28) with appropriate boundary conditions. The result is (3)

$$V_x(y) = \left(\frac{-\Delta P}{mL}\right)^n \frac{H^{n+1}}{n+1} \left[1 - \left(\frac{y}{H}\right)^{n+1}\right] \quad (56)$$

where $n = \frac{1}{\nu}$ and Δp is the pressure drop over L. The maximum velocity occurs at $y = 0$. Its value is given by (3)

$$V_m = \left(\frac{-\Delta P}{mL}\right)^n \frac{H^{n+1}}{n+1} \quad (57)$$

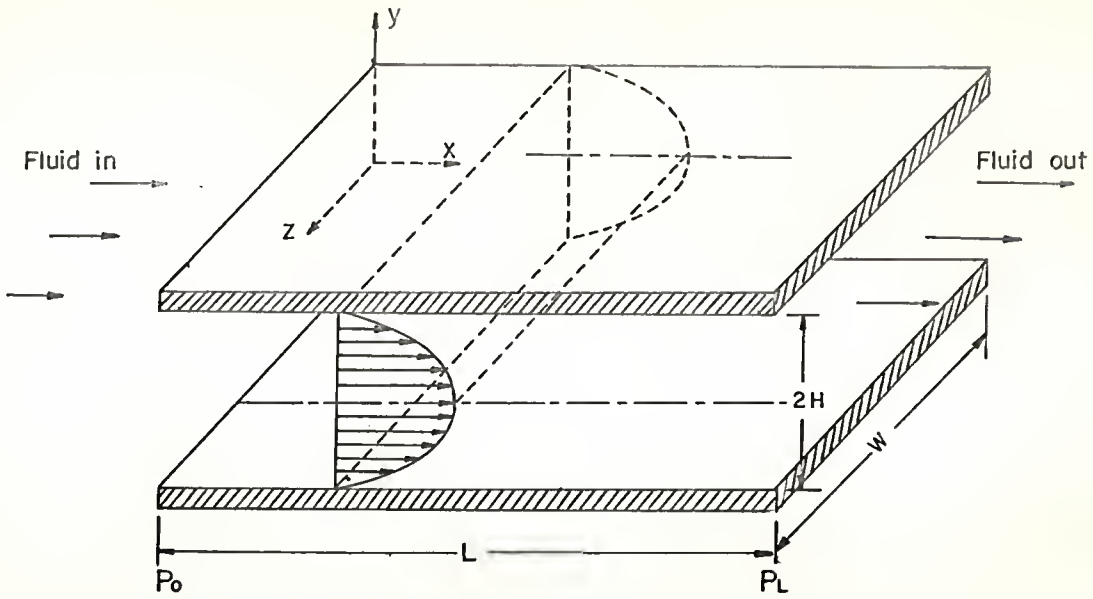

Fig. 10. Velocity profile of the Ostwald-de Waele model fluid in a slit.

Combination of Equations (56) and (57) gives

$$V_x(y) = V_m \left[1 - \left(\frac{y}{H}\right)^{n+1}\right] \tag{58}$$

The average velocity, $\bar{V}_x$, is

$$\bar{V}_x = \frac{1}{WH} \int_0^W \int_0^H V_x(y)\, dy\, dz = \left(\frac{-\Delta P}{mL}\right)^n \frac{H^{n+1}}{n+2} \tag{59}$$

The ratio of maximum to average velocity is then represented by the following relationship:

$$\bar{V}_x = \frac{n+1}{n+2} V_m \tag{60}$$

When the entrance effect cannot be neglected (a short channel) the $\underline{F}$-function is given by

$$\underline{F}(\theta) = \frac{1}{WH} \int_0^W \int_0^y dy\, dz \tag{61}$$

Substituting Equations (58) and (60) into Equation (61) and simplifying the integrand, we have

$$\left.\begin{aligned} \underline{F}(\theta) &= \int_{\frac{n+1}{n+2}}^{\theta} \frac{1}{n+2} \frac{d\theta}{\theta^2 \left[1 - \frac{1}{(\frac{n+2}{n+1})\theta}\right]^{\frac{n}{n+1}}} \\ &\qquad \text{for } \theta > \frac{n+1}{n+2} \\ &= 0 \qquad \text{for } \theta < \frac{n+1}{n+2} \end{aligned}\right\} \tag{62}$$

The response to a Dirac delta function input, the $\underline{E}$-function is

$$\underline{E}(\theta) = \frac{1}{n+2} \frac{1}{\theta^2 \left[1 - \frac{1}{(\frac{n+2}{n+1})\theta}\right]^{\frac{n}{n+1}}} \quad \text{for } \theta > \frac{n+1}{n+2}$$

$$= 0 \quad \text{for } \theta < \frac{n+1}{n+2} \qquad (63)$$

When n = 1 Equations (62) and (63) reduce to those for the Newtonian flow.

When the entrance effect can be neglected (a long channel), the response to a unit step input is

$$\underline{F}(\theta) = \frac{1}{H\bar{V}_x} \int_o^y V_x(y)dy = \int_{\frac{n+1}{n+3}}^{\theta} \frac{1}{n+2} \frac{d\theta}{\theta^3 \left[1 - \frac{1}{(\frac{n+2}{n+1})\theta}\right]^{\frac{n}{n+1}}} \quad \text{for } \theta > \frac{n+1}{n+2}$$

$$= 0 \quad \text{for } \theta < \frac{n+1}{n+2} \qquad (64)$$

and the response to a Dirac Delta function input, i.e., the $\underline{E}$-function is obtained as

$$\underline{E}(\theta) = \frac{1}{n+2} \frac{1}{\theta^3 \left[1 - \frac{1}{(\frac{n+2}{n+1})\theta}\right]^{\frac{n}{n+1}}} \quad \text{for } \theta > \frac{n+1}{n+2}$$

$$= 0 \quad \text{for } \theta < \frac{n+1}{n+2} \qquad (65)$$

Equations (54) and (55) can be obtained by setting n = 1 in Equations (64) and (65).

FLOW OF THE OSTWALD-DE WAELE FLUID WITH SLIP VELOCITY AT THE TUBE WALL

Velocity profile of this model obtained by applying boundary conditions of $V_x = V_R$ at r = R in Equation (29) gives

$$V_x(r) = V_R + V_m \left[1 - \left(\frac{r}{R}\right)^{n+1}\right] \tag{66}$$

The velocity is maximum at r = 0. It is

$$V'_m = V_R + V_m$$

Thus

$$V_m = V'_m - V_R \tag{67}$$

Therefore, Equation (66) can be rewritten as

$$V_x(r) = V_R + (V'_m - V_R) \left[1 - \left(\frac{r}{R}\right)^{n+1}\right] \tag{68}$$

The average velocity, $\bar{V}_x$, is calculated in the same way as shown by using Equation (33) as

$$\bar{V}_x = \frac{(n+1)\, V'_m + 2V_R}{n + 3} \tag{69}$$

The minimum residence time will be defined as

$$\theta_{min} = \frac{\bar{V}_x}{V'_m} = \frac{n+1}{(n+3) - 2\gamma} \tag{70}$$

Where γ is a slip velocity factor and is defined by $\gamma = \frac{V_R}{V_x}$, when there is no slip velocity at the wall, γ becomes zero. When the entrance effect cannot be neglected, from Equation (68), we have

$$\frac{r}{R} = \left[1 - \frac{(n+1)(\frac{1}{\theta} - \gamma)}{(n+3)(1 - \gamma)}\right]^{\frac{1}{n+1}} \tag{71}$$

Differentiating Equation (71) with respect to θ yields

$$d(\frac{r}{R}) = \frac{1}{(n+3)(1-\gamma)} \frac{d\theta}{\theta^2\left[1 - \frac{(n+1)(\frac{1}{\theta} - \gamma)}{(n+3)(1-\gamma)}\right]^{\frac{n}{n+1}}}$$

In response to a unit step function input, one has

$$\left.\begin{aligned} \underline{F}(\theta) &= \int_{\frac{n+1}{(n+3)-2\gamma}}^{\theta} \frac{2}{(n+3)(1-\gamma)} \frac{d\theta}{\theta^2\left[1 - \frac{(n+1)(\frac{1}{\theta} - \gamma)}{(n+3)(1-\gamma)}\right]^{\frac{n-1}{n+1}}} \\ &\qquad \text{for } \frac{n+1}{(n+3) - 2\gamma} < \theta < \frac{1}{\gamma} \\ &= 0 \qquad \text{for } \theta < \frac{n+1}{(n+3) - 2\gamma} \\ &= 1 \qquad \text{for } \frac{1}{\gamma} < \theta \end{aligned}\right\} \tag{72}$$

The response to a Dirac delta function input the $\underline{E}$-function is

$$\underline{E}(\theta) = \frac{2}{(n+3)(1-\gamma)} \quad \frac{1}{\theta^2\left[1 - \frac{(n+1)(\frac{1}{\theta} - \gamma)}{(n+3)(1-\gamma)}\right]^{\frac{n-1}{n+1}}} \qquad \text{for } \frac{n+1}{(n+3) - 2\gamma} < \theta < \frac{1}{\gamma}$$

$$= 0 \qquad \text{for } \theta < \frac{n+1}{(n+3) - 2\gamma} \text{ and } \frac{1}{\gamma} < \theta \qquad (73)$$

When the entrance effect is neglected, the corresponding $\underline{F}$-function is

$$\underline{F}(\theta) = \int_{\frac{n+1}{(n+3)-2\gamma}}^{\theta} \frac{2}{(n+3)(1-\gamma)} \quad \frac{d\theta}{\theta^3\left[1 - \frac{(n+1)(\frac{1}{\theta} - \gamma)}{(n+3)(1-\gamma)}\right]^{\frac{n-1}{n+1}}} \qquad \text{for } \frac{n+1}{(n+3)-2\gamma} < \theta < \frac{1}{\gamma}$$

$$= 0 \qquad \text{for } \theta < \frac{n+1}{(n+3)-2\gamma}$$

$$= 1 \qquad \text{for } \frac{1}{\gamma} < \theta \qquad (74)$$

and the corresponding $\underline{E}$-curve is then

$$\underline{E}(\theta) = \frac{2}{(n+3)(1-\gamma)} \quad \frac{1}{\theta^3\left[1 - \frac{(n+1)(\frac{1}{\theta} - \gamma)}{(n+3)(1-\gamma)}\right]^{\frac{n-1}{n+1}}} \qquad \text{for} \quad \frac{n+1}{(n+3) - 2\gamma} < \theta < \frac{1}{\gamma}$$

$$= 0 \qquad \text{for} \quad \theta < \frac{n+1}{(n+3)-2\gamma} \text{ and } \frac{1}{\gamma} < \theta \qquad (75)$$

When there is no slip velocity at the wall of the tube, that is, when $\gamma = 0$, Equations (72), (73), (74), and (75) reduce to Equations (36), (37), (38), and (39). When $\gamma = 0$ and $n = 1$, the above equations reduce to those for the Newtonian flow, i.e., Equations (3.1), (3.2), (3.3), and (3.4).

Equations (72), (73), (74), and (75) have been numerically computed. A computer program for this purpose written for the IBM 1620 is given in Appendix 11. A family of $\underline{F}$ and $\underline{E}$ curves, shown in Figures 11 through 20, are plotted with flow behavior index, n, and slip velocity factor, γ, as parameters. The $\underline{F}$ and $\underline{E}$ curves for the plug flow cases, $n = \infty$, are also shown in Figures 11 through 20 for comparison. However, it should be noted that the slip velocity at the wall is actually plug flow velocity itself.

MAXIMUM POINTS ON $\underline{E}$-CURVES

In order to know the characteristics of $\underline{E}$ curves for

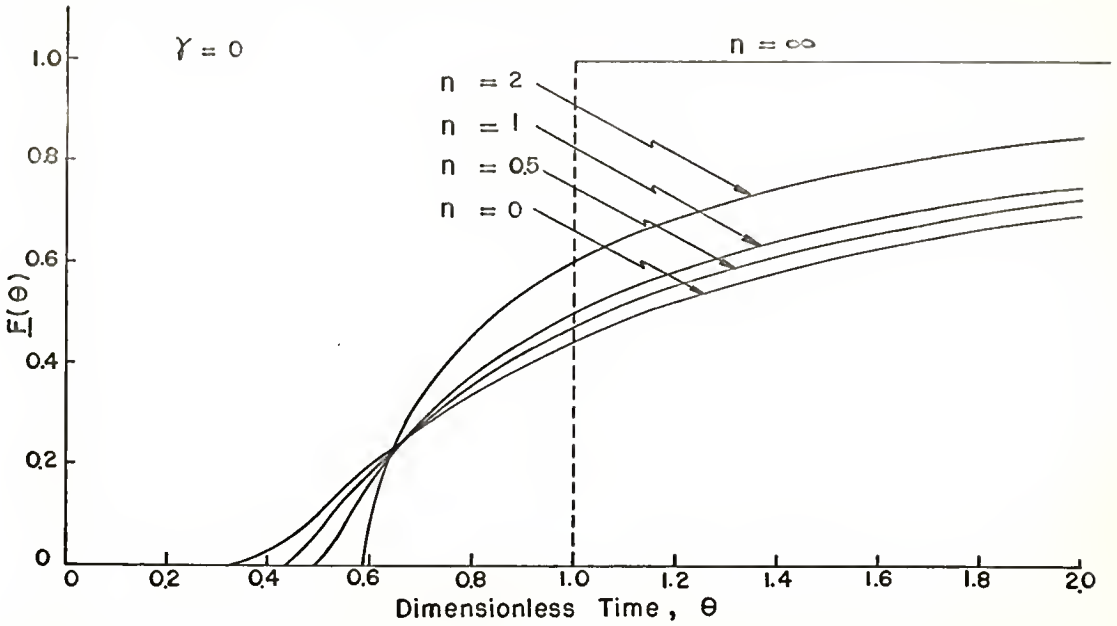

Fig. 11. F curves for laminar flow of Ostwald-de Waele model fluids in a cylindrical tube with $\gamma = 0$, entrance effect considered.

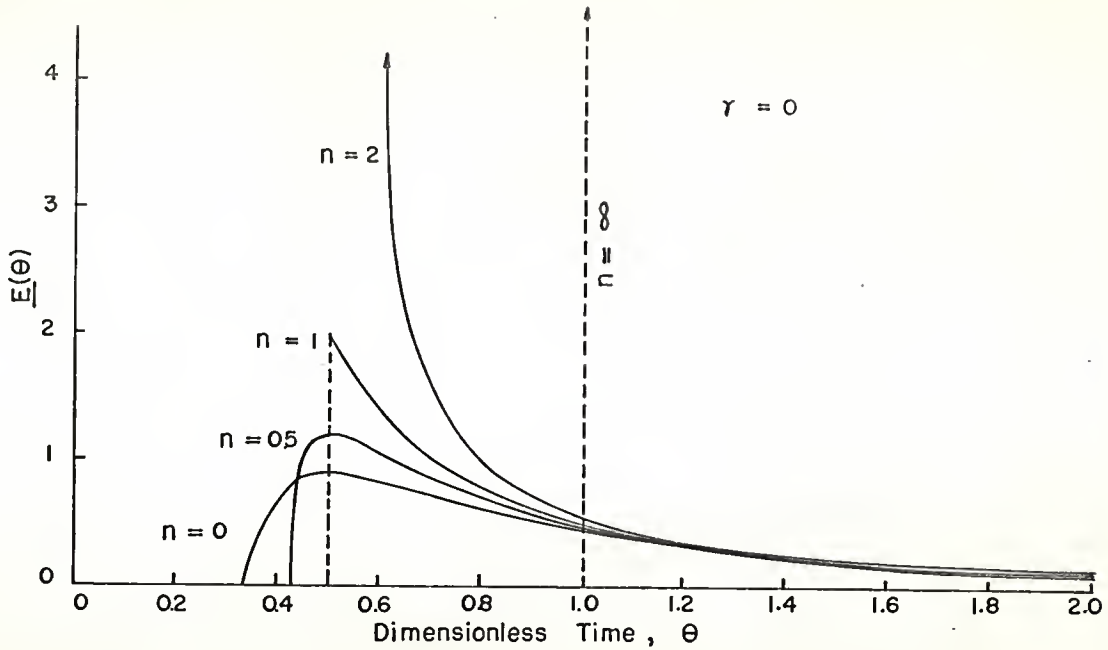

Fig. 12. $\underline{E}$ curves for laminar flow of Ostwald-de Waele model fluids in a cylindrical tube with $\gamma = 0$, entrance effect considered.

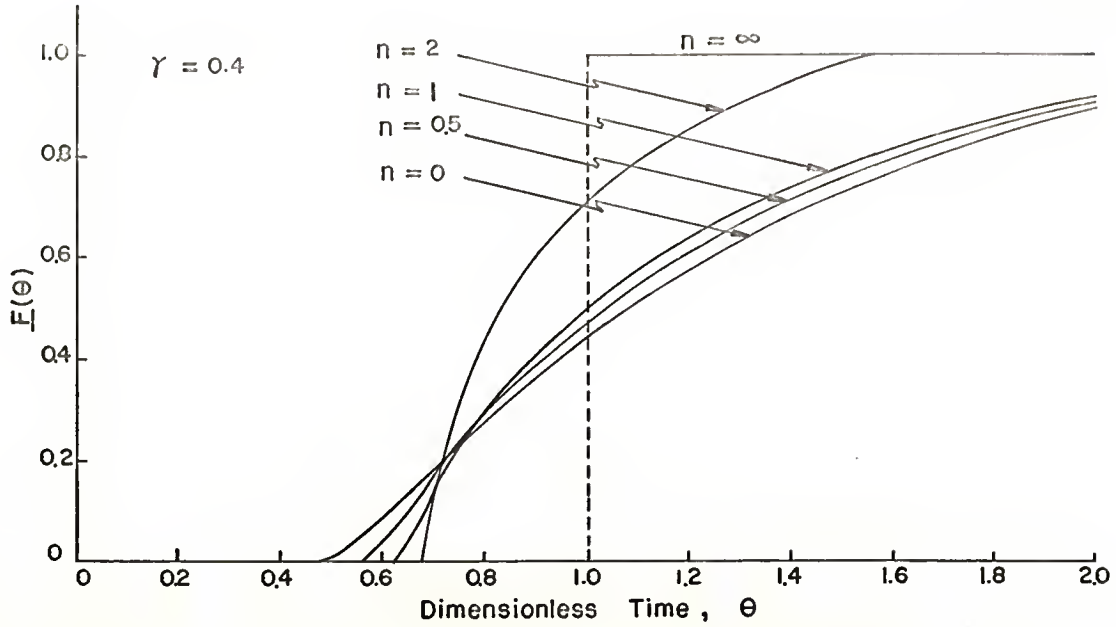

Fig. 13. F curves for laminar flow of Ostwald-de Waele model fluids in a cylindrical tube with $\gamma = 0.4$, entrance effect considered.

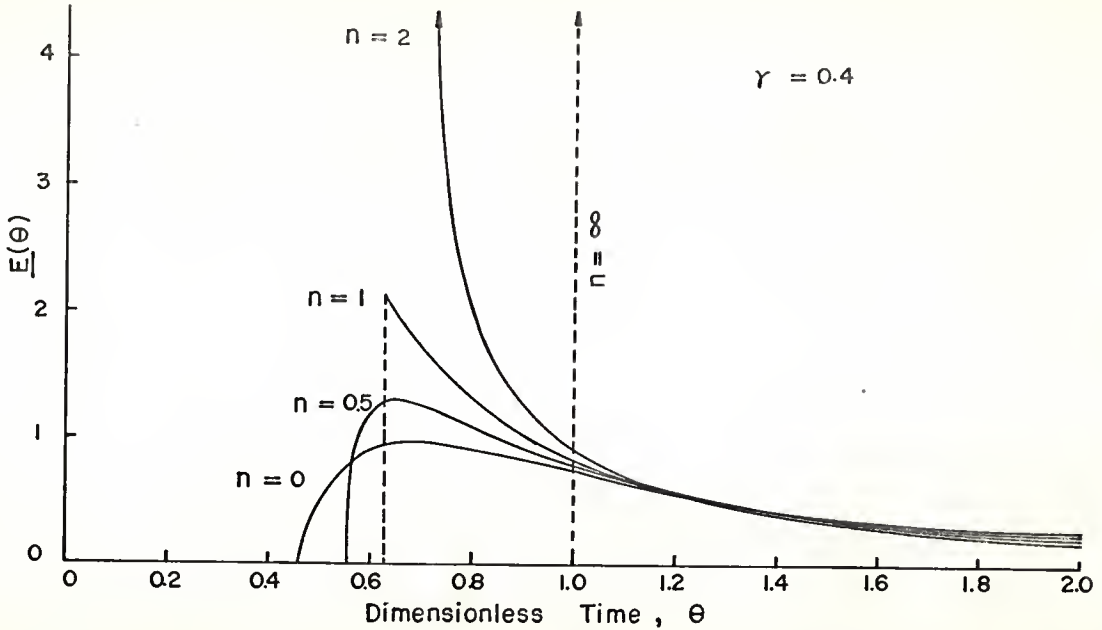

Fig. 14. E curves for laminar flow of Ostwald-de Waele model fluids in a cylindrical tube with $\gamma = 0.4$, entrance effect considered.

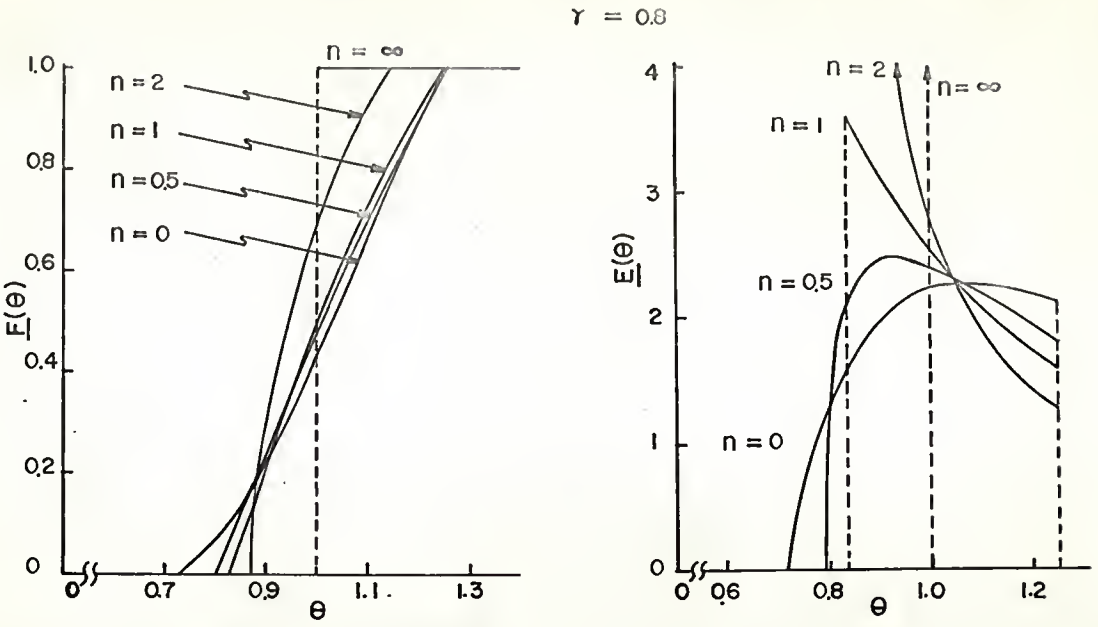

Fig. 15. F and E curves for laminar flow of Ostwald-de Waele model fluids in a cylindrical tube with $\gamma = 0.8$, entrance effect considered.

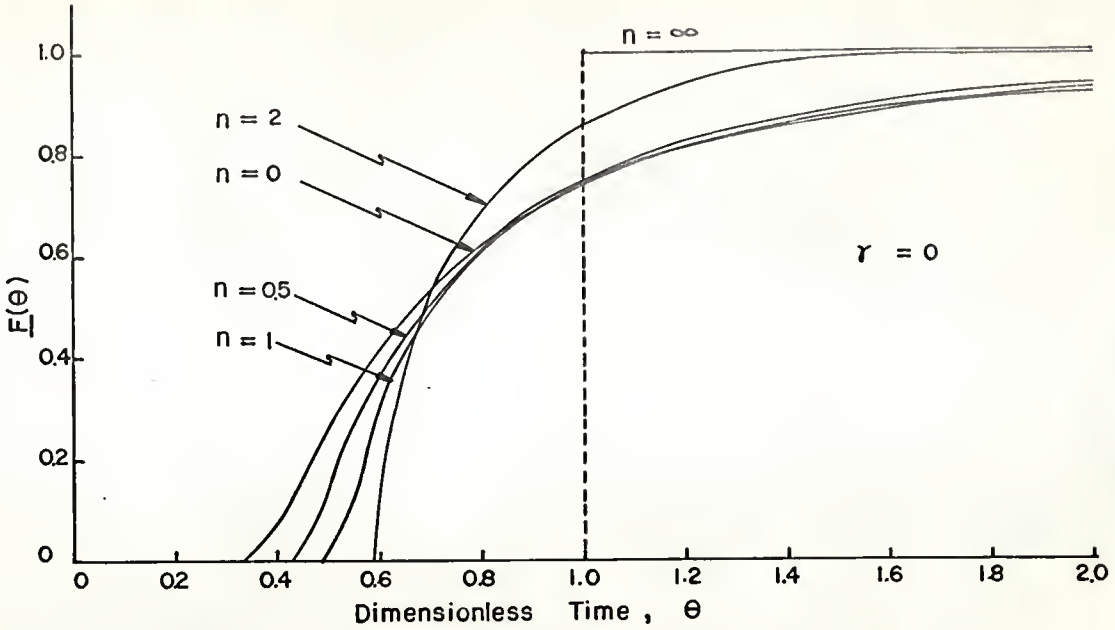

Fig. 16. F curves for laminar flow of Ostwald-de Waele model fluids in a cylindrical tube with $\gamma = 0$, entrance effect neglected.

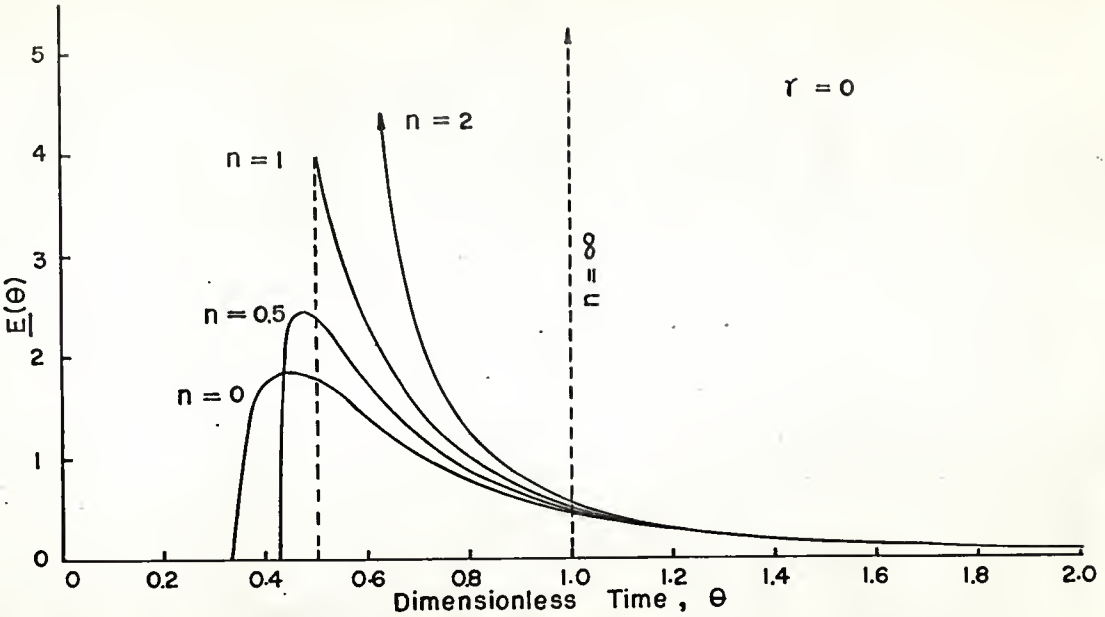

Fig. 17. $\underline{E}$ curves for laminar flow of Ostwald-de Waele model fluids in a cylindrical tube with $\gamma = 0$, entrance effect neglected.

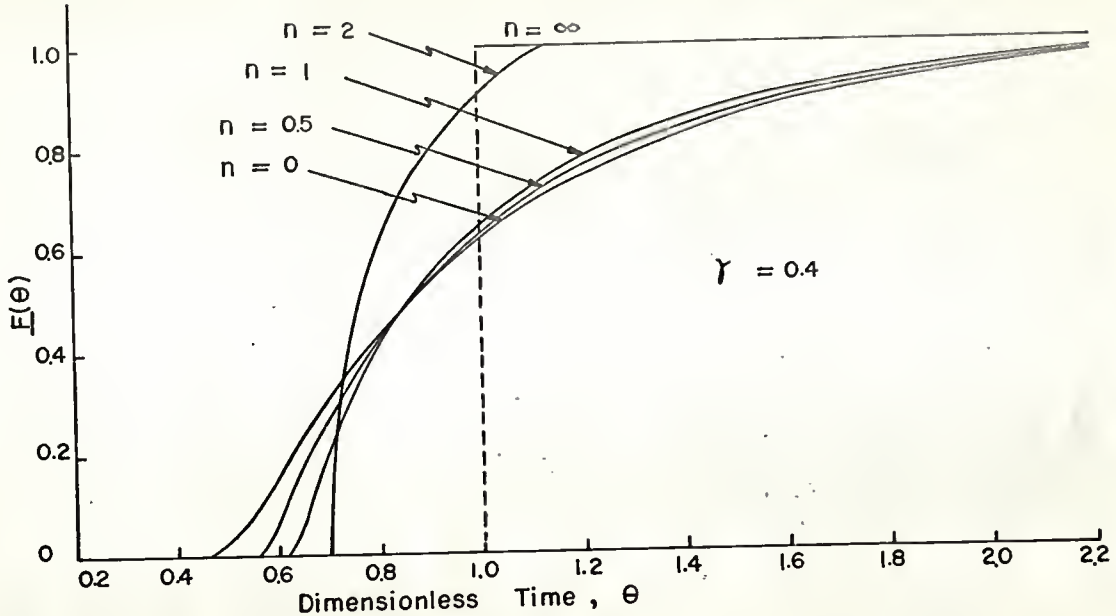

Fig. 18. F curves for laminar flow of Ostwald-de Waele model fluids in a cylindrical tube with $\gamma = 0.4$, entrance effect neglected.

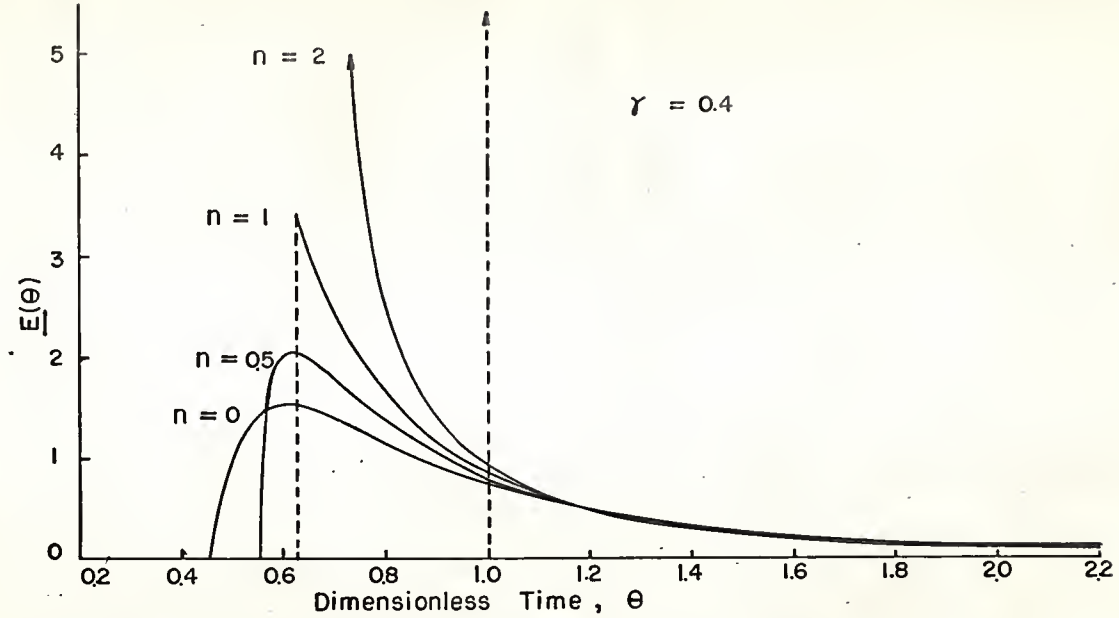

Fig. 19. $\underline{E}$ curves for laminar flow of Ostwald-de Waele model fluids in a cylindrical tube with $\gamma = 0.4$, entrance effect neglected.

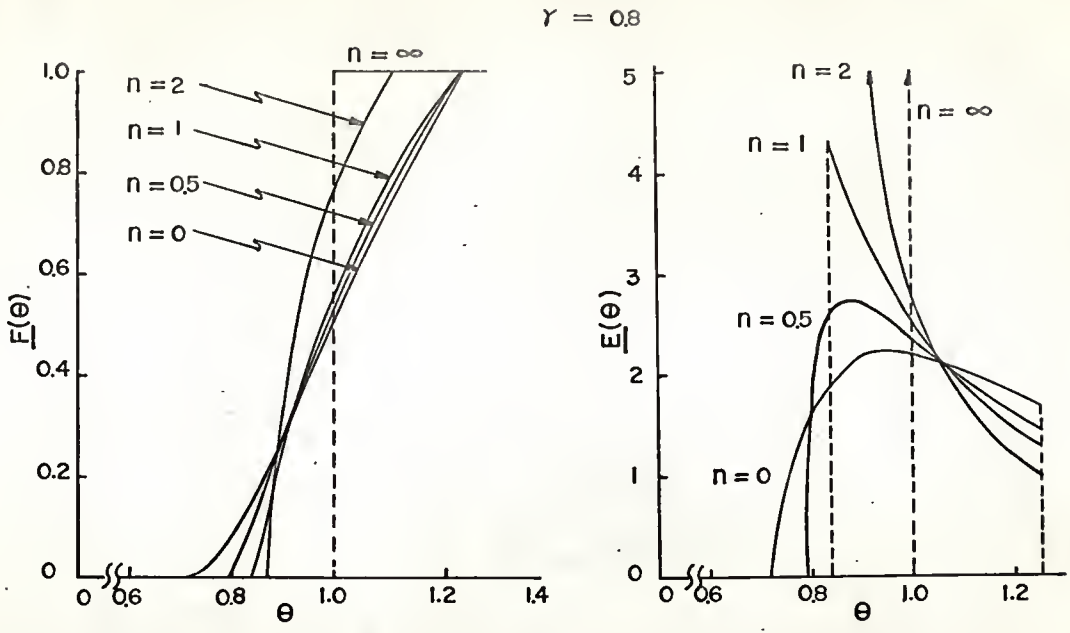

Fig. 20. $\underline{F}$ and $\underline{E}$ curves for laminar flow of Ostwald-de Waele model fluids in a cylindrical tube with $\gamma = 0.8$, entrance effect neglected.

Ostwald-de Waele fluid developed previously in detail, the position of the maximum concentration on the E-curves as given by Equations (73) and (75) are determined.

When the entrance effect cannot be neglected, differentiating Equation (73) with respect to θ and equating the derivative to zero, one has

$$\theta = \frac{1}{2}\left[\frac{n+3}{(n+3)-2\gamma}\right] \tag{76}$$

Substituting this equation into Equation (73), one obtains

$$\underline{E}(\theta)_m = \frac{2}{(n+3)(1-\gamma)} \cdot \frac{1}{\theta_m^2\left[1 - \frac{(n+1)(\frac{1}{\theta_m} - \gamma)}{(n+3)(1-\gamma)}\right]^{\frac{n-1}{n+1}}} \tag{77}$$

where θ_m is θ given by Equation (76).

When the entrance effect can be neglected, dimensionless residence time corresponding to the maximum point on E curve, is

$$\theta = \frac{2}{3}\left[\frac{n+2}{(n+3) - 2\gamma}\right] \tag{78}$$

Hence, the corresponding maximum is

$$\underline{E}(\theta)_m = \frac{2}{(n+3)(1-\gamma)} \cdot \frac{1}{\theta_m^3\left[1 - \frac{(n+1)(\frac{1}{\theta_m}) - \gamma)}{(n+3)(1-\gamma)}\right]^{\frac{n-1}{n+1}}} \tag{79}$$

where θ_m is θ given by Equation (78)

DISCUSSION AND CONCLUSION

In this treatment of the convective models (velocity profile models) steady state and isothermal laminar flow situations are assumed. The velocity profile of the fluid is a function of r, for cylindrical coordinates, or y, for rectangular coordinates, only, and thus a one-dimensional statement of shear stress-shear rate relationship for non-Newtonian fluids is valid.

Based on these simplifications, $\underline{F}$ and $\underline{E}$ curves for the Bingham plastic flowing through a cylindrical tube and a slit between two parallel plates have been derived for the case without entrance effect. The possibility of slip at the tube wall has been neglected. For the Ostwald-de Waele fluid, however, the two different cases, with and without entrance effects, as well as the case with the slip velocity at the tube wall have been considered. Each case, of course, can be reduced to the corresponding $\underline{F}$ and $\underline{E}$ curves for Newtonian flow as a limiting or special case.

Comparisons for both cases may be summarized as follows:

(1) Comparing the slopes of $\underline{E}$ curves for the two cases, one sees that when the slip velocity at the tube wall is neglected, Equations (73) and (75) reduce to Equations (3.2) and (3.4) repeated below for Newtonian flow:

$$\underline{E}(\theta) = \frac{1}{2\theta^2} \text{ , for entrance effect considered} \qquad (3.2)$$

and

$$\underline{E}(\theta) = \frac{1}{2\theta^3} \text{ , for entrance effect neglected} \qquad (3.4)$$

Both equations are applicable only when $\theta > 1/2$.

Slopes for the above two equations are

$$\frac{d\underline{E}}{d\theta} = -\frac{1}{\theta^3} \text{ , for } \theta > 1/2 \qquad (80)$$

$$\frac{d\underline{E}}{d\theta} = -\frac{3}{2\theta^4} \text{ , for } \theta > 1/2 \qquad (81)$$

Comparing these two equations, one sees that when the values of θ become infinite or at $\theta = 3/2$, the two curves, $\frac{d\underline{E}}{d\theta}$ vs. θ, coincide. While the values of θ are in the range between 1/2 and 3/2, the values of $\frac{d\underline{E}}{d\theta}$ in Equation (80) are greater than those given by Equation (81) in this range. The situation is, however, reversed when $\theta > 3/2$.

(2) Equation (76) shows that the values of θ corresponding to the maximum points on $\underline{E}$-curves are constant regardless of the values of n for the case without the slip velocity, $\gamma = 0$, but with the entrance effect. However, from Equation (78) one clearly sees that the above explanation is no longer true for the case without the entrance effect.

(3) Maximum points on $\underline{E}$-curves for the case in which the entrance effect can be neglected are always higher than that for the case in which the entrance effect be considered.

Miyauchi (11) indicated that, in actual observation, there will be a deformation in the shape of an $\underline{E}$-curve due to dispersion as shown in Figure 21. In Figure 21, typical $\underline{E}(\theta)$-curves for convective models for Newtonian and non-Newtonian fluids are replotted against θ. The uniaxial Taylor dispersion model for the Newtonian flow with $P_e = 4$ (11) and the tanks-in-series model (11) are also presented for comparison.

The models for non-Newtonian fluids treated in this chapter without considering the diffusion effect clearly show that the deformation of $\underline{E}$ curves is still caused by merely changing the parameter, n, i.e., by deviation from the Newtonian velocity profile alone. For instance, when $n = 0.5$, the $\underline{E}$-curve is a closer approximation to the curve actually observed by Miyauchi than either Taylor's dispersion or tanks-in-series models as shown in Figure 21.

In Chapter III, it has been mentioned that the first limiting condition proposed by Taylor (7) can be considered as an origin of the convective model. Taylor in his paper (7) showed the predicted distribution of average concentrations, C_m, in the tube, generally confirmed by his experiments, for three transients: an impulse, a step, and a finite pulse. During his development, the fluid has been assumed Newtonian. When the fluid is assumed to be the Ostwald-de Waele fluid the predicted response for an impulse input of a tracer will be (Appendix 12)

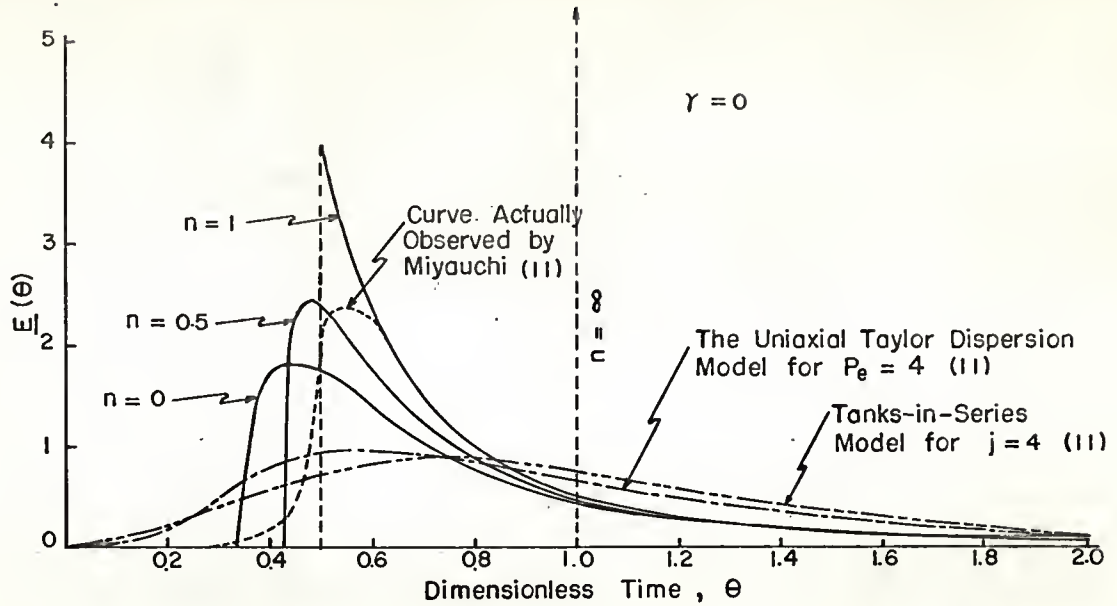

Fig. 21. Comparison of residence time distribution functions for convective (without entrance effect), Taylor's dispersion, and tanks-in-series models with $\gamma = 0$.

$$C_m = \frac{2}{n+1} \frac{C_0 X}{V_m t (1 - \frac{x}{V_m t})^{\frac{n-1}{n+1}}} \quad , \quad 0 < x < V_m t$$

$$= 0 \quad , \quad x < 0 \quad \text{and} \quad x > V_m t \qquad (82)$$

For the case of a step input of a tracer, the distributions of C_m along a tube become (Appendix 12)

$$C_m = C_0 \quad , \quad x < 0$$

$$C_m = C_0 \left[1 - \frac{2}{n+1} \frac{x}{V_m t (1 - \frac{x}{V_m t})^{\frac{n-1}{n+1}}} \right] \quad , \quad 0 < x < V_m t \qquad (83)$$

$$C_m = 0 \quad , \quad x > V_m t$$

When the input of a tracer is of a finite pulse, and if $t < X/V_m$, the distribution will be (Appendix 12)

$$C_m = 0 \quad , \quad x<0$$

$$C_m = \frac{2}{n+1} \frac{C_0 x}{V_m t\left(1 - \frac{x}{V_m t}\right)^{\frac{n-1}{n+1}}} \quad , \quad 0<x<V_m t$$

$$C_m = C_0 \quad , \quad V_m t<x<X$$

$$C_m = C_0\left[1 - \frac{2}{n+1} \frac{x - X}{V_m t\left(1 - \frac{x}{V_m t}\right)^{\frac{n-1}{n+1}}}\right], \quad X<x<X+V_m t$$

(84)

$$C_m = 0 \quad , \quad x>X + V_m t$$

If $t > X/V_m$, it is given by

$$
\left.
\begin{aligned}
C_m &= 0 \quad , \quad x < 0 \\
C_m &= \frac{2}{n+1} \frac{C_o x}{V_m t \left(1 - \frac{x}{V_m t}\right)^{\frac{n-1}{n+1}}} \quad , \quad 0 < x < X \\
C_m &= \frac{2}{n+1} \frac{C_o X}{V_m t \left(1 - \frac{x}{V_m t}\right)^{\frac{n-1}{n+1}}} \quad , \quad X < x < V_m t \\
C_m &= C_o \left[1 - \frac{2}{n+1} \frac{X - x}{V_m t \left(1 - \frac{x}{V_m t}\right)^{\frac{n-1}{n+1}}}\right] \quad , \quad V_m t < x < V_m t + X \\
C_m &= 0 \quad , \quad x > X + V_m t
\end{aligned}
\right\} \quad (85)
$$

Equations (82), (83), (84), and (85) are all derived under the situation without the slip velocity. As an extension for future work the case with the slip velocity can also be investigated. When $n = 1$, all the expressions shown in Equations (82) through (85) reduce to Equations (3.7), (3.8), (3.9), and (3.10) derived by Taylor (7) as a special case.

V. THE DISPERSION (DIFFUSION) MODEL

The mathematical expression of the diffusion equation for an incompressible fluid flowing in a circular tube is Equation (2.26). In case the axial diffusion can be neglected (7, 9) Equation (2.26) becomes

$$\frac{\partial C}{\partial t} = D_R \left(\frac{\partial^2 C}{\partial r^2} + \frac{1}{r}\frac{\partial C}{\partial r}\right) - V_x(r)\frac{\partial C}{\partial x} \qquad (1)$$

This equation describes the variation of tracer concentration with time at a point in a cylindrical tube. Radial diffusion and convection in the axial direction are the principal methods of material transport. For the case in which the diffusion term could not be neglected and also the time for convective transport to effect a change in concentration was long compared with the time of decay of radial concentration gradients by molecular diffusion, Taylor (7) showed that the tracer concentration could be considered dependent only on axial position and time. The criterion he derived is given by Equation (2.11). When the decay of radial concentration could be considered complete, and if the velocity profile is parabolic Equation (1) was found to be equivalent, as mentioned in Chapter III, to Fick's law for molecular diffusion in a moving coordinate system, that is,

$$K\frac{\partial^2 C_m}{\partial x_1^2} = \frac{\partial C_m}{\partial t} \qquad (2)$$

where

$$K = \frac{R^2 V_m^2}{192 D_R}$$

For the case in which the diffusion term in Equation (1) could be neglected, the convective term alone accounts for material transport. This case has been extensively treated in the previous chapter. Starting from Equation (1), this chapter will, then, concentrate on studying the effect of molecular diffusion on the fluid dispersion for Ostwald-de Waele fluids with steady velocity distribution in the isothermal laminar flow region in an open-open round tube (see Figure 22). The analysis employed basically follows Taylor's work (7, 9).

When a one-dimensional rheological statement is valid, the velocity profile of the Ostwald-de Waele fluid in cylindrical coordinates is expressed by Equations (4.31), (4.32) and (4.33),

$$V_x(r) = V_m \left[1 - \left(\frac{r}{R}\right)^{n+1}\right] \tag{3}$$

where

$$V_m = \left(\frac{-\Delta P}{2mL}\right)^n \frac{R^{n+1}}{n+1} \tag{4}$$

and

$$V_m = \left(\frac{n+3}{n+1}\right) \bar{V}_x \tag{5}$$

EFFECT OF MOLECULAR DIFFUSION ON THE FLUID DISPERSION

The equation for diffusion can be written by combining

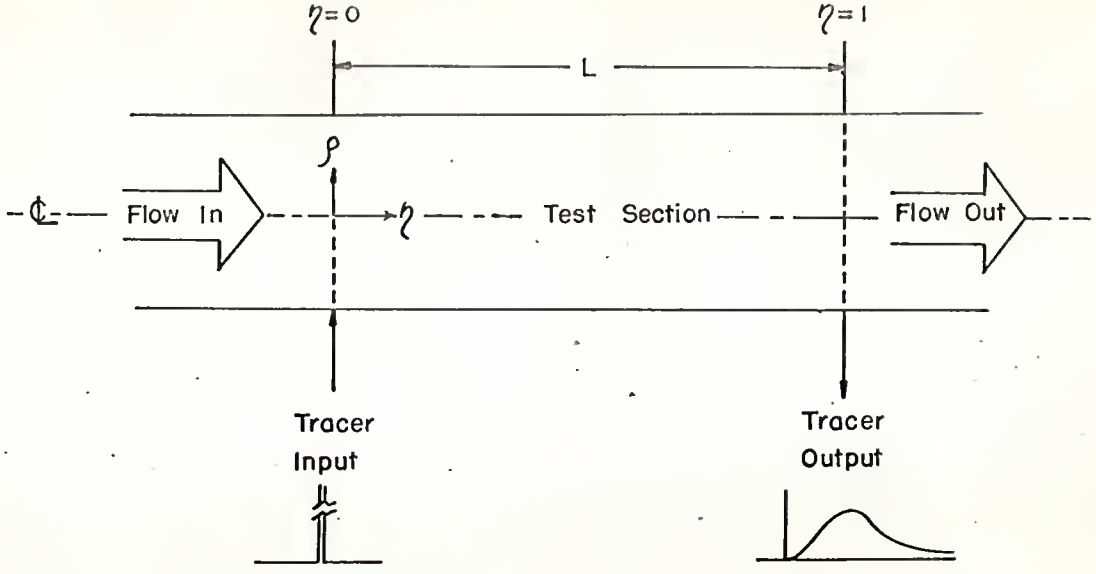

Fig. 22. Determination of dispersion associated with laminar flow of non-Newtonian fluids in an open-open cylindrical tube.

Equations (1), (3), and (5) as

$$\frac{\partial C}{\partial t} = D_R\left(\frac{\partial^2 C}{\partial r^2} + \frac{1}{r}\frac{\partial C}{\partial r}\right) - \left(\frac{n+3}{n+1}\right)\bar{V}_x\left[1 - \left(\frac{r}{R}\right)^{n+1}\right]\frac{\partial C}{x} \qquad (6)$$

Introducing the following dimensionless variables

C^* = dimensionless concentration = C/C^o

θ = dimensionless time = $\frac{t}{\bar{t}} = \frac{t\bar{V}_x}{L}$

ρ = dimensionless radial distance = $\frac{r}{R}$

η = dimensionless axial distance = $\frac{x}{L}$

Equation (6) becomes

$$\frac{\partial C^*}{\partial \theta} = \frac{D_R \bar{t}}{R^2}\left(\frac{\partial^2 C^*}{\partial \rho^2} + \frac{1}{\rho}\frac{\partial C}{\partial \rho}\right) - \left(\frac{n+3}{n+1}\right)\left(1 - \rho^{n+1}\right)\frac{\partial C^*}{\partial \eta} \qquad (7)$$

Since the wall of the tube is impermeable, one of the boundary conditions is

$$\left.\frac{\partial C^*}{\partial \rho}\right|_{\rho = 1} = 0 \qquad (8)$$

However, it would be difficult to find complete solutions to Equation (7) giving the value of C^* for all values of ρ, η and θ when the distribution of C^* at time $\theta = 0$ is known; on the other hand, approximate solutions can be found, which are valid for the second limiting condition proposed by Taylor (7) and mentioned in Chapter III. For reference, it is repeated below

> "The time necessary for appreciable effects to appear, owing to convective transport, is long compared with the 'time of decay' during which radial variations of concentration are reduced to a fraction of their initial value through the action of molecular diffusion."

In order to find the conditions under which this limiting condition may be expected to be valid, it is necessary to calculate how rapidly a concentration, which varies with radial position, becomes a uniform concentration.

Since it is assumed that the time for convective transport to effect an appreciable change in concentration is long as compared with the 'time of decay' of the radial concentration gradient by molecular diffusion, the axial concentration gradient $\partial C^*/\partial \eta$ may be considered approximately zero. But it should be noted that the first velocity profile of the fluid flow still exists. For the case with such an assumption the solution of Equation (7) is of the form (Appendix 13) (40)

$$C^*(\theta, \rho) = \sum_{m=1}^{\infty} A_m \exp(-\alpha_m^2 \theta) J_o\left[\frac{\alpha_m R}{(D_R t)^{\frac{1}{2}}} \rho\right]$$

$$m = 1, 2, \ldots \qquad (9)$$

where

A_m = m-th eigen constant

α_m = m-th eigen value

Since the rapid convergence of Equation (9) is expected, only the first term of the summation, that is, m = 1 is considered as an approximate solution of Equation (7). Besides, a boundary condition

$C^* = 1$ when $\theta = 0$ and $\rho = 0$

ensures that

$$C^*(\theta, \rho) = \exp(-\alpha_1^2 \theta) J_o \left[\frac{\alpha_1 R}{(D_R \bar{t})^{\frac{1}{2}}} \rho \right] \tag{10}$$

Furthermore, applying the following boundary condition

$$\left. \frac{\partial C^*}{\partial \rho} \right|_{\rho=1} = 0$$

to Equation (10), one has

$$J_1 \left[\frac{\alpha_1 R}{(D_R \bar{t})^{\frac{1}{2}}} \right] = 0 \tag{11}$$

The root of this equation corresponding to the lowest value of α_1 is

$$\frac{\alpha_1 R}{(D_R \bar{t})^{\frac{1}{2}}} = 3.83$$

or

$$\alpha_1 = (3.83) \frac{(D_R \bar{t})^{\frac{1}{2}}}{R} \tag{12}$$

It is necessary to find the time required for a tracer concentration to become uniform in the radial direction of the flow field. The time necessary to decay the radial concentration variation, represented by Equation (10), to the statistically uniform state; that is, e^{-1} of the initial value at the center of the tube, $\rho = 0$; is then (7)

$$\frac{D_R \bar{t}}{R^2} \theta_1 = 0.0682$$

or

$$\frac{D_R t_1}{R^2} = 0.0682$$

Solving for t_1, one has

$$t_1 = 0.0682 \frac{R^2}{D_R} \tag{13}$$

Therefore, in order that Taylor's assumption may be valid, or the time necessary for convective transport, L/V_m, to make an appreciable change in a tracer concentration is comparatively long, the following inequality should be satisfied.

$$\frac{L}{V_m} \gg 0.0682 \frac{R^2}{D_R}$$

or

$$\frac{L}{\bar{V}_x} \gg 0.0682 \left(\frac{n+3}{n+1}\right) \frac{R^2}{D_R} \tag{14}$$

because

$$V_m = \left(\frac{n+3}{n+1}\right) \bar{V}_x$$

SOLUTION OF TWO-DIMENSIONAL DIFFUSION EQUATION FOR NON-NEWTONIAN FLUIDS BY REDUCING TO ONE DIMENSION

Since the axial dispersion has been neglected, as shown in

Equation (7), the whole of the axial material transport is thus due to convection only. Equation (7) signifies that the distribution of tracer concentration in the steady, laminar flow region is due to the combined action of convection along the tube due to variation of velocity over the cross-section and radial dispersion due to molecular diffusion.

For convenience the concentration and velocity will be defined relative to axes which move with mean fluid velocity, that is,

$$x_1 = x - \bar{V}_x t \tag{15}$$

With these simplifications Equation (6) becomes (Appendix 14)

$$\frac{\partial C}{\partial t} = D_R\left(\frac{\partial^2 C}{\partial r^2} + \frac{1}{r}\frac{\partial C}{\partial r}\right) - \bar{V}_x\left[\frac{2}{n+1} - \frac{n+3}{n+1}\left(\frac{r}{R}\right)^{n+1}\right]\frac{\partial C}{\partial x_1} \tag{16}$$

Normalizing Equation (16) by introducing the dimensionless variables C^*, θ, ρ, η, and η_1 defined previously, one obtains

$$\frac{\partial C^*}{\partial \theta} = \frac{D_R \bar{t}}{R^2}\left(\frac{\partial^2 C^*}{\partial \rho^2} + \frac{1}{\rho}\frac{\partial C^*}{\partial \rho}\right) - \left(\frac{2}{n+1} - \frac{n+3}{n+1}\right)^{n+1}\frac{\partial C^*}{\partial \eta_1} \tag{17}$$

where $\eta_1 = \eta - \theta$,

Here $\frac{\partial}{\partial \theta}$ represents differentiation with respect to time at a point fixed relative to axes moving with the mean fluid velocity. Since the moving axes have been introduced, the transfer of tracer concentration across the plane at which η_1 is constant depends only on the radial variation of tracer concentration because the mean velocity across such planes is zero. In solving

Equation (17), Taylor (7) further assumed that the radial variation of tracer concentration is small and thus $\partial C^*/\partial \theta$ is also small. It should be noted that the transfer of mass across the constant plane η_1 depends only on the radial variation of tracer concentration. Now it can be approximately calculated from the equation by first neglecting $\frac{\partial C^*}{\partial \theta}$ term, as

$$\frac{D_R \bar{t}}{R^2} \left(\frac{\partial^2 C^*}{\partial \rho^2} + \frac{1}{\rho} \frac{\partial C^*}{\partial \rho} \right) = \left(\frac{2}{n+1} - \frac{n+3}{n+1} \rho^{n+1} \right) \frac{\partial C^*}{\partial \eta_1} \tag{18}$$

In solving this equation, $\frac{\partial C^*}{\partial \rho_1}$ is independent of ρ because the moving coordinate is used. The boundary condition

$$\frac{\partial C^*}{\partial \rho} = 0 \text{ at } \rho = 1 \tag{19}$$

is employed. The result for the case n is zero or a positive integer is (Appendix 15)

$$C^* = C_o^* + A_2 \left(\rho^2 - \frac{2}{n+3} \rho^{n+3} \right) \tag{20}$$

where C_o^* is the value of C^* at $\rho = 0$, and A_2 is a constant.

Substituting Equation (20) into Equation (18) and simplifying, the constant, A_2, is found as

$$A_2 = \frac{1}{2(n+1)} \left(\frac{R^2}{D_R \bar{t}} \right) \frac{\partial C^*}{\partial \eta_1} \tag{21}$$

Taylor in his later paper (9) mentioned that using the mean concentration C_m^* over any section was more convenient than using C_o^* in solving the problem. Here, C_m^* is defined by

$$C^*_m = \frac{\int_0^{2\pi}\int_0^1 C^* \rho d\rho d\theta}{\int_0^{2\pi}\int_0^1 \rho d\rho d\theta} = 2\int_0^1 C^* \rho d\rho \qquad (22)$$

Equation (20), therefore, may be modified to the form (Appendix 16)

$$C^* = C^*_m + \frac{1}{2(n+1)}\left(\frac{R^2}{D_R\bar{t}}\right)\left(\frac{\partial C^*_m}{\partial \eta_1}\right)\left[-\frac{1}{2} + \frac{4}{(n+3)(n+5)} + \rho^2 - \frac{2}{n+3}\rho^{n+3}\right] \qquad (23)$$

The volumetric flow rate at which C* is transported across a section at η_1 is

$$Q = 2\pi R^2 \int_0^1 C^* V_x(\rho)\rho \, d\rho \qquad (24)$$

and also one knows that from Equation (16),

$$V_x(\rho) = \bar{V}_x\left(\frac{2}{n+1} - \frac{n+3}{n+1}\rho^{n+1}\right) \qquad (25)$$

Substituting Equations (23) and (25) into Equation (24) and integrating over the range (0,1), one obtains (Appendix 17)

$$Q = -\frac{\pi R^4 \bar{V}_x^2}{2(n+3)(n+5)D_R L}\left(\frac{\partial C^*_m}{\partial \eta_1}\right) = -\frac{R^2\bar{V}_x^2}{D_R}\left[\frac{1}{2(n+3)(n+5)}\right]\pi R^2\left(\frac{\partial C^*_m}{\partial \eta_1}\right) \qquad (26)$$

From Equation (26) it can be seen that C^*_m is dispersed relative to a plane which moves with mean fluid velocity, $\bar{V}_x$, exactly as though it were being diffused by a process which obeys Fick's law of diffusion, but with the overall dispersion

coefficient E defined by (7)

$$E = \frac{R^2 \bar{V}_x^2}{D_R} \left[\frac{1}{2(n+3)(n+5)} \right] \tag{27}$$

Equation (26) then becomes

$$Q = - E \frac{\pi R^2}{L} \left(\frac{\partial C^*_m}{\partial \eta_1} \right) \tag{28}$$

It is important to remember that Equation (28) has been derived on the assumptions (7) that mass transport across the plane at which η_1 is constant depends only on the radial variation of tracer concentration and the radial concentration gradient is also small so that $\partial C^*/\partial \theta$ is small. These assumptions will also be applied to derive an unsteady, one-dimensional diffusion equation by correlating Equation (28) with Fick's second law of diffusion (6). First of all, starting from the equation of continuity for the one-dimensional problem without chemical change occurring in the system, one has (6)

$$\frac{\partial C^*_m}{\partial t} = - \frac{1}{\pi R^2} \left(\frac{\partial Q}{\partial x_1} \right)$$

or in dimensionless form

$$\frac{\partial C^*_m}{\partial \theta} = - \frac{1}{\pi R^2 \bar{V}_x} \left(\frac{\partial Q}{\partial \eta_1} \right) \tag{29}$$

From Equation (28) it is clear that

$$\frac{\partial Q}{\partial \eta_1} = - E \frac{\pi R^2}{L} \left(\frac{\partial^2 C^*_m}{\partial \eta_1^2} \right) \tag{30}$$

Hence combining Equations (29) and (30) gives the governing partial differential equation of axial dispersion (7)

$$\frac{\partial C^*_m}{\partial \theta} = \left(\frac{E}{\bar{V}_x L}\right) \frac{\partial^2 C^*_m}{\partial \eta_1^2} \tag{31}$$

Solution of Equation (31) subject to the following initial and boundary conditions (Appendix 18)

I.C. $C^* = 0$ for $\theta = 0$ and $\eta_1 \neq 0$

B.C.1. $C^* = 0$ for $\theta > 0$ and $\eta_1 \rightarrow \pm \infty$

B.C.2. $C^* = \delta(\theta)$ for all θ and $\eta_1 = 0$

gives C^* in terms of θ and η_1 (7, 41, 42), as

$$C^* = \frac{1}{2\left[\pi\left(\frac{E}{\bar{V}_x L}\right)\theta\right]^{\frac{1}{2}}} \exp\left[\frac{\eta_1^2}{4\left(\frac{E}{\bar{V}_x L}\right)\theta}\right] \tag{32}$$

Since

$$\eta_1 = \eta - \theta \text{ and } E = \frac{R^2 \bar{V}_x^2}{D_R}\left[\frac{1}{2(n+3)(n+5)}\right],$$

Equation (32) becomes

$$C^* = \frac{1}{2\left[\left(\frac{R^2 \bar{V}_x}{D_R L}\right)\frac{\pi\theta}{2(n+3)(n+5)}\right]^{\frac{1}{2}}} \exp\left[-\frac{(\eta-\theta)^2}{\left(\frac{R^2 \bar{V}_x}{D_R L}\right)\frac{2\theta}{(n+3)(n+5)}}\right] \tag{33}$$

The distribution function of the tracer concentration at the

outlet of the experimental section (See Figure 22) of the cylindrical tube can be obtained by setting $\eta = 1$. Thus one obtains

$$C^* = \underline{C}(\theta) = \underline{E}(\theta)$$

$$= \frac{1}{2\left[\frac{\pi M \theta}{2(n+3)(n+5)}\right]^{\frac{1}{2}}} \exp\left[-\frac{(1-\theta)^2}{\frac{2 M \theta}{(n+3)(n+5)}}\right] \qquad (34)$$

where

$$M = \frac{R^2 \bar{V}_x}{D_R L}$$

The residence time distribution functions or exit age distribution curves for various combinations of the dimensionless parameter M, and flow-behavior index, n, have been calculated by using Equation (34) and are plotted on Figures 23 through 29. When M is very small or n is very large, the values of $\underline{E}(\theta)$ are essentially zero except for the value of θ close to 1.0. In this situation, Equation (34) can be approximately reduced to (5)

$$\underline{E}(\theta) = \frac{1}{2\left[\frac{\pi M}{2(n+3)(n+5)}\right]^{\frac{1}{2}}} \exp\left[-\frac{(1-\theta)^2}{\frac{2 M}{(n+3)(n+5)}}\right] \qquad (35)$$

Curves of $\underline{E}(\theta)$ at $\theta = 1.0$ and $n = \infty$ are also shown in figures. At $\theta = 1.0$ and $n = \infty$, $\underline{E}(\theta)$ curves become infinite. They are consistent with plug (slug) flow situation.

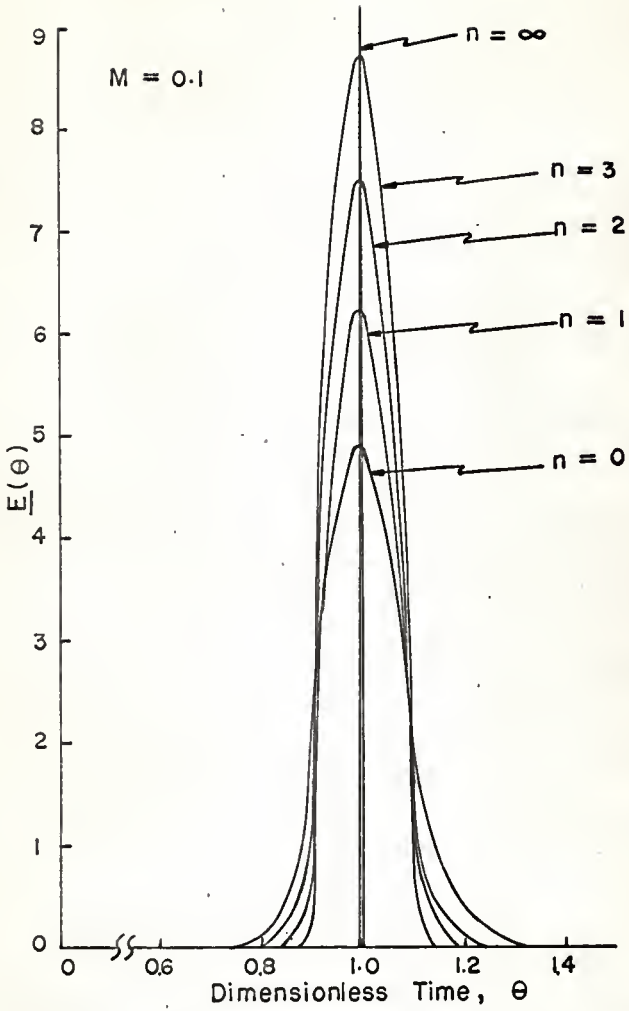

Fig. 23. Calculated $\underline{E}$ curves for laminar flow of Ostwald-de Waele model fluids with $M = 0.1$.

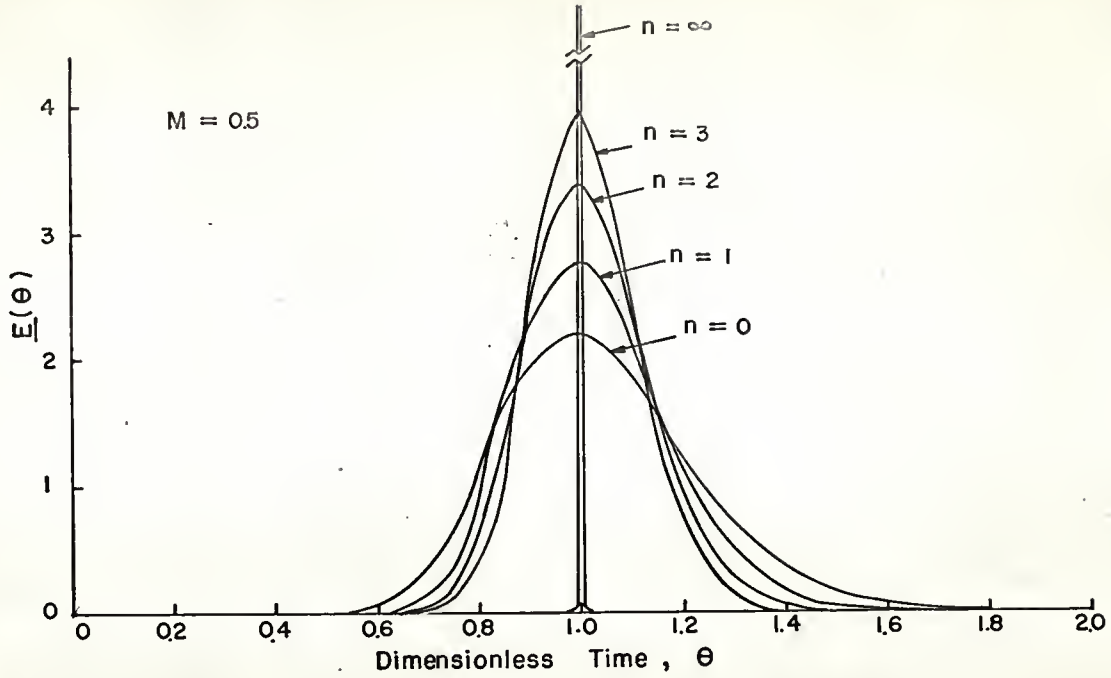

Fig. 24. Calculated E curves for laminar flow of Ostwald-de Waele model fluids with M=0.5 .

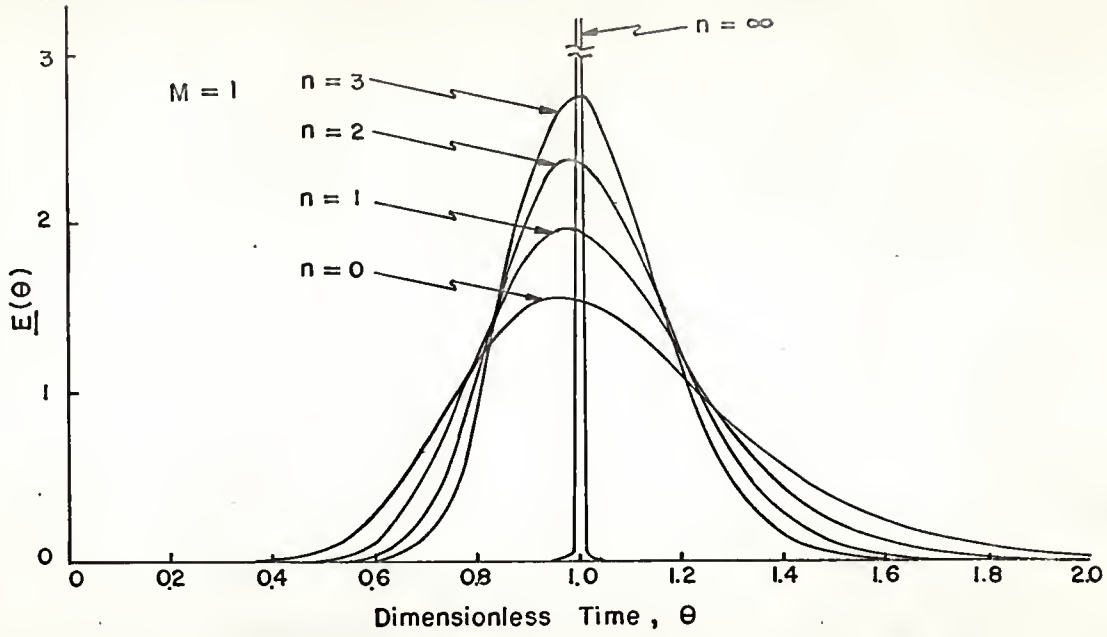

Fig. 25. Calculated $\underline{E}$ curves for laminar flow of Ostwald-de Waele model fluids with $M = 1$.

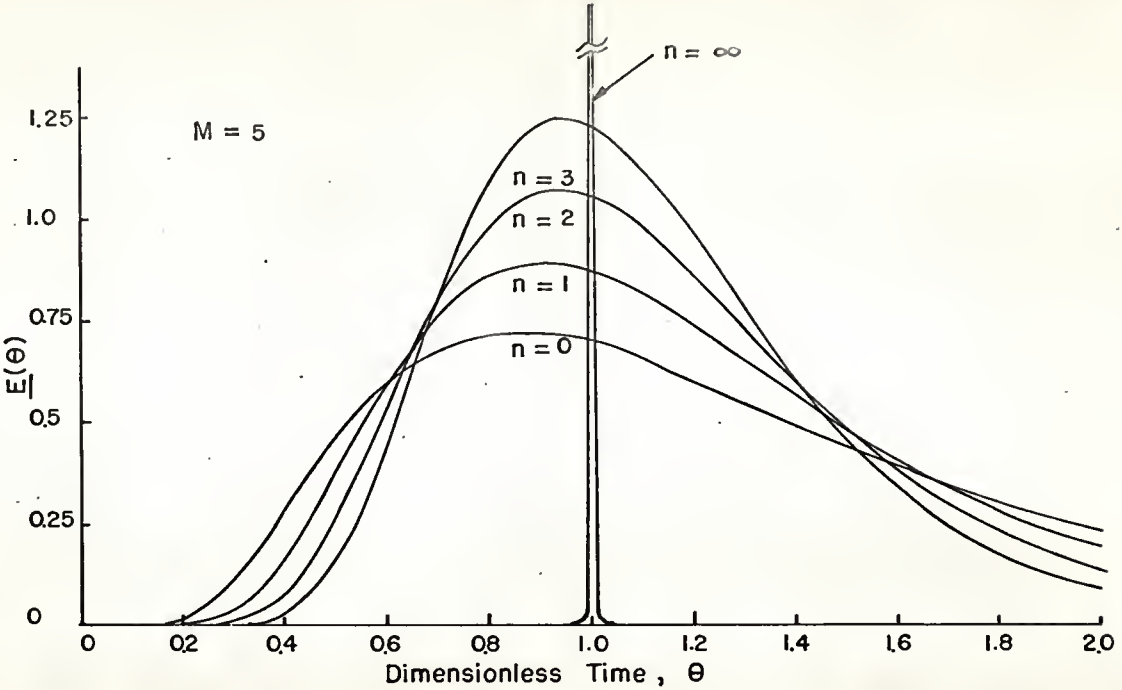

Fig. 26. Calculated $\underline{E}$ curves for laminar flow of Ostwald-de Waele model fluids with $M = 5$.

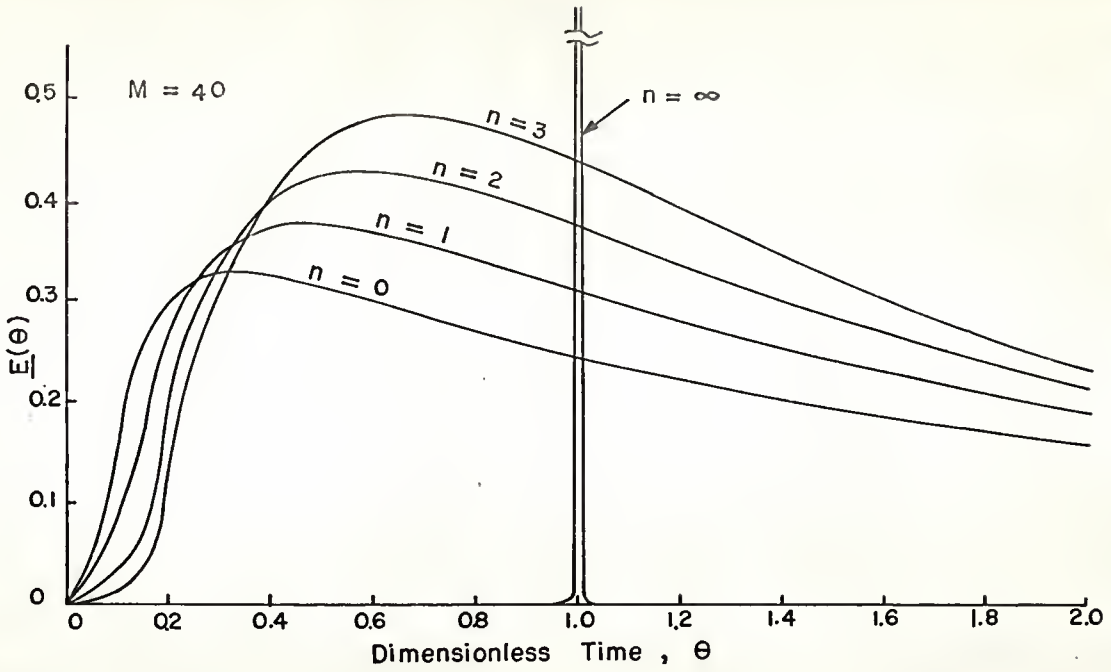

Fig. 27. Calculated $\underline{E}$ curves for laminar flow of Ostwald-de Waele model fluids with $M = 40$.

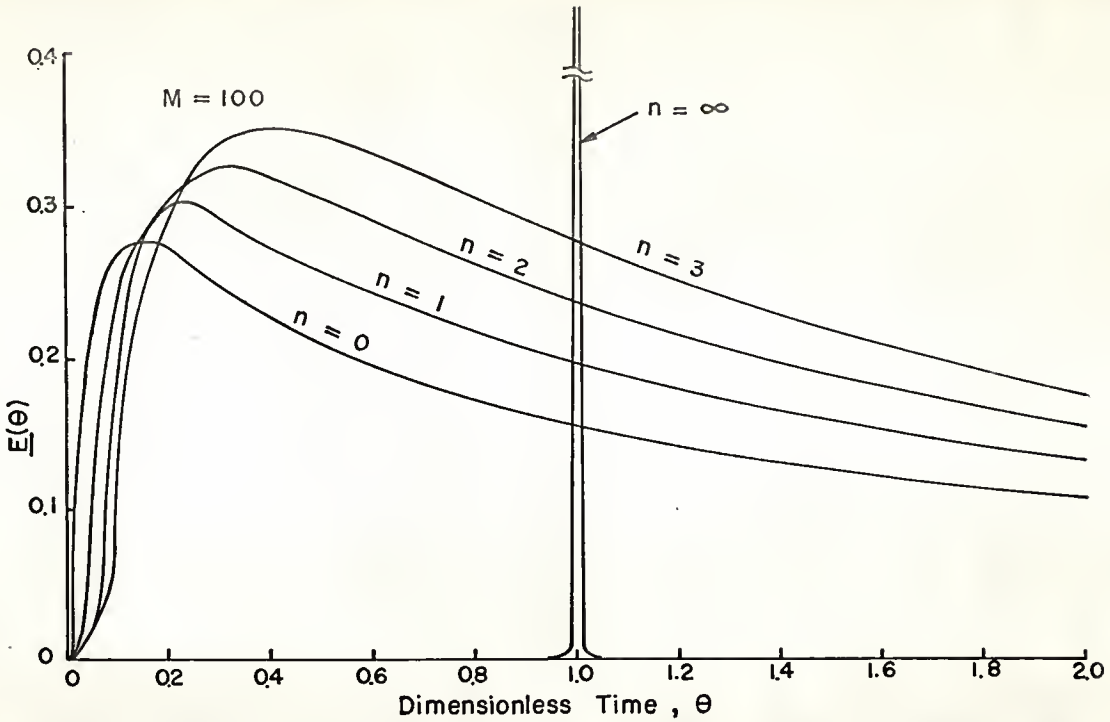

Fig. 28. Calculated $\underline{E}$ curves for laminar flow of Ostwald-de Waele model fluids with M = 100.

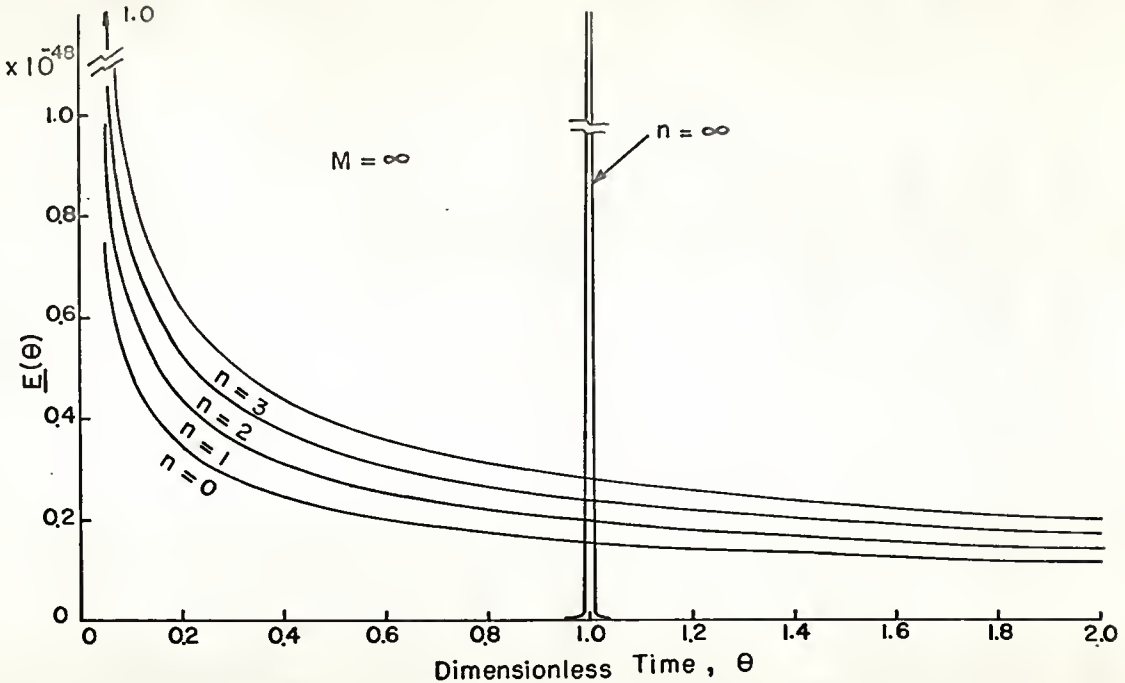

Fig. 29. Calculated $\underline{E}$ curves for laminar flow of Ostwald-de Waele model fluids with $M = \infty$.

It can be seen from the figures that it is sufficiently accurate to assume that the maximum value of $\underline{E}(\theta)$ occurs at $\theta = 1$ when the values of M are less than 1. But it is not quite true when the values of M are greater than 1, due to the cause of skewness.

MAXIMUM POINTS ON $\underline{E}$-CURVES

Equation (34) is differentiated with respect to θ and the derivative equated to zero the solution which represents the time θ_m, at which the maximum value, $\underline{E}(\theta)_m$, occurs, is evaluated as

$$\theta_m = \left\{ \left(\frac{E}{\bar{V}_x L}\right)^2 + 1 \right\}^{\frac{1}{2}} - \left(\frac{E}{\bar{V}_x L}\right) \tag{36}$$

where

$$\frac{E}{\bar{V}_x L} = \frac{M}{2(n+3)(n+5)} \tag{37}$$

Equation (36) can also be written as

$$\theta_m = \frac{1}{\left[\left(\frac{E}{\bar{V}_x L}\right)^2 + 1 \right]^{\frac{1}{2}} + \frac{E}{\bar{V}_x L}} \tag{38}$$

This equation shows that, when $\frac{E}{\bar{V}_x L}$ or $M/2(n+3)(n+5)$ is very small, θ_m reduces to 1 at which the maximum point occurs. But θ_m becomes approximately $\frac{1}{2\left(\frac{E}{\bar{V}_x L}\right)}$ when the value of $\frac{E}{\bar{V}_x L}$ is of higher order. The general expression of the maximum point of the

residence time distribution obtained by substituting Equations (36), (37), and (38) into Equation (34) is

$$\underline{E}(\theta)_m = \frac{1}{2\left[\frac{\pi M}{2(n+3)(n+5)}\right]^{\frac{1}{2}}\left\{\left[\left(\frac{M}{2(n+3)(n+5)}\right)^2 + 1\right]^{\frac{1}{2}} - \frac{M}{2(n+3)(n+5)}\right\}^{\frac{1}{2}}}$$

$$\cdot \exp\left\{-\frac{\left\{\left[\frac{M}{2(n+3)(n+5)}\right]^2 + 1\right\}^{\frac{1}{2}} - 1}{\frac{M}{(n+3)(n+5)}}\right\} \qquad (39)$$

For the case when $\theta = 1$, Equation (34) reduces to

$$\underline{E}(\theta) = \frac{1}{2\left[\frac{\pi M}{2(n+3)(n+5)}\right]^{\frac{1}{2}}} \qquad (40)$$

Comparing Equations (39) and (40), we see that $\underline{E}(\theta)_m$ and $\underline{E}(\theta)$ are practically identical except when values of M are large (43).

MEAN AND VARIANCE OF RESIDENCE TIME DISTRIBUTION

The first moment about the origin and the second moment about the mean, commonly called the mean, μ, and the variance, σ^2, respectively are used to describe the distribution of the $\underline{E}$-curve. The former is also called the centroid of the distribution and is the location parameter of the distribution while the latter measures the spread of the distribution about the mean. The formulas used to evaluate μ and σ^2 are (5)

$$\mu = \int_0^\infty \theta\, \underline{E}(\theta) d\theta \qquad (41)$$

and

$$\sigma^2 = \int_0^\infty (\theta - \mu)^2 \, \underline{E}(\theta) d\theta \tag{42}$$

or

$$\sigma^2 = \int_0^\infty \theta^2 \underline{E}(\theta) d\theta - \left[\int_0^\infty \theta \underline{E}(\theta) d\theta \right]^2 \tag{43}$$

By substituting Equation (34) into Equation (41) and integrating, the resulting equation (Appendix 19) is

$$\mu = 1 + \frac{M}{(n+3)(n+5)} \tag{44}$$

The variance of the residence time distribution is obtained by substituting Equations (34) and (44) into Equation (43) as

$$\sigma^2 = \int_0^\infty \frac{\theta^2}{2\left[\frac{\pi M \theta}{2(n+3)(n+5)}\right]^{\frac{1}{2}}} \exp\left[- \frac{(1-\theta)^2}{\frac{2 M \theta}{(n+3)(n+5)}} \right] d\theta$$

$$- \left[1 + \frac{M}{(n+3)(n+5)} \right]^2 \tag{45}$$

or (35, 43) (Appendix 20)

$$\sigma^2 = 2\left[\frac{M}{(n+3)(n+5)} \right]^2 + \frac{M}{(n+3)(n+5)} \tag{46}$$

Solving for M gives

$$M = \frac{(n+3)(n+5)}{4} \left[(8\sigma^2 + 1)^{\frac{1}{2}} - 1 \right] \tag{47}$$

Equations (44) and (46) or (47) are used to find M for the fluid

of known n by injecting an impulse of tracer into the system and finding the variance of the experimental concentration data by either graphical or numerical integration.

In case the value of M is very small, that is, D_R is very large, Equations (44) and (46) can be approximately reduced to

$$u = 1 \tag{48}$$

$$\sigma^2 = \frac{M}{(n+3)(n+5)} \tag{49}$$

The curves corresponding to the above equations can be approximated well by the Gaussian distribution (44).

CORRELATION FOR DISPERSION COEFFICIENT

It has been mentioned (10) that the dimensionless group $E/\bar{V}_x d_t$ is dependent on the Reynolds number, Schmidt number, and pipe roughness. But the pipe roughness has been shown to be important only in turbulent flow (45). Hence in the laminar flow region one may write (44):

$$\frac{E}{\bar{V}_x d_t} = \phi\left[\left(\frac{d_t \bar{V}_x \rho}{m}\right), \left(\frac{m}{\rho D_R}\right)\right] \tag{50}$$

and consequently a plot of $E/\bar{V}_x d_t$ vs. $d_t \bar{V}_x \rho/m$ with $m/\rho D_R$ as a parameter should result in a family of curves.

Repeating Equation (27), one has

$$E = \frac{R^2 \bar{V}_x^2}{D_R}\left[\frac{1}{2(n+3)(n+5)}\right] \tag{27}$$

Rewriting this in dimensionless form according to Equation (50),

one obtains

$$\frac{E}{\bar{V}_x d_t} = \frac{1}{8(n+3)(n+5)} \left(\frac{d_t \bar{V}_x \rho}{m}\right) \left(\frac{m}{\rho D_R}\right) \tag{51}$$

This correlation is shown in Figure 30. Equation (51) can also be written simply as

$$\frac{E}{\bar{V}_x d_t} = \frac{1}{8(n+3)(n+5)} \left(\frac{d_t \bar{V}_x}{D_R}\right) \tag{52}$$

This relationship is plotted in Figure 31.

DISCUSSION AND CONCLUSION

The dispersion of a tracer injected in laminar flow of Ostwald-de Waele fluid in an open-open, cylindrical tube is extensively studied in this work. In the analysis M and n are considered to be independent of x-r coordinates. The approach used is basically that of Taylor (7, 9). A family of curves, $\underline{E}(\theta)$ vs. θ, with M and n as parameters is plotted by using Equation (34). Typical results are those shown in Figures 23 through 29.

The condition for which the Taylor's second limiting condition can be satisfied has been shown by the inequality in Equation (14), that is

$$\frac{L}{\bar{V}_x} >> 0.0682 \left(\frac{n+3}{n+1}\right) \frac{R^2}{D_R}$$

This condition can be realized by using a long experimental tube with a small diameter. By using Taylor's assumptions (7) and

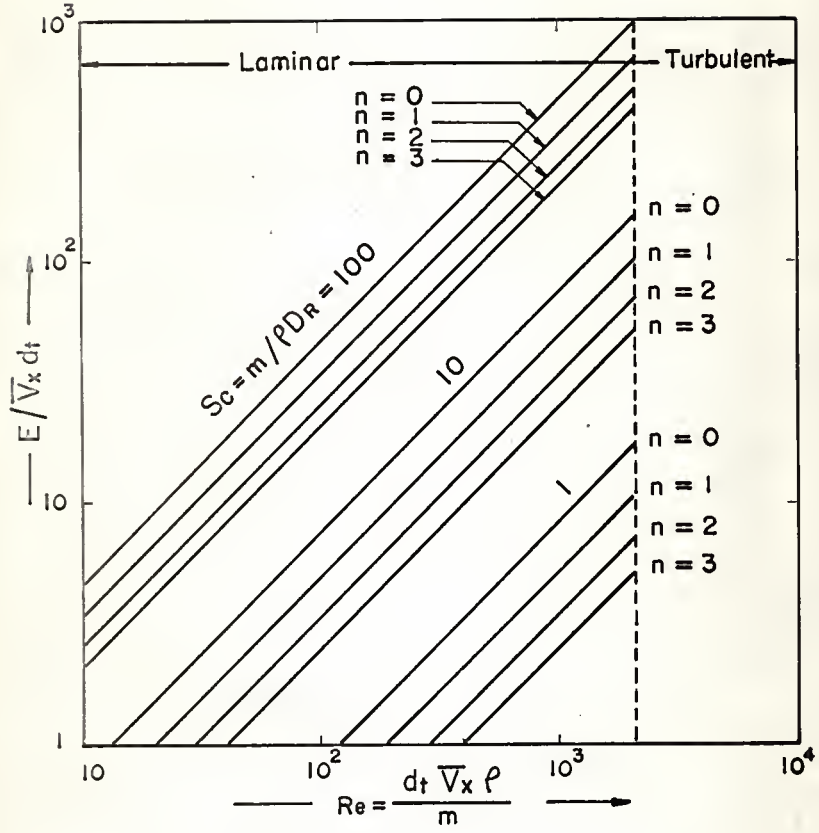

Fig. 30. Correlation of the dispersion coefficient in a cylindrical tube with Schmidt number as a parameter.

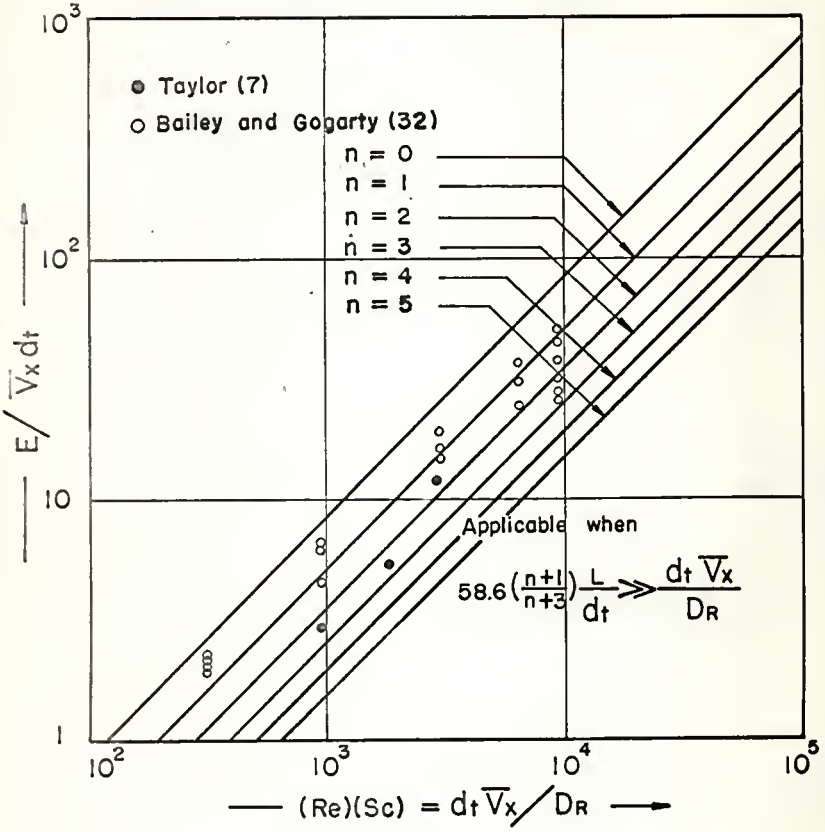

Fig. 31. Correlation of dispersion coefficient in laminar flow in a cylindrical tube as a function of the product of Reynolds and Schmidt numbers.

axes which move with the mean fluid velocity, Equation (7) can be reduced to a one-dimensional diffusion equation represented by Equation (31) with the overall dispersion coefficient E defined by

$$E = \frac{R^2 \bar{V}_x^2}{D_R}\left[\frac{1}{2(n+3)(n+5)}\right]$$

In order to derive Equation (31) analytically, it has been assumed that n is either zero or a positive integer. If n is a positive non-integer, solution of Equation (18), a consequence after a transformation of Equation (7), becomes impossible without the aid of a numerical analysis. Figures 23 through 29 have only shown the cases when the values of n are 0, 1, 2, 3, and infinity. When n is a positive non-integer, $\underline{E}(\theta)$ can still be found by merely using interpolation techniques. However, in order to enable one to obtain accurate values of $\underline{E}(\theta)$ for n different from either zero or a positive integer, a family of curves, $\underline{E}(\theta)$ vs. n for M = 1 with θ as a parameter has been presented on Figure 32 based on Equation (34). This figure shows that $\underline{E}(\theta)$ becomes infinite or finite depending on the value of θ as n increases without bound.

As the dimensionless parameter, M, decreases to zero the behavior of fluid flow becomes the plug flow case. When M increases to infinity, the model used approaches the backmix flow case. It is also true that the model becomes plug flow as $n \longrightarrow \infty$. Naturally, all equations so far derived from Equation (7) can be reduced to the result predicted by Taylor

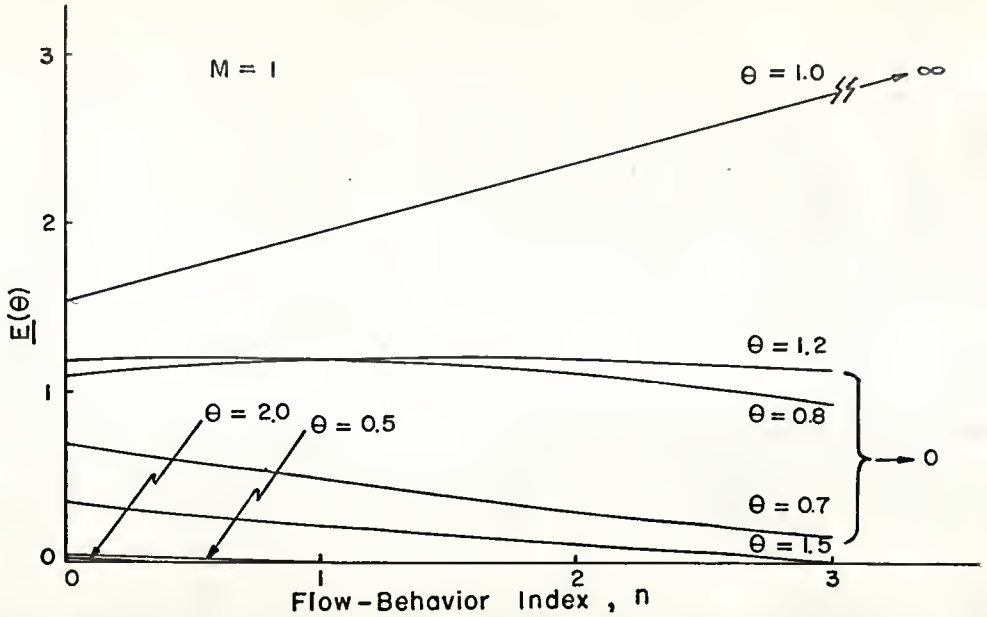

Fig. 32. E curves vs. n for laminar flow of Ostwald-de Waele model fluids with M and Θ as parameters.

for n = 1, i.e., for Newtonian flow.

The first moment about the origin and the second moment about the mean for the dispersion model are also presented to indicate the mean and the spread of the exit age distribution curve about the mean. The $\underline{E}(\theta)$ curves coupled with Equations (44) and (46) or (47) enable one to calculate M and consequently E for the fluid of known n.

Recently, Bailey and Gogarty (32) solved Equation (7) directly for the case n = 1 by using a numerical method. The range of dimensionless time, $D_R t/R^2$, considered by them was from 0 to 6. Experiments on measuring dispersion coefficient of a dilute solution of potassium permanganate (0.15 % by weight) in water flowing in a capillary tube of 0.1 cm in diameter were performed. They obtained a good agreement between a numerical solution and experimental results. They also compared their numerical solutions with Taylor's two approximate solutions of Equation (7). The first solution was presented as a variation from the concentration at the center of the tube, C_o^*, and was given in his first paper as (7)

$$C_1^* = C_o^* + \left(\frac{R^2}{4D_R\bar{t}}\right)\left(\frac{\partial C_o^*}{\partial \eta_1}\right)\left(\rho^2 - \frac{1}{2}\rho^4\right) \tag{53}$$

The second solution was given as a variation from the mean concentration, C_m^*, and was presented in his third paper as (9)

$$C_2^* = C_o^* + \left(\frac{R^2}{4D_R\bar{t}}\right)\left(\frac{\partial C_m^*}{\partial \eta_1}\right)\left(-\frac{1}{3} + \rho^2 - \frac{1}{2}\rho^4\right) \tag{54}$$

It should be noted that the latter can also be obtained from the result of this work, Equation (23), by setting n = 1.

Mathematically, the above two equations differ only by a constant ratio. However, in analyzing the data, it is more logical to use Equation (54) rather than to use Equation (53) because C_m^* is the quantity more directly measurable than C_o^* (9). The numerical solution by Bailey et al. also showed that both solutions, Equations (53) and (54), are good approximations but that the use of C_2^* yields somewhat better agreement than C_1^*.

Farrel and Leonard (33) also solved Equation (7) for the case n = 1, however, they did not directly use a numerical method. They first obtained the Laplace transformation of the residence time distribution function resulting from a Dirac delta function input as shown in Equation (3.21). Second, they used a numerical method to solve the transformed equation and to compare with Taylor's work (7, 9) for a definite range of operating conditions. However, from observation of their results (33), Taylor's model still has merit in representing real systems because of its simplicity when the assumptions proposed by Taylor are valid.

However, it is important to remember that neither Bailey and Gogarty's work (32) nor Farrel and Leonard's work (33) treated non-Newtonian flow.

It has been mentioned that one is able to calculate the overall dispersion coefficient, E, for the fluid of known n by using $\underline{E}(\theta)$ curves and Equations (44) and (46). In addition, E can also be estimated by using Figure 31. Figure 31 is the

correlation of $E/\bar{V}_x d_t$ of the fluid in laminar flow region in a tube as a function of the product of Reynolds and Schmidt numbers, $d_t \bar{V}_x / D_R$. The value of n appears as a parameter in the figure. It clearly shows that when n = 1, the curve is the same as that derived by Taylor (7, 9). Experimental data by Taylor (7) and Bailey and Gogarty (32) are also presented in Figure 31 for comparison. The figure shows that the experimental results of Bailey and Gogarty agree fairly closely with the Taylor's solution. But the agreement is not equally good over the entire time range considered.

In conclusion, all the results of this work reduce to those obtained for Newtonian flow when the flow-behavior index, n, approaches one. Also, for a given flow condition, the degree of dispersion decreases inversely proportional to $8(n + 3)(n + 5)$ as given by Equation (52) as the fluid behavior changes from dilatant characteristics ($n<1$) to pseudoplastic characteristics ($n>1$).

VI. OUTLINE OF PROPOSED RESEARCH WORK

In the previous chapters, treatment is confined to dispersion of Bingham plastics and Ostwald-de Waele fluids with steady velocity profiles in the isothermal laminar flow region. Geometrical configurations used in developing convective models are those of circular and rectangular conduits while an open-open cylindrical tube has been used to develop the dispersion model.

In this chapter, some of the problems of considerable importance, which may be investigated by immediate applications or minor modifications of the methods developed in this work, are summarized.

1. Laminar Flow of non-Newtonian Fluids other than Ostwald-de Waele Fluids and Bingham Plastics in Circular Pipes

So far, attention has been focused on the Ostwald-de Waele fluid and Bingham plastics. Other non-Newtonian fluids, however, are also worthy of consideration. Dilatant fluids, for instance, display a rheological behavior opposite to that of the Ostwald-de Waele fluid in that the apparent viscosity increased with increasing shear rate, or ν is greater than unity in Equation (2.37). Examples of dilatant fluids are those of starch, potassium silicate and gum arabic in water. Therefore, it would be most interesting to have the work extended to include these non-Newtonians.

2. Non-Newtonian Fluid Dispersions in Non-Circular Conduits

Most analytical and experimental investigations on fluid dispersion have been confined mainly to Newtonian fluids in circular tubes, probably for simplicity. Many problems arising in industry are those of non-Newtonian fluids in non-circular conduits. Therefore, research on the fluid dispersion of non-Newtonian fluids in such geometrical configurations is of great importance.

3. The Convective and Dispersion Models for Non-Newtonian flow with Slip Velocity

Development of convective models for Bingham plastic fluids and dispersion models for both Bingham plastic fluids and Ostwald-de Waele fluids in a cylindrical tube with slip velocity at the wall is suggested.

4. Solutions of Equation (5.7) Using a Numerical Method and Following the Farrel and Leonard (33) Approach

Equation (5.31) was derived by assuming flow behavior index, n, to be zero or a positive integer, since the overall dispersion coefficient, E, in Equation (5.31) is defined as

$$E = \frac{R^2 \bar{V}_x^2}{D_R} \left[\frac{1}{2(n+3)(n+5)} \right]$$

where n is a positive integer or zero. In case n is not a positive integer, the solution of Equation (5.7) will be difficult to obtain without the aid of a numerical method.

Furthermore, the original two-dimensional diffusion equation may be solved using Farrel and Leonard's approach, i.e., Laplace transformation, the method of separation of variables, and power series solution are suggested (46). The mean, variance, and skewness of the $\underline{E}(\theta)$ curves may then be computed. The results can be compared with the uniaxial Taylor dispersion, and a perfectly-mixed-tanks-in-series models. The extension of the method of analysis used for the laminar flow region to the turbulent flow region is also recommended.

5. Experimental Verification of the Models Developed

Mathematical modeling is a very useful, time saving tool, but like any mathematical approach, its validity must be tested by experiment because of assumptions involved in developing a model. The use of radioactive isotopes, electrolytes, dye stuffs, and temperature perturbation are methods by which dispersion mechanisms of fluids can be investigated. The objective can be attained by experimentally measuring $\underline{E}(\theta)$ and comparing the values with those predicted by the use of the models.

Diffusivity and shear rate data for some slurries and a polymer solution are available (47, 48, 49). The following table was presented by Clough et al. (48).

DIFFUSIVITY OF BENZOIC ACID IN A 14.2% ATTACLAY SLURRY AT 25°C

Fluid mix	Shear rate, $sec.^{-1}$	Fluid viscosity, centipoise	Diffusivity, sq. cm./sec.
I	1,480	11.	0.90×10^{-5}
I	6,200	7.0	1.21
I	9,100	5.7	0.96
II	3,260	63.	0.69
II	10,500	45.	0.60

6. Extension of Taylor (7, 8) and Tichacek (10) Models to Non-Newtonian Turbulent Flow

One of the difficulties in extending Taylor's work into the transition or lower turbulent regions arises from his use of a universal velocity profile. This profile is valid only in fully developed turbulence. Tichacek et al. repeated Taylor's analysis by using measured profiles. Vanderveen (36) determined the dispersion coefficients in the lower turbulent region of flow between Reynolds numbers of 4,000 and 10,000. All of their work considered only Newtonian flow.

In this phase of the proposed research an experimental approach can be employed in determining the dispersion coefficient in terms of $D_L/\bar{V}_x d_t$ versus Reynolds numbers, Re, for non-Newtonian fluids in circular pipes in the transition and fully developed turbulent regions. Work can also be extended to include non-circular conduits. The effect of enhanced dispersions induced by mechanical as well as gas agitations also should be considered.

7. Effects of Bends, Elbows, Valves, etc. on the Dispersion Coefficients of Non-Newtonian Fluids

Industrially, fittings such as bends, elbows, and valves, etc., bring about major effects on fluid dispersion. Determination of equivalent length of the fittings in terms of straight pipe from the stand point of fluid dispersion effects would be most interesting. The information obtained could be used for better piping design.

8. Minimization of Axial Dispersion for Non-Newtonians by Using Secondary Flow in Helical Tubes (50)

It has been known (5) that many continuous chemical reactors give the greatest conversion when axial dispersion is minimized, that is, when plug flow occurs. It has been suggested that the use of helical tubes promote plug flow by producing secondary currents. Experimental work for such an approach is of importance.

9. Study of Drag Reduction for Non-Newtonian Systems

Drag or friction reduction of Non-Newtonians in laminar and turbulent pipe flows may be attained by adding certain types of solvent in the fluids (51). For example, friction reduction as great as 35% was reported by adding 5 ppm of polymeric material to water (52).

10. Viscoelastic Stability and Flow Noise for Non-Newtonian Fluids

It has been reported (53) that the stability of the laminar

boundary layer in an annular test section is increased when small concentrations of a polymeric additive are introduced into the fluid stream. It has been shown that, in turbulent flow, the flow noise associated with the turbulence is appreciably increased when the additive is present. Further study of such phenomena in relation to dispersion may be desirable.

11. Effects of the Fluid Dispersion on the Chemical Reaction

For simplicity, first-order chemical reaction occurring in laminar flow of Ostwald-de Waele fluids with axial and radial diffusion should be considered first. The work could then be extended to include other fluids and reactions.

12. Extension of the Techniques Developed to Non-Newtonian Liquid-Solid Fluidized Beds

Dynamic analysis of liquid-solid fluidized beds by using non-Newtonian fluids instead of water, which has always been used heretofore, is suggested.

13. Extension of the Convective and Dispersion Models to Polar Fluids

The fluid dynamics of polar fluids have been discussed recently (54). The stress tensor for polar fluids was described as being composed of two parts, $\overrightarrow{\overrightarrow{\tau}} = \overrightarrow{\overrightarrow{\tau}}_s + \overrightarrow{\overrightarrow{\tau}}_a$, where $\overrightarrow{\overrightarrow{\tau}}_s$ (the symmetric part) depends upon the rate of strain associated with the symmetrized velocity gradient tensor in a manner identical to a structureless Newtonian fluid, and $\overrightarrow{\overrightarrow{\tau}}_a$ (the skew-symmetric part) depends only upon the strain arising from opposition

between internal spin and external spin or vorticity. Based on these facts, velocity profiles of polar fluids will be different from those derived by merely assuming fluids to be Newtonian or non-Newtonian. Hence, the development of convective and dispersion models for polar fluids becomes interesting.

14. The Application of Wolf and Resnick's Model (55) and other Similar Models to Non-Newtonian Dispersions

A method of representing a residence time distribution in real systems has been presented by Wolf and Resnick (55). The use of their model and other models (37, 56) for non-Newtonian fluids in analyzing residence time distribution functions will be an important tool in the study of continuous flow systems.

15. Continuous Mixing of Non-Newtonian Fluids in an Annular Channel and Flowing Through a Rotating Tube (37, 57, 58)

Continuous mixing of two or more than two streams of non-Newtonians such as molten polymer in an cylindrical annulus and/or flowing through a rotating tube is of practical importance.

16. Effects of Magnetic Fields on the Taylor Dispersion for Newtonian and Non-Newtonian Fluids

Suppose that there are impurities in fluids such as liquid metals, imposed in magnetic fields, the study of the effect of such fields on the dispersion of impurities in the fluids flowing through a slit between two parallel plates is of considerable interest. Since the analytical solutions to the

equation of motion have been given by Sarpkaya (59), direct application of his results may be helpful.

ACKNOWLEDGEMENT

The author wishes to express his sincere appreciation to Dr. Liang-tseng Fan, for his constant enthusiasm and advice during the process of this work, and for his permission to use his unpublished note on fluid dispersion; Dr. William H. Honstead, Head of the Department of Chemical Engineering, for his help and encouragement; Dr. William L. Stamey, for reading the manuscript; the K. S. U. Engineering Experiment Station for supporting this work (Project 299 supervised by Dr. Liang-tseng Fan); and the K. S. U. Computer Center for use of IBM 1620.

APPENDICES

1. Step Function (40)

The unit step function $U_s(t-a)$ is defined as follows:

$$U_s(t-a) = \begin{cases} 0 \ , & t<a \\ 1 \ , & t>a \end{cases} \tag{1}$$

The Laplace transformation of $U_s(t-a)$ is

$$L\left\{U_s(t-a)\right\} = \int_0^\infty e^{-st}\, U_s(t-a)dt = \int_a^\infty e^{-st}\, dt$$

$$= -\frac{1}{s} e^{-st} \Big|_a^\infty$$

Hence, we have

$$L\left\{U_s(t-a)\right\} = \frac{1}{s} e^{-sa} \tag{2}$$

2. Dirac Delta Function

The delta function is the idealization of functions that vanish outside a short interval. It is, therefore, possible to approximate the delta function by such functions (60).

Let $f_n(t)$ be a function on $(-\infty,\infty)$ satisfying the following conditions (61, 62):

$$f_n(t) = \begin{cases} 0 \ , & t<0 \\ n \ , & 0\leq t\leq 1/n \\ 0 \ , & 1/n<t \end{cases} \tag{3}$$

If n is very large this differs from zero only in a small neighborhood of the origin. For all n

$$\int_{-\infty}^{\infty} f_n(t)dt = \int_{0}^{\infty} f_n(t)dt = \int_{0}^{1/n} n\,dt = n\int_{0}^{1/n} dt = 1 \qquad (4)$$

If g(t) is any other function, then

$$\int_{-\infty}^{\infty} f_n(t)g(t)dt = \int_{0}^{\infty} f_n(t)g(t)dt = n\int_{0}^{1/n} g(t)dt$$

$$= n\int_{0}^{1/n} \left[g(0) + tg'(0) + \frac{1}{2!}t^2 g''(0) + \ldots \right] dt$$

$$= g(0) + \frac{1}{2!n}g'(0) + \frac{1}{3!n^2}g''(0) + \ldots \qquad (5)$$

Now let $n \to \infty$ and call

$$\lim_{n\to\infty} f_n(t) = \delta(t) \qquad (6)$$

Then if the limit exists within the integral, one has

$$\int_{-\infty}^{\infty} \delta(t)g(t)dt = \lim_{n\to\infty} \int_{-\infty}^{\infty} f_n(t)g(t)dt = g(0) \qquad (7)$$

Similarly,

$$\int_{-\infty}^{\infty} \delta(t-a)g(t)dt = g(a) \quad , \quad a>0 \qquad (8)$$

Other properties of the Dirac delta function are

$$\delta(t-a) = 0 \quad , \quad t \neq a$$

$$\int_{-\infty}^{\infty} \delta(t-a)dt = 1$$

$$L\left\{\delta(t-a)\right\} = e^{-sa} \quad , \quad a \geq 0$$

$$U_s'(t-a) = \delta(t-a)$$

3. Derivation of Equations (4.5) and (4.6)

General rheological statements of the Bingham plastic are (6)

$$\vec{\vec{\tau}} = -\left\{\mu_o - \frac{\tau_o}{\left[\frac{1}{2}(\vec{\vec{\Delta}} : \vec{\vec{\Delta}})\right]^{\frac{1}{2}}}\right\} \quad , \quad \frac{1}{2}(\vec{\vec{\tau}} : \vec{\vec{\tau}}) > \tau_o^2 \tag{9}$$

$$\vec{\vec{\Delta}} = 0 \quad , \quad \frac{1}{2}(\vec{\vec{\tau}} : \vec{\vec{\tau}}) < \tau_o^2 \tag{10}$$

From Equation (9) and also because τ_{rx} and Δ_{rx} are the only non-vanishing components of $\vec{\vec{\tau}}$ and $\vec{\vec{\Delta}}$ respectively, one obtains

$$(\vec{\vec{\Delta}} : \vec{\vec{\Delta}}) = \Delta_{ij}\Delta_{ji} = \Delta_{rx}\Delta_{xr} + \Delta_{xr}\Delta_{rx}$$

$$= 2\Delta_{rx}^2 = 2\left(\frac{dV_x}{dr}\right)^2 \tag{11}$$

for the symmetric system. Similarily, one obtains

$$(\vec{\vec{\tau}} : \vec{\vec{\tau}}) = 2\tau_{rx}^2 \tag{12}$$

Based on Equations (11) and (12), Equations (9) and (10) can thus be simplified to Equations (4.5) and (4.6) as

$$\tau_{rx} = \tau_o - \mu_o \frac{dV_x}{dy_r} \quad , \quad \tau_{rx} > \tau_o \tag{4.5}$$

$$\frac{dV_x}{dr} = 0 \quad , \quad \tau_{rx} < \tau_o \tag{4.6}$$

4. Derivation of Equation (4.11)

From Bird et al. (6) (Equation (2.3-25) in p. 50 of TRANSPORT PHENOMENA)

$$V_x(r) = \frac{(-\Delta P)R^2}{4\mu_o L}\left[1 - \left(\frac{r}{R}\right)^2\right] - \frac{\tau_o R}{\mu_o}\left[1 - \left(\frac{r}{R}\right)\right] \quad \text{for } r \geq r_o \tag{13}$$

where

$$\tau_o = \frac{(-\Delta P)r_o}{2L} \tag{14}$$

This is equivalent to

$$V_x(r) = \frac{(-\Delta P)R^2}{4\mu_o L}\left[1 - \left(\frac{r}{R}\right)^2\right] - \frac{(-\Delta P)r_o R}{2\mu_o L}\left[1 - \left(\frac{r}{R}\right)\right]$$

$$= \frac{(-\Delta P)R^2}{4\mu_o L}\left[1 - \left(\frac{r}{R}\right)^2 - \frac{2r_o}{R} + \left(\frac{r}{R}\right)\left(\frac{2r_o}{R}\right)\right]$$

$$= \frac{V_m}{(1-\xi)^2}\left[1 - \left(\frac{r}{R}\right)^2 - 2\xi + 2\left(\frac{r}{R}\right)\xi\right] \tag{15}$$

where

$$V_m = \frac{(-\Delta P)R^2}{4\mu_o L}(1-\xi)^2$$

$$\xi = \frac{r_o}{R}$$

Equation (15) can be rewritten as

$$V_x(r) = \frac{V_m}{(1-\xi)^2}\left[(1-\xi)^2 - (1-\xi)^2 + 1 - \left(\frac{r}{R}\right)^2 - 2\xi + 2\left(\frac{r}{R}\right)\xi\right]$$

$$= V_m\left[1 - \frac{\left(\frac{r}{R}-\xi\right)^2}{(1-\xi)^2}\right] \qquad (4.11)$$

5. Derivation of Equation (4.12)

Starting from Equation (2.3-27) on p. 50 of TRANSPORT PHENOMENA by Bird et al. (6), and Equation (4.11), one obtains

$$Q = \int_0^{2\pi}\int_0^R V_x(r)\, r\, d\, r\, d\, \theta \qquad (16)$$

$$= 2\pi\left[\int_0^{r_o} V_m r\, d\, r + \int_{r_o}^R V_x(r) r\, d\, r\right]$$

$$= 2\pi V_m\left[\frac{R^2}{2} - \frac{1}{(1-\xi)^2}\int_{r_o}^R \left(\frac{r}{R}-\xi\right)^2 r\, d\, r\right]$$

$$= 2\pi V_m\left\{\frac{R^2}{2} - \frac{1}{(1-\xi)^2}\left[\frac{1}{4R^2}\left(R^4 - r_o^4\right) + \frac{\xi^2}{2}\left(R^2 - r_o^2\right) - \frac{2\xi}{3R}\right.\right.$$

$$\left.\left.\cdot\left(R^3 - r_o^3\right)\right]\right\}$$

$$= 2\pi V_m R^2\left[\frac{1}{2} - \frac{1}{(1-\xi)^2}\left(\frac{1}{4} - \frac{2}{3}\xi + \frac{1}{2}\xi^2 - \frac{1}{12}\xi^4\right)\right]$$

$$= \frac{(-\Delta P)\pi R}{8\mu_o L}\left(1 - \frac{4}{3}\xi + \frac{1}{3}\xi^4\right)$$

or

$$\bar{V}_x = \frac{Q}{\pi R^2} = \frac{(-\Delta P)R^2}{8\mu_o L}\left(1 - \frac{4}{3}\xi + \frac{1}{3}\xi^4\right) \qquad (4.12)$$

6. Derivation of Equation (4.24)

Equation (4.18) can be written as

$$\underline{F_2}(\theta) = \int_{r_o}^{r} \frac{2V_m}{\bar{V}_x} \left[1 - \frac{(\frac{r}{R} - \xi)^2}{(1 - \xi)^2}\right] (\frac{r}{R}) d(\frac{r}{R}) \tag{17}$$

From Equations (4.11) and (4.14), we know that

$$\frac{r}{R} = \xi + (1-\xi) \left[1 - \frac{V_x(r)}{V_m}\right]^{\frac{1}{2}}$$

$$= \xi + (1-\xi) \left[1 - \frac{V_x(r)}{2\bar{V}_x}\right]^{\frac{1}{2}}$$

$$= \xi + (1-\xi) \left[1 - \frac{\alpha L/\bar{V}_x}{2L/V_x(r)}\right]^{\frac{1}{2}}$$

$$= \xi + (1-\xi) (1 - \frac{\alpha}{2\ t/\bar{t}})^{\frac{1}{2}}$$

$$= \xi + (1-\xi) (1 - \frac{\alpha}{2\theta})^{\frac{1}{2}} \tag{18}$$

and

$$d(\frac{r}{R}) = \frac{(1-\xi)\alpha}{4\theta^2} \frac{d\theta}{(1 - \frac{\alpha}{2\theta})^{\frac{1}{2}}} \tag{19}$$

Substituting Equations (18), (19), and (4.14) into Equation (17) yields

$$\underline{F}_2(\theta) = \int_{\frac{\alpha}{2}}^{\theta} \frac{(1 - \xi)^{\alpha}}{2\theta^3} \left[\frac{\xi}{\sqrt{(1 - \frac{\alpha}{2\theta})}} + 1 - \xi \right] d\theta \qquad (4.24)$$

7. Derivation of Equations (4.28) and (4.29)

Repeating Equation (2.37)

$$\vec{\vec{\tau}} = - \left\{ m \left| \left[\frac{1}{2} \left(\vec{\vec{\Delta}} : \vec{\vec{\Delta}} \right) \right]^{\frac{1}{2}} \right|^{\nu - 1} \right\} \vec{\vec{\Delta}} \qquad (2.37)$$

For a one-dimensional rheological problem (37), the following expressions are valid:

$$\left(\vec{\vec{\Delta}} : \vec{\vec{\Delta}} \right) = 2 \left(\frac{dV_x}{dr} \right)^2$$

$$\vec{\vec{\tau}} = \tau_{rx}$$

Therefore, Equation (4.28) can be obtained as

$$\tau_{rx} = - m \left| \frac{dV_x}{dr} \right|^{\nu - 1} \frac{dV_x}{dr} \qquad (4.28)$$

Because, in pipe flow, $\frac{dV_x}{dr}$ is everywhere negative, the above equation becomes

$$\tau_{rx} = m \left(- \frac{dV_x}{dr} \right)^{\nu} \qquad (4.29)$$

8. Derivation of Equation (4.43)

From the equation of motion, we have

$$\frac{\partial \tau_{yx}}{\partial y} = - \frac{\partial P}{\partial x} \qquad (20)$$

Combining this equation with Equation (4.40) and solving the resulting equation subject to the boundary conditions.

$$\tau_{yx} = 0 \quad \text{at} \quad y = 0 \tag{21}$$

$$V_x(y) = 0 \quad \text{at} \quad y = H \tag{22}$$

One has

$$V_x(y) = \frac{(-\Delta P)H^2}{2\mu_o L}\left[1 - \left(\frac{y}{H}\right)^2\right] - \frac{\tau_o H}{\mu_o}\left[1 - \left(\frac{y}{H}\right)\right], \quad y \geq y_o \tag{23}$$

$$V_m = \frac{(-\Delta P)H^2}{2\mu_o L}(1 - \zeta)^2, \quad y \leq y_o \tag{24}$$

where

$$\zeta = \frac{y_o}{H}$$

Since $\tau_o = (\frac{-\Delta P}{L})y_o$, Equation (23) becomes

$$V_x(y) = \frac{(-\Delta P)H^2}{2\mu_o L}\left[1 - \left(\frac{y}{H}\right)^2\right] - \frac{(-\Delta P)H}{\mu_o L}\left[1 - \left(\frac{y}{H}\right)\right] \tag{25}$$

Using the same technique of manipulation employed in 4, one obtains

$$V_x(y) = V_m\left[1 - \frac{\left(\frac{y}{H} - \zeta\right)^2}{(1 - \zeta)^2}\right] \tag{4.43}$$

9. Derivation of Equation (4.44)

Since

$$Q = \int_0^W \int_{-H}^{H} V_x(y)\, dydZ$$

$$= 2W\left\{\int_0^{y_o} V_m dy + \int_{y_o}^{H} V_x(y)dy\right\} \qquad (26)$$

Equations (4.42) and (4.43) can be substituted into the above equation to obtain Q by using the same technique employed in 5. Thus,

$$Q = 2W\left\{\int_o^{y_o} V_m dy + \int_{y_o}^{H} V_m \left[1 - \frac{(\frac{V}{H} - \zeta)^2}{(1 - \zeta)^2}\right] dy\right\}$$

$$= \frac{2}{3}\frac{(-\Delta P)WH^3}{\mu_o L}(1 - \frac{3}{2}\zeta + \frac{1}{2}\zeta^3) \qquad (27)$$

where

$$\zeta = \frac{y_o}{H}$$

Since $\bar{V}_x = \frac{Q}{2WH}$, one obtains

$$\bar{V}_x = \frac{(-\Delta P)H^2}{3\mu_o L}(1 - \frac{3}{2}\zeta + \frac{1}{2}\zeta^3) \qquad (4.44)$$

10. Derivation of Equation (4.51)

From Equation (4.43), one has

$$\frac{V}{H} = \zeta + (1 - \zeta)\left[1 - \frac{V_x(y)}{V_m}\right]^{\frac{1}{2}}$$

$$= \zeta + (1 - \zeta)\left[1 - \frac{2\beta\, V_x(y)}{3\,\bar{V}_x}\right]^{\frac{1}{2}}$$

$$= \zeta + (1 - \zeta)\left(1 - \frac{2\beta}{3\theta}\right)^{\frac{1}{2}}$$

Hence,

$$d\left(\frac{y}{H}\right) = \frac{(1 - \zeta)\beta}{3\theta^2} \frac{d\theta}{\left(1 - \frac{2\beta}{3\theta}\right)^{\frac{1}{2}}} \tag{28}$$

Substituting this equation into Equation (4.49) yields

$$\underline{F_2}(\theta) = \int_{\frac{2}{3}\beta}^{\theta} \frac{(1 - \zeta)\beta}{3\theta^2} \frac{d\theta}{\left(1 - \frac{2\beta}{3\theta}\right)^{\frac{1}{2}}} \tag{4.51}$$

11. Computer Program (IBM 1620, FORTRAN II) for Computing Equations (4.72), (4.73), (4.74), and (4.75).

Notations Used In The Computer Program

R = γ , B = n , C = θ , DELTC = $d\theta$

A = (n+3)(1-γ) , F = (n+1)$\left(\frac{1}{\theta} - \gamma\right)$

$$G = \left[1 - \frac{(n+1)\left(\frac{1}{\theta} - \gamma\right)}{(n+3)(1 - \gamma)}\right]^{\frac{n-1}{n+1}}$$

D = $\underline{E}(\theta)$ in Equation (4.73)

E = $\underline{E}(\theta)$ in Equation (4.75)

S = $\underline{F}(\theta)$ in Equation (4.72)

P = $\underline{F}(\theta)$ in Equation (4.74)

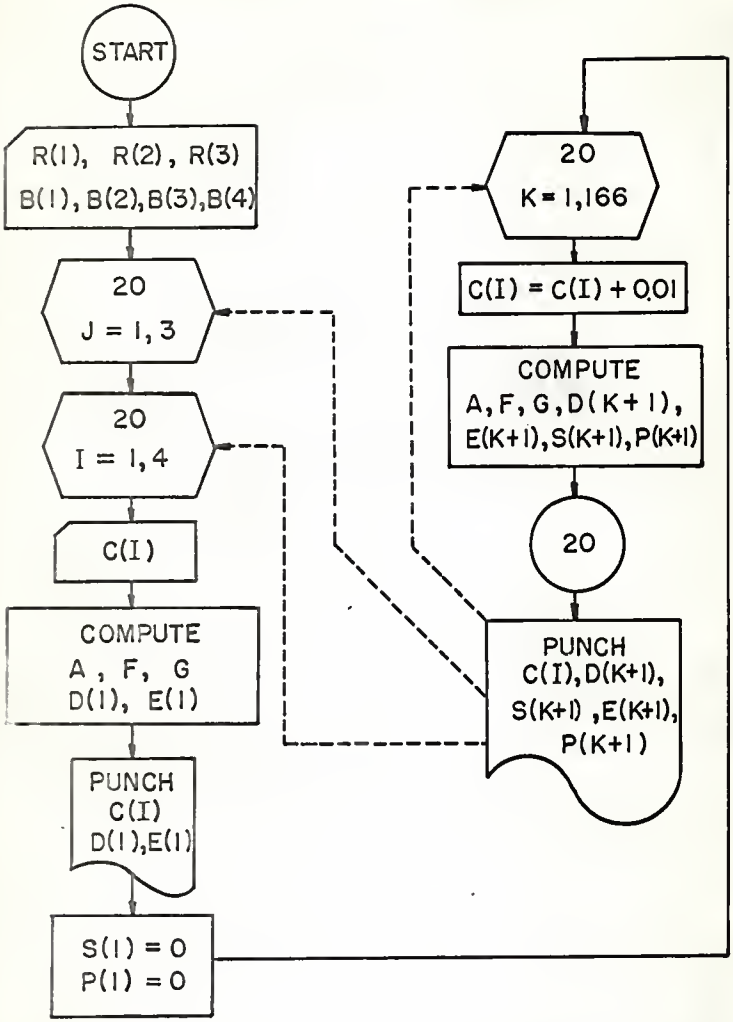

Fig. 33. Flow chart for computing Equations (4.72), (4.73), (4.74), and (4.75).

```
C       F AND E CURVES WITH SLIP VEL AT WALL
C       BY TRAPEZOIDAL RULE WITH DELTC=0.01
        DIMENSION R (3),B(4),E(167),D(167),S(167),P(167),C(4)
      1 FORMAT (3F4.1)
      2 FORMAT (4F4.1)
     10 FORMAT (3E10.4)
     21 FORMAT (5E10.4)
        READ 1, R(1), R(2), R(3)
        READ 2, B(1), B(2), B(3), B(4)
        DO 20 J=1,3
        DO 20 I=1,4
        READ 10, C(I)
        A=(B(I)+3.0)*(1.0-R(J))
        F=(B(I)+1.0)*(1.0/C(I)-R(J))
        G=(1.0-F/A)**((B(I)-1.0)/(B(I)+1.0))
        D(1)=(2.0/A)*(1.0/((C(I)**2)*G))
        E(1)=(2.0/A)*(1.0/((C(I)**3)*G))
        PUNCH 10, C(I), D(1), E(1)
        S(1)=0
        P(1)=0
        DO 20 K=1,166
        C(I)=C(I)+0.01
        A=(B(I)*3.0)*(1.0-R(J))
        F=(B(I)+1.0)*(1.0/C(I)-R(J))
        G=(1.0-F/A)**((B(I)-1.0)/(B(I)+1.0))
        D(K+1)=(2.0/A)*(1.0/((C(I)**2)*G))
        E(K+1)=(2.0/A)*(1.0/((C(I)**3)*G))
        S(K+1)=S(K)+0.005*(D(K)+D(K+1))
        P(K+1)=P(K)+0.005*(E(k)+E(K+1))
     20 PUNCH 21, C(I), D(K+1), S(K+1), E(K+1), P(K+1)
        STOP
        END
```

Data Used

γ

.0 0.4 0.8

n

.0 0.5 1.0 2.0

θ

.3334E - 00	for γ = 0, n = 0
.4286E - 00	for γ = 0, n = 0.5
.5001E - 00	for γ = 0, n = 1.0
.6001E - 00	for γ = 0, n = 2.0
.4546E - 00	for γ = 0.4, n = 0
.5556E - 00	for γ = 0.4, n = 0.5
.6251E - 00	for γ = 0.4, n = 1.0
.7143E - 00	for γ = 0.4, n = 2.0
.7143E - 00	for γ = 0.8, n = 0
.7895E - 00	for γ = 0.8, n = 0.5
.8334E - 00	for γ = 0.8, n = 1.0
.8824E - 00	for γ = 0.8, n = 2.0

12. Derivation of Equations (4.82), (4.83), (4.84) (7)

The velocity profile of the Ostwald-de Waele fluid is, repeating Equation (4.32),

$$V_x(r) = V_m \left[1 - \left(\frac{r}{R}\right)^{n+1} \right] \tag{4.32}$$

If the tracer at time t = 0 is distributed symmetrically, the concentration of a tracer, C, can be written as

$$C = C(x, r) \tag{29}$$

Then, after time t, the concentration will be

$$C = C(x, r, t) = C \left[x - V_x(r)\, t, r \right] \tag{30}$$

The mean value, C_m of the tracer concentration over a cross-

section of a tube is defined by

$$C_m = \frac{2}{R^2} \int_0^R C\, r\, dr \tag{31}$$

The response to an impulse input of a tracer is derived as follows:

Initially the space between two planes x = 0 and x = X (X/R being small) is filled with a tracer of concentration C_o. From Equation (30) it will be seen that the amount of the tracer, which lies between r + δr is constant during the flow and equal to $2\pi r\, C_o \times \delta r$. The tracer will be distorted in time into

$$x = V_m t \left[1 - \left(\frac{r}{R}\right)^{n+1}\right] \tag{32}$$

The total amount of the tracer between x and x + δx is therefore $2\pi r\, C_o \times \frac{dr}{dx}\, \delta x$ and from Equation (32) one has

$$\frac{r dr}{dx} = - \frac{R}{(n+1)V_m t} \left(\frac{R}{r}\right)^{n-1} \tag{33}$$

Substituting the expression of r/R from Equation (32) into Equation (33) one obtains

$$\frac{r dr}{dx} = - \frac{R^2}{n+1} \frac{1}{V_m t \left(1 - \frac{x}{V_m t}\right)^{\frac{n-1}{n+1}}}$$

Therefore,

$$C_m = \frac{1}{\pi R^2 \delta x} 2\pi C_o X \delta x \frac{R^2}{n+1} \frac{1}{V_m t \left(1 - \frac{x}{V_m t}\right)^{\frac{n-1}{n+1}}}$$

or

$$\left.\begin{aligned} C_m &= \frac{2}{n+1} \frac{C_o X}{V_m t \left(1 - \frac{x}{V_m t}\right)^{\frac{n-1}{n+1}}} \quad \text{for} \quad 0 < x < V_m t \\ &= 0 \qquad\qquad\qquad\qquad\qquad\quad \text{for} \quad x < 0 \quad \text{and} \quad x > V_m t \end{aligned}\right\} \quad (4.82)$$

For a step input of a tracer, the response to such a tracer input will be derived as follows:

Suppose that the tracer of constant concentration enters a tube which at time t = 0 congains only the fluid. Here

$$\left.\begin{aligned} C &= C_o \quad , \quad x < 0 \\ C &= 0 \quad , \quad x > 0 \end{aligned}\right\} \text{ at time } t = 0 \qquad (35)$$

This case can be solved by imagining that the constant initial concentration for $x < 0$ consists of a number of thin sections of the type imagined in the case mentioned above. In this way, it is found that

$$
\left.
\begin{aligned}
C_m &= C_o \quad , \quad x<0 \\
C_m &= C_o \left[1 - \frac{2}{n+1} \frac{x}{V_m t \left(1 - \frac{x}{V_m t}\right)^{\frac{n-1}{n+1}}} \right] , \quad 0<x<V_m t \\
C_m &= 0 \quad , \quad x>V_m t
\end{aligned}
\right\} \quad (4.83)
$$

When the input of a tracer is of a finite pulse, the situation is

$$
\left.
\begin{aligned}
C &= 0 \quad , \quad x<0 \\
C &= C_o \quad , \quad 0<x<X \\
C &= 0 \quad , \quad x>X
\end{aligned}
\right\} \text{ at time } t = 0 \qquad (36)
$$

This case can be obtained by superposing two examples of the second case (a response to a step input function), namely

$$
\left.
\begin{aligned}
C &= C_o \quad , \quad x<X \\
C &= 0 \quad , \quad x>X
\end{aligned}
\right\} \quad \text{and} \quad
\left.
\begin{aligned}
C &= -C_o \quad , \quad x<0 \\
C &= 0 \quad , \quad x>0
\end{aligned}
\right\} \qquad (37)
$$

then, if $t<X/V_m$, one can obtain Equation (4.84).

13. Derivation of Equation (5.9)

When $\frac{\partial C^*}{\partial \bar{\eta}} = 0$, Equation (5.7) becomes

$$
\frac{\partial C^*}{\partial \theta} = \frac{D_R \bar{t}}{R^2} \left(\frac{\partial^2 C^*}{\partial \rho^2} + \frac{1}{\rho} \frac{\partial C^*}{\partial \rho} \right) \qquad (38)
$$

The boundary condition is

$$\left.\frac{\partial C^*}{\partial \rho}\right|_{\rho=1} = 0 \tag{39}$$

In using the method of separation of variables, one assumes that the solution of Equation (38) is of the form

$$C^*(\theta,\rho) = F(\theta)\, G(\rho) \tag{40}$$

By differentiating Equation (40), one obtains

$$\frac{\partial C^*}{\partial \theta} = F'G, \qquad \frac{\partial C^*}{\partial \rho} = FG'$$

$$\frac{\partial^2 C^*}{\partial \rho^2} = FG''$$

By substituting these equations into Equation (38), one obtains

$$\frac{F'}{F} = \frac{D_R \bar{t}}{R^2}\left(\frac{G''}{G} + \frac{1}{\rho}\frac{G'}{G}\right) \tag{41}$$

The term on the left hand side of Equation (41) is, by definition, a function of θ, and while the right hand side is a function of ρ only. Since θ and ρ are both independent variables, the only way the equation can hold for all arbitrary values of the two variables is for each side to be a constant. For the time being, let this constant be $-\alpha^2$, then

$$\frac{F'}{F} = \frac{D_R \bar{t}}{R^2}\left(\frac{G''}{G} + \frac{1}{\rho}\frac{G'}{G}\right) = -\alpha^2 \tag{42}$$

This means

$$\frac{F'}{F} = -\alpha^2 \tag{43}$$

and

$$\frac{G''}{G} + \frac{1}{\rho}\frac{G'}{G} = -\alpha^2 \left(\frac{R^2}{D_R \bar{t}}\right) \tag{44}$$

Solving Equation (43) gives

$$F = B_1 \exp(-\alpha^2 \theta) \tag{45}$$

where B_1 is an arbitrary constant. Simplifying Equation (44), one obtains a Bessel equation

$$G'' + \frac{1}{\rho} G' + \left(\frac{\alpha^2 R^2}{D_R \bar{t}}\right) G = 0 \tag{46}$$

A general solution to this equation is (40)

$$G = B_2 J_o \left[\frac{\alpha R}{(D_R \bar{t})^{\frac{1}{2}}} \rho\right] + B_3 Y_o \left[\frac{\alpha R}{(D_R \bar{t})^{\frac{1}{2}}} \rho\right] \tag{47}$$

where B_2 and B_3 are constants and J_o and Y_o are the Bessel functions of the first and second kind of order zero respectively. Since the concentration of the tracer in the fluid is always finite while Y_o becomes infinite as ρ approaches zero, we cannot thus use Y_o and must choose $B_3 = 0$. Clearly, one thus has

$$C^*(\theta,\rho) = \sum_{m=1}^{\infty} A_m \exp\left(-\alpha_m^2 \theta\right) J_o \left[\frac{\alpha_m R}{(D_R \bar{t})^{\frac{1}{2}}} \rho\right]$$

$$m = 1, 2, 3, \ldots \qquad (48)$$

where

A_m = m-th eigen constant

α_m = m-th eigen value

14. Derivation of Equations (5.16) and (5.17)

Since the axes which move with the mean fluid velocity, we may write

$$x_1 = x - \bar{V}_x t = x - \left(\frac{n+1}{n+3}\right) V_m t \qquad (49)$$

where x_1 = moving axial position relative to the mean fluid velocity.

It is known that C is a function of x, r, and t only; that is

$$C = C\ (x, r, t) \qquad (50)$$

By using the chain rule of differentiation on Equations (49) and (50) one obtains

$$\frac{\partial C}{\partial x} = \frac{\partial C}{\partial x_1}$$

$$\frac{\partial C}{\partial t} = \frac{\partial C}{\partial t} - \bar{V}_x \frac{\partial C}{\partial x_1}$$

$$\frac{\partial C}{\partial r} = \frac{\partial C}{\partial r}$$

$$\frac{\partial^2 C}{\partial r^2} = \frac{\partial^2 C}{\partial r^2}$$

Substituting these relations into Equation (5.6) yields

$$\frac{\partial C}{\partial t} = D_R\left(\frac{\partial^2 C}{\partial r^2} + \frac{1}{r}\frac{\partial C}{\partial r}\right) - \bar{V}_x \left[\frac{2}{n+1} - \frac{n+3}{n+1}\left(\frac{r}{R}\right)^{n+1}\right] \frac{\partial C}{\partial x_1} \qquad (5.16)$$

By normalizing Equation (5.16) one obtains

$$\frac{\partial C^*}{\partial \Theta} = \frac{D_R \bar{t}}{R^2}\left(\frac{\partial^2 C^*}{\partial \rho^2} + \frac{1}{\rho}\frac{\partial C^*}{\partial \rho}\right) - \left(\frac{2}{n+1} - \frac{n+3}{n+1}\rho^{n+1}\right)\frac{\partial C^*}{\partial \eta_1} \qquad (5.17)$$

where

$$C^* = C/C^o$$

$$\Theta = \frac{t}{\bar{t}}$$

$$\rho = \frac{r}{R}$$

$$\eta_1 = \frac{x_1}{L}$$

15. Derivation of Equation (5.20)

Since $\frac{\partial C^*}{\partial \eta}_1$ has been taken as a constant in order to solve Equation (5.16), we may let

$$\beta = \left(\frac{R}{D_R \bar{t}}\right) \left(\frac{1}{n+1}\right) \frac{\partial C^*}{\partial \eta}_1 \tag{51}$$

Then Equation (5.18) becomes

$$\frac{d^2 C^*}{d\rho^2} + \frac{1}{\rho} \frac{dC^*}{d\rho} = \beta \left[2 - (n+3)\rho^{n+1} \right] \tag{52}$$

Equation (52) is a linear non-homogeneous ordinary differential equation, so that the general solution is the sum of a general solution C_h^* of the corresponding homogeneous equation and an arbitrary particular solution C_p^* of Equation (52) i.e.,

$$C^* = C_h^* + C_p^* \tag{53}$$

The corresponding homogeneous equation is

$$\frac{d^2 C^*}{d\rho^2} + \frac{1}{\rho} \frac{dC^*}{d\rho} = 0 \tag{54}$$

and its solution is

$$C^* = C_h^* = k_1 \ln \rho + k_2 \tag{55}$$

where k_1 and k_2 are integration constants.

Knowing that

$$\frac{\partial C^*}{\partial \rho} = 0 \quad \text{at} \quad \rho = 1,$$

and

$$C^* = C_o^* \text{ at } \rho = 0$$

One has

$$k_1 = 0 \quad \text{and} \quad k_2 = C_0^*$$

Equation (55) is, therefore,

$$C_h^* = C_0^* \tag{56}$$

It is first assumed that the solution is of the form

$$C^* = C_p^* = A_1 \rho + A_2 \rho^2 + \sum_{m=o}^{\infty} A_{m+3} \rho^{m+3}, \quad m = 1, 2, 3,.. \tag{57}$$

Substituting Equation (57) and its derivatives into Equation (52), one has

$$2A_2 + \sum_{m=o}^{\infty} (m+3)(m+2)A_{m+3} \rho^{m+1}$$

$$+ \frac{1}{\rho} A_1 + 2A_2 \rho + \sum_{m=o}^{\infty} (m+3)A_{m+3} \rho^{m+2}$$

$$= 2\beta - (n+3)\beta \rho^{n+1} \tag{58}$$

Simplifying the above equation, regardless if n is an integer or not, it becomes

$$\frac{A_1}{\rho} + (4A_2 - 2\beta) + \sum_{m=o}^{\infty} A_{m+3}(m+3)^2\rho^{m+1} + (n+3)\beta\rho^{n+1} = 0 \tag{59}$$

Assuming that the flow-behavior index n is a positive integer or zero, the third term in Equation (59) can be broken into three terms, first summing m from m = 0 to m = n-1, second m = n, and third from m = n+1 to infinity as follows:

$$\frac{A_1}{\rho} + (4A_2 - 2\beta) + \sum_{m=o}^{n-1} A_{m+3}(m+3)^2\rho^{m+1} + (n+3)\left[A_{n+3}(n+3) + \beta\right]\rho^{n+1}$$

$$+ \sum_{m=n+1}^{\infty} A_{m+3}(m+3)^2\rho^{m+1} = 0 \tag{60}$$

Comparing the coefficients of both sides, one has

$$A_1 = 0$$

$$4A_2 - 2\beta = 0$$

$$A_{m+3}(m+3)^2 = 0 \quad \text{when} \quad m = 0 \sim n-1$$
$$\text{and} \quad m = n+1 \sim \infty$$

$$(n+3)\left[A_{n+3}(n+3) + \beta\right] = 0$$

Solving these four simultaneous equations, one obtains

$$A_1 = 0$$

$$A_2 = \text{an arbitrary constant}$$

$$A_3 = A_4 = A_5 = \cdots = A_{n+1} = A_{n+2} = 0$$

$$A_{n+3} = -\frac{2A_2}{n+3}$$

$$A_{n+4} = A_{n+5} \cdots = 0$$

Therefore, one has

$$C_p^* = A_2 \left(\rho^2 - \frac{2}{n+3}\rho^{n+3}\right) \tag{61}$$

Equation (53) is then

$$C^* = C_o^* + A_2\left(\rho^2 - \frac{2}{n+3}\rho^{n+3}\right) \tag{5.20}$$

16. Derivation of Equation (5.23)

From Equations (5.20) and (5.22) we know that

$$C_m^* = 2\int_0^1 \left[C_o^* + \frac{1}{2(n+1)}\left(\frac{R^2}{D_R t}\right)\left(\frac{\partial C^*}{\partial \eta}\right)_1\left(\rho^2 - \frac{2}{n+3}\rho^{n+3}\right)\right]\rho\, d\rho \tag{62}$$

which can be integrated to obtain

$$C_m^* = C_o^* + \frac{1}{n+1}\left(\frac{R^2}{D_R t}\right)\left(\frac{\partial C^*}{\partial \eta}\right)_1\left[\frac{1}{4} - \frac{2}{(n+3)(n+5)}\right] \tag{63}$$

or

$$C_o^* = C_m^* - \frac{1}{n+1}\left(\frac{R^2}{D_R t}\right)\left(\frac{\partial C^*}{\partial \eta}\right)_1\left[\frac{1}{4} - \frac{2}{(n+3)(n+5)}\right] \tag{64}$$

Substituting Equation (64) into Equation (5.20), one has

$$C^* = C_m^* + \frac{1}{2(n+1)} \left(\frac{R^2}{D_R \bar{t}}\right)\left(\frac{\partial C^*}{\partial \eta_1}\right) \left[-\frac{1}{2} + \frac{4}{(n+3)(n+5)} + \rho^2 - \frac{2}{n+3}\rho^{n+3} \right] \tag{65}$$

Now, $\frac{\partial C^*}{\partial \eta_1}$ is replaced by $\frac{\partial C_m^*}{\partial \eta_1}$ because radial variation of tracer concentration has been assumed to be small (7). Then Equation (65) may be modified to become

$$C^* = C_m^* + \frac{1}{2(n+1)} \left(\frac{R^2}{D_R \bar{t}}\right)\left(\frac{\partial C_m^*}{\partial \eta_1}\right) \left[-\frac{1}{2} + \frac{4}{(n+3)(n+5)} + \rho^2 - \frac{2}{n+3}\rho^{n+3} \right] \tag{5.23}$$

17. Derivation of Equations (5.26)

From Equations (5.23), (5.24), and (5.25), one has

$$Q = 2\pi R^2 \int_0^1 \left[C_m^* + \alpha\left(\beta + \rho^2 - \frac{2}{n+3}\rho^{n+3}\right) \right] \bar{V}_x \left(\frac{2}{n+1} - \frac{n+3}{n+1}\rho^{n+1} \right) \rho \, d\rho \tag{66}$$

where

$$\alpha = \frac{1}{2(n+1)} \left(\frac{R^2}{D_R \bar{t}}\right) \frac{\partial C_m^*}{\partial \eta_1}$$

and

$$\beta = -\frac{1}{2} + \frac{4}{(n+3)(n+5)}$$

Factoring out common term in Equation (66) gives

$$Q = \frac{2\pi R^2 \bar{V}_x}{n+1} \left\{ \int_0^1 (C_m^* + \alpha\beta) \left[2\rho - (n+3)\rho^{n+2} \right] d\rho \right.$$

$$\left. + \int_0^1 \alpha\rho^2 \left[2\rho - (n+3)\rho^{n+2} \right] d\rho - \frac{2\alpha}{n+3} \int_0^1 \rho^{n+3} \left[2\rho - (n+3)\rho^{n+2} \right] d\rho \right\}$$

$$= \frac{2\pi R^2 \bar{V}_x \alpha}{n+1} \left[\left(\frac{1}{2} - \frac{n+3}{n+5}\right) - \frac{2}{n+3} \left(\frac{2}{n+5} - \frac{1}{2}\right) \right]$$

$$= - \frac{\pi R^2 \bar{V}_x (n+1)}{(n+3)(n+5)} \alpha = - \frac{\pi R^2 \bar{V}_x}{2(n+3)(n+5)} \left(\frac{R^2}{D_R \bar{t}}\right) \frac{\partial C_m^*}{\partial \eta_1}$$

$$= - \frac{\pi R^4 \bar{V}_x^2}{2(n+3)(n+5) D_R L} \left(\frac{\partial C_m^*}{\partial \eta_1}\right) \qquad (5.26)$$

18. Derivation of Equation (5.32)(41, 42)

Rewriting Equation (5.31), one has

$$\frac{\partial C_m^*}{\partial \theta} = \left(\frac{E}{\bar{V}_x L}\right) \frac{\partial^2 C_m^*}{\partial \eta_1^2} \qquad (67)$$

For simplicity, let $\frac{E}{\bar{V}_x L} = \alpha$ and $C^* = C_m^*$, then Equation (67) becomes

$$\frac{\partial C^*}{\partial \theta} = \alpha \frac{\partial^2 C^*}{\partial \eta_1^2} \qquad (68)$$

Consider the expression

$$C^* = \frac{A}{\theta^{\frac{1}{2}}} \exp\left(-\frac{\eta_1^2}{4\alpha\theta}\right) \tag{69}$$

where A is an arbitrary constant

Since

$$\frac{\partial C^*}{\partial \theta} = -\frac{A}{2\theta^{3/2}} \exp\left(-\frac{\eta_1^2}{4\alpha\theta}\right) + \frac{A}{4\alpha\theta^{5/2}} \exp\left(-\frac{\eta_1^2}{4\alpha\theta}\right) \tag{70}$$

and

$$\frac{\partial^2 C^*}{\partial \eta_1^2} = -\frac{A}{2\alpha\theta^{3/2}} \exp\left(-\frac{\eta_1^2}{4\alpha\theta}\right) + \frac{A}{4\alpha\theta^{5/2}} \exp\left(-\frac{\eta_1^2}{4\alpha\theta}\right) , \tag{71}$$

one can substitute Equations (70) and (71) into Equation (68) to show that Equation (69) satisfies the equation for diffusion in axial direction.

Equation (69) is symmetrical with respect to $\eta_1 = 0$, and has the following initial and boundary conditions:

I.C. $C^* = 0$ for $\theta = 0$ and $\eta_1 \neq 0$

B.C.1 $C^* = 0$ for $\theta > 0$ and $\eta_1 \to \pm \infty$

B.C.2 $C^* = \delta(\theta)$ for all θ and $\eta_1 = 0$

The total amount of tracer injected in the cylindrical tube of infinite length is given by

$$\int_{-\infty}^{\infty} C^* d\eta_1 = 1 \tag{72}$$

If the concentration distribution is that of expression shown in Equation (69) letting

$$\frac{\eta_1^2}{4\alpha\theta} = X \ , \quad d\eta_1 = 2(\alpha\theta)^{\frac{1}{2}} dX \ , \tag{73}$$

one sees that, combining Equations (69), (72), and (73)

$$2A\alpha^{\frac{1}{2}} \int_{-\infty}^{\infty} \exp(-X^2)dX = 2A(\pi\alpha)^{\frac{1}{2}} = 1 \tag{74}$$

or

$$A = \frac{1}{2(\pi\alpha)^{\frac{1}{2}}} \tag{75}$$

Expression in Equation (74) shows that the amount of tracer diffusing remains constant and equal to the amount originally deposited in the plane $\eta_1 = 0$. Therefore, on substituting Equation (75) into Equation (69), one has

$$C^* = \frac{1}{2(\pi\alpha\theta)^{\frac{1}{2}}} \exp\left(-\frac{\eta_1^2}{4\alpha\theta}\right) \tag{76}$$

where

$$\alpha = \frac{E}{\bar{V}_x L}$$

19. Derivation of Equation (5.44) (63)

For the time being, let

$$\frac{M}{2(n+3)(n+5)} = \alpha \tag{77}$$

then from Equations (5.34) and (5.41), one has

$$\mu = \int_0^\infty \theta \frac{1}{2(\pi\alpha\theta)^{\frac{1}{2}}} \exp\left[-\frac{(1-\theta)^2}{4\alpha\theta}\right] d\theta \tag{78}$$

The exponent of e containing the expression

$$\frac{(1-\theta)^2}{\theta} = \frac{1-2\theta+\theta^2}{\theta} = \frac{1}{\theta} - 2 + \theta = (\theta^{\frac{1}{2}} - \theta^{-\frac{1}{2}})^2 \tag{79}$$

Consequently the integrand in Equation (78) will be simplified if we set

$$x = \theta^{\frac{1}{2}} - \theta^{-\frac{1}{2}}$$

or

$$\theta^{\frac{1}{2}} = \frac{x + (x^2 + 4)^{\frac{1}{2}}}{2} , \tag{80}$$

from which it can be calculated that

$$d\theta = \frac{2\theta}{(x^2+4)^{\frac{1}{2}}} dx \tag{81}$$

With this substitution the integral takes the form

$$\int_{-\infty}^{\infty} \theta \frac{1}{2(\pi\alpha\theta)^{\frac{1}{2}}} \exp\left(-\frac{x}{4\alpha}\right) \frac{2\theta}{(x^2+4)^{\frac{1}{2}}}\, dx$$

$$= \frac{1}{(\pi\alpha)^{\frac{1}{2}}} \int_{-\infty}^{\infty} \frac{\theta^{3/2}}{(x^2+4)^{\frac{1}{2}}} \exp\left(-\frac{x^2}{4\alpha}\right) dx$$

$$= \frac{1}{(\pi\alpha)^{\frac{1}{2}}} \int_{-\infty}^{\infty} \frac{x^3+3x^2(x^2+4)^{\frac{1}{2}}+3x(x^2+4)+(x^2+4)^{3/2}}{8(x^2+4)^{\frac{1}{2}}} \exp\left(-\frac{x^2}{4\alpha}\right) dx \qquad (82)$$

because

$$\theta^{\frac{1}{2}} = \frac{x+(x^2+4)^{\frac{1}{2}}}{2}$$

Rearranging and simplifying terms in Equation (82), one obtains

$$\frac{1}{2(\pi\alpha)^{\frac{1}{2}}} \int_{-\infty}^{\infty} (x^2+1) \exp\left(-\frac{x^2}{4\alpha}\right) dx + \frac{1}{2(\pi\alpha)^{\frac{1}{2}}} \int_{-\infty}^{\infty} \frac{x^3+1}{(x^2+4)^{\frac{1}{2}}} \exp\left(-\frac{x}{4\alpha}\right) dx$$

$$= \frac{1}{(\pi\alpha)^{\frac{1}{2}}} \int_{0}^{\infty} (x^2+1) \exp\left(-\frac{x^2}{4\alpha}\right) dx + 0 \qquad (83)$$

because, in the first integral of the first line, the integral is an even function and, in the second the integral is an odd function.

Let

$$\frac{x^2}{4\alpha} = y \qquad \text{or} \qquad x^2 = 4\alpha y \qquad (84)$$

Since relation between the differentials is

$$dx = \left(\frac{\alpha}{y}\right)^{\frac{1}{2}} dy \tag{85}$$

one finally arrives at

$$\frac{1}{(\pi\alpha)^{\frac{1}{2}}} \int_0^{\infty} (4\alpha y + 1) \exp(-y) \left(\frac{\alpha}{y}\right)^{\frac{1}{2}} dy$$

$$= \frac{1}{\pi^{\frac{1}{2}}} \left[4\alpha \int_0^{\infty} y^{\frac{1}{2}} \exp(-y) dy + \int_0^{\infty} y^{-\frac{1}{2}} \exp(-y)\, dy \right]$$

$$= \frac{1}{\pi^{\frac{1}{2}}} \left[4\alpha \Gamma\left(\frac{3}{2}\right) + \Gamma\left(\frac{1}{2}\right) \right]$$

$$= \frac{1}{\pi^{\frac{1}{2}}} \left[4\alpha \frac{1}{2} \Gamma\left(\frac{1}{2}\right) + \Gamma\left(\frac{1}{2}\right) \right]$$

$$= 2\alpha + 1 \tag{86}$$

where $\Gamma\left(\frac{1}{2}\right) = \pi^{\frac{1}{2}}$

Equation (86) can also be obtained from the mathematical table (64). Therefore,

$$\mu = 1 + 2\alpha = 1 + \frac{M}{(n+3)(n+5)} \tag{5.44}$$

20. Derivation of Equation (5.46) (63)

Let $\frac{M}{2(n+3)(n+5)} = \alpha$ then

Equation (5.45) can be written as

$$\sigma^2 = \int_0^\infty \theta^2 \frac{1}{2(\pi\alpha\theta)^{\frac{1}{2}}} \exp\left[-\frac{(1-\theta)^2}{4\alpha\theta}\right] d\theta - \mu^2 \qquad (87)$$

where

$$\mu = 1 + \frac{M}{(n+3)(n+5)} \qquad (5.44)$$

Integrand in Equation (87) can be evaluated as follows:

Using a similar manner given in 19 and introducing

$$\theta^{\frac{1}{2}} = \frac{x+(x^2+4)^{\frac{1}{2}}}{2} \quad , \qquad (80)$$

one has

$$\frac{1}{(\pi\alpha)^{\frac{1}{2}}} \int_{-\infty}^{\infty} \theta^2 \frac{1}{2(\pi\alpha\theta)^{\frac{1}{2}}} \exp\left(-\frac{x^2}{4\alpha}\right) \frac{2\theta}{(x^2+4)^{\frac{1}{2}}} dx$$

$$= \frac{1}{(\pi\alpha)^{\frac{1}{2}}} \int_{-\infty}^{\infty} \frac{\theta^{5/2}}{(x^2+4)^{\frac{1}{2}}} \exp\left(-\frac{x^2}{4\alpha}\right) dx \qquad (88)$$

Substituting Equation (80) into Equation (88) and simplifying the terms, one obtains

$$\frac{1}{2(\pi\alpha)^{\frac{1}{2}}} \int_{-\infty}^{\infty} (x^4+3x^2+1) \exp\left(-\frac{x^2}{4\alpha}\right)dx$$

$$+ \frac{1}{2(\pi\alpha)^{\frac{1}{2}}} \int_{-\infty}^{\infty} \frac{x^5+5x^3+5x}{(x^2+4)^{\frac{1}{2}}} \exp\left(-\frac{x^2}{4\alpha}\right)dx$$

$$= \frac{1}{2(\pi\alpha)^{\frac{1}{2}}} \int_{-\infty}^{\infty} (x^4+3x^2+1) \exp\left(-\frac{x^2}{4\alpha}\right)dx + 0$$

$$= \frac{1}{(\pi\alpha)^{\frac{1}{2}}} \int_{0}^{\infty} (x^2+3x^2+1) \exp\left(-\frac{x^2}{4\alpha}\right)dx \qquad (89)$$

Now substituting Equations (84) and (85) into Equation (89), one obtains

$$\frac{1}{(\pi\alpha)^{\frac{1}{2}}} \int_{0}^{\infty} (16\alpha^2y^2 + 12\alpha y + 1) \exp(-y)\left(\frac{\alpha}{y}\right)^{\frac{1}{2}}dy$$

$$= \frac{1}{\pi^{\frac{1}{2}}}\left[16\alpha^2\int_{0}^{\infty} y^{3/2}\exp(-y)dy + 12\alpha\int_{0}^{\infty} y^{\frac{1}{2}}\exp(-y)dy\right.$$

$$\left. + \int_{0}^{\infty} y^{-\frac{1}{2}}\exp(-y)dy\right]$$

$$= \frac{1}{\pi^{\frac{1}{2}}}\left[16\alpha^2\Gamma\left(\frac{5}{2}\right) + 12\alpha\Gamma\left(\frac{3}{2}\right) + \Gamma\left(\frac{1}{2}\right)\right]$$

$$= 12\alpha^2 + 6\alpha + 1 \qquad (90)$$

where $\Gamma\left(\frac{1}{2}\right) = \pi^{\frac{1}{2}}$

Therefore, substituting Equations (86) and (90) into Equation (87) one obtains

$$\sigma^2 = 12\alpha^2 + 6\alpha + 1 - (2\alpha + 1)^2$$

$$= 8\alpha^2 + 2\alpha$$

$$= 2\left[\frac{M}{(n+3)(n+5)}\right]^2 + \frac{M}{(n+3)(n+5)} \qquad (5.46)$$

LITERATURE CITED

1. Metzner, A. B., and J. S. Taylor, A.I.Ch.E. Journal, 6, 109 (1960).
2. Metzner, A. B. and K. W. Norwood, A.I.Ch.E. Journal, 6, 432 (1960).
3. McKelvey, J. M., "Polymer Processing," John Wiley and Sons, Inc., New York (1962).
4. Danckwerts, P. V., Chem. Engg. Sci., 2, 1 (1953).
5. Levenspiel, O., "Chemical Reaction Engineering," John Wiley and Sons, Inc., New York (1962).
6. Bird, R. B., W. E. Steward and E. N. Lightfoot, "Transport Phenomena," John Wiley and Sons, Inc., New York (1960).
7. Taylor, G. I., Proc. Roy. Sco. (London), A219, 186 (1953).
8. Taylor, G. I., Proc. Roy. Soc. (London), A223, 446 (1954).
9. Taylor, G. I., Proc. Roy. Soc. (London), A225, 473 (1954).
10. Tichacek, L. J., C. H. Barkelew, and T. Baron, A.I.Ch.E. Journal, 3, 439 (1957).
11. Miyauchi, T., "Operations of Flow Systems and Mixing Characteristics," (Japanese Ed.), Nikan Kogyo News Publications Co., Tokyo (1960).
12. Sheppard, C. W., "Basic Principles of the Tracer Method," John Wiley and Sons, Inc., New York (1962).
13. Kirschbaum, E., "Distillation and Rectification," trans. by M. Wulfinghoff, Brooklyn Publ. Co. (1948).
14. Kramers, H. and G. Alberda, Chem. Engg. Sci., 2, 35 (1953).

15. Levenspiel, O., and K. B. Bischoff, "Advances in Chemical Engineering," Vol. 4, Academic Press Inc., New York (1963).

16. Trambouze, P. J., Rev. Inst. Franc. Petrole, 15, 1948 (1960).

17. van der Laan, E. T., Chem. Eng. Sci., 7, 187 (1958).

18. Philippoff, W., "Viskosität Der Kolloide," (1942). Lithoprinted by J. W. Edwards, Ann Arbor, Mich. (1944).

19. Kruyt, H. R. and F. G. van Selms, Rec. trav. chim., 62, 415 (1943).

20. Metzner, A. B., Chemical Engineering Program, 50, 27 (1954).

21. Metzner, A. B., "Advances in Chemical Engineering," Vol. I, Academic Press Inc., New York (1956).

22. Reiner, M., "Deformation and Flow," Lewis, London (1949).

23. Perry, J. H., "Chemical Engineers' Handbook," 3rd Ed., McGraw-Hill, New York (1950).

24. Bosworth, R. C. L., Phil. Mag., 39, 847 (1948).

25. Gonzalez-Fernandez, J. M., "Symposium on Use of Indicator-Dilution Techniques in the Study of the Circulation," American Heart Association Monograph, No. 4 (1962).

26. Aris, R. B., Proc. Roy. Soc. (London) A235, 67 (1956).

27. Blockwell, A. J., Paper presented at local section of A.I.Ch.E., Glaverton, Texas, Oct. 18, 1957.

28. Carberry, J. J., and R. H. Bretton, A.I.Ch.E. Journal, 4, 367 (1958).

29. Ebach, E. A. and R. R. White, A.I.Ch.E. Journal, 4, 161 (1958).

30. Liles, A. W., and C. J. Geankoplis, A.I.Ch.E. Journal, 6, 591 (1960).

31. McHenry, K. W., Jr., and R. H. Wilhelm, A.I.Ch.E. Journal, 3, 83 (1957).

32. Bailey, H. R., and W. B. Gogarty, Proc. Roy. Soc. (London), A269 352 (1962).

33. Farrel, M. A., and E. F. Leonard, A.I.Ch.E. Journal, 9, 190 (1963).

34. Nicholas, D. C., and D. E. Lamb, Unpublished paper, University of Delaware, Newark, Delaware (1963).

35. Bischoff, K. B., Ph.D. thesis, Illinois Institute of Technology, Chicago, Illinois (1961).

36. Vanderveen, J. W., M.S. Ch.E. thesis, University of Nebraska, Lincoln, Nebraska (1961).

37. Fredrickson, A. G., "Principles and Applications of Rheology," Prentice-Hall, Inc., Englewood Cliffs, N. J. (1964).

38. Schechter, R. S., and E. H. Wissler, Nuclear Sci. and Eng., 6, 371 (1959).

39. Fan, L. T., Unpublished Note on Fluid Dispersion, K.S.U., Manhattan, Kansas (1963).

40. Kreyszig, E., "Advanced Engineering Mathematics," John Wiley and Sons, Inc., New York (1962).

41. Crank, J., "The Mathematics of Diffusion," Oxford Univ. Press (1956).

42. Carslaw, H. S. and J. C. Jaeger, "Conduction of Heat in Solid," (2nd Ed.), Oxford Univ. Press (1959).

43. Levenspiel, O., and W. K. Smith, Chem. Eng. Sci., 6, 227 (1957).

44. Levenspiel, O., Ind. Engg. Chem., 50, 345 (1958).

45. Rouse, H., "Elementary Mechanics of Fluids," Chapter 7, John Wiley and Sons, Inc., New York (1946).

46. Fan, L. T., "Fluid Dispersion Associated with Flow of Non-Newtonian Fluids," A proposal for basic research submitted to National Science Foundation, Washington, D.C., Engineering Experiment Station, Kansas State University, Manhattan, Ks. (1963).

47. Clough, S. B., M.S.Ch.E. thesis, Univ. of Delaware, Newark, Delaware (1961).

48. Clough, S. B., H. E. Read, A. B. Metzner, and V. C. Behn, A.I.Ch.E. Journal, 8, 346 (1962).

49. Read, H. E., M.S.M.E. thesis, Univ. of Delaware, Newark, Delaware (1961).

50. Koutsky, J. A., and R. J. Adler, Paper presented at the 13th Ch. E. Conference, Chemical Institute of Canada, Oct. 21-23, 1963.

51. Savins, J. G., Paper presented at 56th Annual A.I.Ch.E. Meeting at Houston, Texas, Dec. 1-5, 1963.

52. Pruitt, G. T., and H. R. Crawford, Paper presented at 56th Annual A.I.Ch.E. Meeting at Houston, Texas, Dec. 1-5, 1963.

53. Giles, W. B., Paper presented at 56th Annual A.I.Ch.E. Meeting at Houston, Texas, Dec. 1-5, 1963.

54. Gondiff, D. W., Paper presented at 56th Annual A.I.Ch.E. Meeting at Houston, Texas, Dec. 1-5, 1963.

55. Wolf, D., and W. Resnick, Ind. Eng. Chem. Fundamentals, 2, 287 (1963).

56. Williams, M. C., and R. B. Bird, A.I.Ch.E. Journal, 8, 378 (1962).

57. Schrenk, W. J., D. S. Chisholm, and T. Alfrey, Jr., ASME Paper No. 63-WA-303 (1963).

58. Schrenk, W. J., K. J. Cleereman, and T. Alfrey, Jr., ASME Paper No. 62-WA-336 (1962).

59. Sarpkaya, T., A.I.Ch.E. Journal, 7, 324 (1961).

60. Beckenbach, E. F., "Modern Mathematics for the Engineers," McGraw-Hill Book Co., Inc., New York (1961).

61. Aris, R., "Notes on Chemical Reactor Analysis," Chem. Eng. Dept., Univ. of Minnesota, Minneapolis, Minnesota (1961).

62. Churchill, R. V., "Operational Mathematics," McGraw-Hill Book Co., Inc., New York (1958).

63. Bischoff, K. B., Private Communication, April, 1964.

64. Ryshik, I. M., and I. S. Gradstein, "Tables of Series, Products, and Integrals," (2nd rev. ed.), Plenum Press, New York (1963).

NOMENCLATURE

A_m = m-th eigen constant

C = concentration, m/l^3

C_i = molar concentration of component i, mols./l^3

$\underline{C}(\theta)$ = dimensionless tracer response curve to a unit impulse input, a function of θ

C^* = dimensionless concentration, C/C^o

$\overline{\underline{C}}$ = Laplace transform of the two-dimensional residence time distribution function (r.t.d.f.)

C_o = concentration of tracer in inlet stream, m/l^3

C^o = mean concentration of pulse of tracer if uniformly distributed in experimental section of vessel, m/l^3

C_m = area mean concentration, m/l^3

D = dispersion coefficient, l^2/t

D_e = effective axial diffusivity, a function of D_L, D_R, and $\overline{V}x(5)$, l^2/t

D_L = axial dispersion coefficient, l^2/t

D_R = radial dispersion coefficient, l^2/t

D_m = molecular diffusivity, l^2/t

d_t = inside diameter of round tube, l

E = overall dispersion coefficient, $\frac{R^2\overline{V}_x^2}{D_R}\left[\frac{1}{2(n+3)(n+5)}\right]$

$\underline{E}(\theta)$ = exit age distribution function or r.t.d.f., a function of θ

$\underline{E}(\theta)_m$ = maximum concentration

$\underline{F}(\theta)$ = dimensionless response curve to a step input of tracer, a function of θ

F_m = m-th eigen function

f = Fanning friction factor

$\vec{g}$ = gravitational acceleration, l/t^2

$\vec{g}_i$ = total body force per unit mass of component i, l/t^2

$\underline{I}(\theta)$ = internal age distribution function, a function of θ

H = a distance between two parallel plates, l

$\vec{J}_i$ = molecular flux of component i, mols./tl^2

$\vec{J}_i(l)$ = laminar contribution to molar flux of component i, mols./tl^2

$\vec{J}_i(t)$ = turbulent contribution to molar flux of component i, mols./tl^2

J_o = Bessel function of the first kind of order zero

j = parameter in the perfectly mixed tanks in series model

K = effective axial dispersion coefficient for laminar flow defined by Taylor (7)

k = first-order rate constant for bulk phase chemical reaction, l/t

L = characteristic length of system, l, or Laplace transform operator in Appendices

M = parameter, $R^2\bar{V}_x/D_RL$

m = parameter in Ostwald-de Waele model, dimensions depend on n

n = flow-behavior index in Ostwald-de Waele model, dimensionless, l/v

P = pressure, m/lt^2

ΔP = pressure drop over L, m/lt^2

Pe = Peclet number, $\bar{V}_x L/D$

Q = volumetric flow rate, l^3/t

$\vec{q}$ = energy flux, m/t^3

R = tube radius, l

Re = Reynolds number, $d_t \bar{V}_x \rho/m$

r = radial coordinate

r_i = molar rate of production of component i, mols./tl^3

s = Laplace parameter

Sc = Schmidt number, $m/\rho D_R$

t = time, t

$\bar{t}$ = mean residence time, t

Us = a unit step function

V_R = wall velocity, l/t

$\bar{V}_x$ = mean velocity in axial direction, l/t

$V_x(r)$ = axial velocity, a function of r, l/t

V_m = center line velocity for laminar flow, l/t

V'_m = center line velocity for laminar flow if a slip velocity at the wall is considered, l/t

$\vec{v}$ = velocity vector, l/t

W = width of plate in z-direction, l

X = length of the system, l

x = axial distance, l

x_1 = $x - 1/2\ (V_m t)$ = axial position relative to a coordinate system moving with the mean fluid velocity, l

Y_o = Bessel function of the second kind of order zero

Greek Letters

α = dimensionless constant

α_m = m-th eigen value

β = dimensionless constant

γ = a slip velocity factor

$\overrightarrow{\overrightarrow{\Delta}}$ = rate of deformation tensor

$\delta(\theta)$ = Dirac delta function, a function of θ

$\delta(\eta-\eta_o)$ = Dirac delta function, a function of

ϵ_D = eddy diffusivity, l^2/t

ζ = dimensionless position variable, y_o/H or τ_o/τ_H

η = dimensionless axial distance, x/L

θ = dimensionless time, $t/\bar{t}$ or $t\bar{V}_x/L$

θ_m = dimensionless time at maximum concentration

μ = mean of the r.t.d.f. or the first moment about the origin

μ_o = parameter in Bingham model, m/lt

ν = parameter in Ostwald-de Waele model, dimensionless

ξ = dimensionless radial distance, r_o/R or τ_o/τ_R

π = 3.1416

$\overrightarrow{\overrightarrow{\Pi}}$ = pressure tensor, m/lt^2

ρ = dimensionless radial distance, r/R

ρ = fluid density, m/l^3

ρ_i = mass concentration of component i, m/l^3

σ^2 = variance of the r.t.d.f. or the second moment about the mean

$\overrightarrow{\overrightarrow{\tau}}$ = shear stress tensor, m/t^2l

$\overrightarrow{\overrightarrow{\tau}}(l)$ = laminar contribution to shear stress tensor, m/t^2l

$\overrightarrow{\overrightarrow{\tau}}(t)$ = turbulent contribution to shear stress tensor, m/t^2l

τ_o = parameter or yield stress in Bingham model, m/t^2l

τ_R = shear stress or momentum flux at the wall, m/t^2l

τ_{yx} = tangential shear stress parallel to y plane and in direction of x axis, m/t^2l

Φ = a function of Reynolds and Schmidt numbers

$\psi(C)$ = rate of production, a function of concentration

∇ = the "del" or "nabla" operator

FLUID DISPERSION ASSOCIATED WITH LAMINAR FLOW OF NON-NEWTONIAN FLUIDS

by

WEI SHIN HWANG

B. S., National Taiwan University, 1955

AN ABSTRACT OF A MASTER'S THESIS

submitted in partial fulfillment of the

requirements for the degree

MASTER OF SCIENCE

Department of Chemical Engineering

KANSAS STATE UNIVERSITY
Manhattan, Kansas

1964

The principal purpose of this work was to develop mathematical models to characterize dispersion of non-Newtonian fluids in continuous flow systems in the laminar flow region. First, the basic notions of fluid dispersion and residence time distributions are presented. The analysis of residence time distributions is one of the most commonly used tools in the study of fluid dispersion in continuous flow systems.

The convective models (velocity profile models) of fluid dispersion are derived for Bingham and the Ostwald-de Waele fluids. It has been indicated that deformation in the shape of the residence time distribution curve is caused solely by the dispersion effect. The present analysis, however, reveals that the deformation of the residence time distribution curve can also be caused by deviation of the flow-behavior from Newtonian characteristics.

Finally, the dispersion (diffusion) model is developed for the Ostwald-de Waele fluid. Expressions for the residence time distributions as well as a correlation of dispersion coefficients are obtained. It is noted that the results include Newtonian flow as a special case. Also for a given flow condition, the degree of dispersion decreases as the fluid changes its characteristics from dilatant ($n<1$) to pseudoplastic ($n>1$).